ANTIVIRAL POTENTIAL OF CANNABIS-DERIVED COMPOUNDS

Aphrodite Savva

Department of Biomedical and Life Sciences Faculty of Health and Medicine

Lancaster University

Thesis for the degree of MSc by Research

2024

Declaration

I declare that all the content in this dissertation is my original work and does not contain any material from other sources. This document has not been previously presented in a similar format to obtain a higher degree or qualification elsewhere.

Aphrodite Savva

Abstract

Cannabis-derived compounds show promise as antiviral agents, offering an innovative approach to facing growing viral resistance to existing therapies. Cannabinoids demonstrate immunomodulatory and anti-inflammatory effects, suggesting further effectiveness in inhibiting viral replication. Therefore, their bioactivity suggests the prospect of enhancing current antiviral treatments.

This project focused on addressing current gaps in understanding the mechanisms of cannabinoids, terpenes, and flavonoids, including the optimal dosage and potential efficacy of compound combinations against the Influenza A virus *in vitro*. The aim was to screen a range of these promising compounds for their ability to inhibit the virus. A549 and MDCK cells were cultured and passaged for cell viability and antiviral plaque assays. Cell viability and cytotoxicity were assessed after 24-hour cannabinoid pre-treatment, using PrestoBlue™ and CytoTox-Glo™ assays, and IC50 values were determined. The cytotoxicity of ethanol and methanol vehicles was also evaluated. Influenza A H1N1/PR8 was inoculated in chicken embryonated eggs and propagated in MDCK cells. The antiviral activity was assessed by plaque assay. The viral plaque areas were quantified using ImageJ software. The research shortlisted two compounds that demonstrate the most potent antiviral activity against H1N1. Furthermore, the results provided foundational information for the development of drug testing portfolios for future pre-clinical evaluation.

According to the antiviral plaque assay results, 5.93 µM CBG and 3.13 µM CBD reduced viral load by approximately 85% and 75%, respectively, and appeared to be the most effective among the compounds. Sesquiterpenes with a concentration of 425 mg/mL also reduced the viral load, with an increased plaque size compared to the control. The results support a strong antiviral potential for CBG and CBD, which could be of clinical significance in the treatment of Influenza virus infections. Further investigation is required to assess the specific antiviral effects of these compounds down to a molecular level, as well as their longevity, potential compound combinations, and antiviral potential against other respiratory viruses.

Abbreviations

2-AG	2-Arachidonoylglycerol
A549	Human alveolar basal epithelial cell line
AAF	Allantoic Fluid
ACA	ε-Aminocaproic Acid
ACE2	Angiotensin-Converting Enzyme 2
AEA	Anandamide
AR	Acute Respiratory
ARDS	Acute Respiratory Distress Syndrome
BCP	β-Caryophyllene
BHK-21	Baby Hamster Kidney fibroblasts
BSA	Bovine Serum Albumin
BSC	Biosafety Cabinet
BSL-3	Biosafety Level 3
CBC	Cannabichromene
CBCV	Cannabichromevarin
CBCVA	Cannabichromevarinolic Acid
CBD	Cannabidiol
CBDA	Cannabidiolic Acid
CBDV	Cannabidivarin
CBDVA	Cannabidivarinolic Acid
CBG	Cannabigerol
CBGA	Cannabigerolic Acid
CBN	Cannabinol
CB1	Cannabinoid Type 1
CB2	Cannabinoid Type 2
CDC	Centers for Disease Control and Prevention
CL3	Containment Level 3
COVID-19	Coronavirus Disease 2019
CVH	Cell Culture Virus Harvest

Cytotox-Glo	Cytotoxicity assay kit
DAB	3,3’-Diaminobenzidine
DENV-2	Dengue Virus Serotype 2
DMEM	Dulbecco's Modified Eagle Medium
DMSO	Dimethyl Sulfoxide
Δ9-THC	Delta-9-tetrahydrocannabinol
EDTA	Ethylenediaminetetraacetic Acid
ECS	Endocannabinoid System
EOs	Essential Oils
FAAH	Fatty Acid Amide Hydrolase
FBS	Fetal Bovine Serum
FDA	Food and Drug Administration
FITC	Fluorescein isothiocyanate
GRP55	G Protein-Coupled Receptor 55
HA	Hemagglutination
HAU	Hemagglutination Unit
HBV	Hepatitis B Virus
HCV	Hepatitis C Virus
HEK293	Human Embryonic Kidney cells
HEPES	N-2-Hydroxyethylpiperazine-N-2-ethane Sulfonic Acid
HIV	Human Immunodeficiency Virus
HNECs	Primary Human Nasal Epithelial Cells
HSV	Herpes Simplex Virus
HSV-1	Herpes Simplex Virus 1
IC_{50}	Half-Maximal Inhibitory Concentration
IAV	Influenza A Virus
KSHV	Kaposi's Sarcoma-Associated Herpesvirus
LRTI	Lower Respiratory Tract Infection
MAGL	Monoacylglycerol Lipase
MDCK	Madin-Darby Canine Kidney
MEM	Minimum Essential Medium
MOI	Multiplicity of Infection

NiV	Nipah Virus
PARP	Poly (ADP-ribose) polymerase
Pen-Strep	Penicillin-Streptomycin
PFU	Plaque Forming Unit
PI	Propidium Iodide
PPARγ	Peroxisome Proliferator-Activated Receptor Gamma
PrestoBlue	Cell viability assay reagent
PR8	Puerto Rico 8 (Influenza A H1N1 strain)
RBC	Red Blood Cell
RIP1	Receptor-interacting protein kinase 1
RIP3	Receptor-interacting protein kinase 3
RNP	Ribonucleoprotein
ROS	Reactive Oxygen Species
RSV	Respiratory Syncytial Virus
RT	Room Temperature
RT-PCR	Reverse Transcription Polymerase Chain Reaction
SARS-CoV-2	Severe Acute Respiratory Syndrome Coronavirus 2
SEM	Standard Error of the Mean
TCID50	50% Tissue Culture Infectious Dose
THC	Tetrahydrocannabinol
TMPRSS2	Transmembrane Protease, Serine 2
TPCK	L-1-Tosylamide-2-phenylethyl chloromethyl ketone
TR146	Buccal carcinoma cell line
TRPV	Transient Receptor Potential Vanilloid Channels
UV	Ultraviolet
WHO	World Health Organisation
ZIKV	Zika Virus
µM	Micromolar

Contents

Figures and Tables

Acknowledgements

I would like to express my appreciation to my supervisors Dr Muhammad Munir and Dr Karen Wright for offering me the opportunity to work on this exciting project, and for their patience, guidance and support throughout this research. Throughout this journey I gained a wealth of expertise and had the opportunity to engage with great researchers and most of all kind and positive people.

I have great respect for and would like to thank Dr Rohaim Mohammed and Dr Mustafa Ozan Atasoy for their knowledge, advice and assistance with complicated virology experiments and virus handling.

Thank you to all my colleagues, who are now my friends, from both groups; Asmaa Nasr, Vidya Manju and Daniel Baines for their willingness to provide assistance and advice when necessary, since my first day in the lab.

Special thanks to my wonderful partner, Lord Matthew David Franks for his positivity and emotional support.

Finally, I would like to give a massive thank you to my family. Without their massive support with everything, I would not have been able to accomplish nearly as much.

Chapter 1 Introduction

1.1. Introduction

The Cannabis plant consists of over 400 secondary metabolites, which include 120 cannabinoids, and over half of the remaining compounds consist of terpenes and phenolic compounds. These compounds have also been investigated for a variety of pharmacological actions, with evidence of inhibiting viral replication and decreasing viral plaque formation of SARS-CoV-2 and HSV-1.

Past pandemics such as H1N1 and COVID-19 illustrate the persistent threat of viral infections globally, which emphasises the necessity of preparedness, surveillance, and continuous development of broad-spectrum antivirals (Gonçalves et al., 2020). Current antiviral options are limited by drug resistance, viral mutation, and host toxicity (Gonçalves et al., 2020). Consequently, interest has grown in plant-derived metabolites such as cannabinoids and terpenes, because they have demonstrated in vitro antiviral and immunomodulatory activity against a range of RNA and DNA viruses. (Jones et al., 2022). The unique properties of cannabinoids include their ability to modulate the endocannabinoid system via CB1 and CB2 receptors. This interaction influences numerous physiological processes, including anti-inflammatory and immunomodulatory effects. As such, further research into cannabis-derived compounds could lead to the development of more effective antiviral therapies. As an example, CBD can modulate immune responses via CB2 receptors and can offer therapeutic potential without psychoactive effects (Janecki et al., 2022).

According to previous research, cannabidiol (CBD) and cannabigerol (CBG) can inhibit SARS-CoV-2 through inhibiting viral entry and replication (Classen et al., 2024; Devi & Yadav, 2023). These cannabinoids downregulate ACE2 transcript levels, a key receptor for viral entry (Devi and YADAV, 2023). In addition, there is evidence supporting that cannabigerolic acid (CBGA), cannabigerol (CBG), and Δ9-Tetrahydrocannabutol effectively block replication and act as inhibitors of the SARS-CoV-2 main protease (Liu *et al.*, 2022). Research based on the antiviral properties of cannabinoids is overall limited, notably on Influenza A virus, and further well-

designed trials are needed to fully confirm their efficacy and safety as antivirals.

1.2. Influenza A virus and SARS-CoV2

1.2.1. Inlfuenza A virus introduction

Influenza A and B viruses, rhinovirus, respiratory syncytial virus (RSV), parainfluenza virus, and adenovirus are the most frequent respiratory viruses in the UK. They can induce acute respiratory failure, which can result in acute respiratory distress syndrome (ARDS). Despite this, there is a scarcity of effective antiviral treatments available.

Influenza A viruses are highly adaptable pathogens that are classified according to their surface proteins, hemagglutinin (HA) and neuraminidase (NA), with 18 HA and 11 NA subtypes identified (Wang et al., 2019). The natural reservoir for all known subtypes is wild aquatic birds, from which all these viruses originate (Palese, 2004). Influenza viruses can infect other animals like pigs, which act as “mixing vessels” for reassortment between avian, human, and swine strains (Ma, Kahn, and Richt, 2008). New viruses can then emerge through antigenic shift, leading to pandemics like the 2009 H1N1 outbreak. Seasonal strains such as H1N1 and H3N2 evolve rapidly via antigenic drift, persisting in humans and resulting in the requirement for constant vaccine updates (Petrova & Russell, 2018).

In the UK, Influenza hospital admissions peaked during week 52 of 2023 and in week 4 of 2024. During this period, there was a relatively equal distribution of admissions for influenza A(H1N1)pdm09 (n=448) and influenza A(H3N2) (n=444), alongside a late-season surge in influenza B admissions starting in week 8 of 2024. Influenza A was the predominant type, with both A(H3N2) and A(H1N1)pdm09 subtypes circulating. Influenza B Victoria lineage was less prominent (GOV.UK, 2024). The data was collected from surveys, completed by a total of 2,545 participants, with a majority residing in England and a higher representation of older age groups (GOV.UK, 2024).

According to Job et al. (2010), pandemic H1N1 influenza A virus strains are resistant to the antiviral activities of innate immune proteins from the collectin and pentraxin superfamilies, resulting in challenges in combating this disease effectively. Additionally, there is vulnerability in certain populations, as women exhibit attenuated innate interferon responses to the 2009 pandemic influenza A virus subtype H1N1 (Forbes et al., 2012).

1.2.2. SARS-CoV-2 introduction

Severe acute respiratory syndrome coronavirus 2 (SARS-CoV-2) emerged in late 2019 in Wuhan, China, causing an outbreak of viral pneumonia that, due to its high transmissibility, escalated rapidly into a global pandemic. It is a positive-sense, single-stranded RNA virus that belongs to the Betacoronavirus genus (Hu et al., 2020). Its host cell entry mechanism involves angiotensin-converting enzyme 2 (ACE2) receptor binding, facilitated by its spike (S) protein, with a higher binding affinity compared to earlier coronaviruses (Jackson et al., 2021). According to genomic analyses, the virus is of zoonotic origin, with close similarities to coronaviruses found in bats and pangolins, indicating possible interspecies transmission events (Hu et al., 2020).

1.2.3. Global perspective of respiratory viruses

Respiratory viruses have a significant level of morbidity and mortality worldwide, especially for children. Particularly in impoverished regions of tropical countries, one-fifth of all childhood deaths are related to respiratory infections (ARIs). It was also observed that SARS coronavirus and avian influenza virus H5N1 have emerged as threats in recent years (Boncristiani et al., 2009).

An approximation of 11.5% of all lower respiratory tract infection (LRTI) episodes that occurred in 2017 were caused by influenza virus infection. This corresponds to about 54 million episodes, 9.4 million of which resulted in hospitalisations (Troeger et al., 2019). The greatest mortality rate belongs to individuals aged >70 (16.4 deaths per 100,000 (95% CI 11.6–21.9)) (Cilloniz et al., 2022). When focusing on RSV-causing acute respiratory infections (ARI),

approximately 1.5 million episodes were recorded in industrialised countries for individuals aged ≥65 years.

In the season of 2022-2023, 11% of confirmed influenza cases were attributed to Influenza A (H1N1)pdm09 strain cases (Iván Martínez-Baz et al., 2023). The overall effectiveness of the vaccine against the virus strain was reported as null, which suggests difficulties in its control. Seasonal influenza epidemics can lead to between 290,000 and 650,000 respiratory disease-related deaths globally each year, and H1N1 influenza viruses have been major contributors to these outbreaks (Al-Naqeeb and Raham, 2021). A recent example is the prevalence of the influenza A (H1N1) pdm09 subtype in China in 2023. When viewed in historical context, the UK reported over 30,000 infections and 457 deaths during the 2009-2010 pandemic, attributed to H1N1 (Lucas, 2010). The annual global recommendation of influenza vaccine production is 230 million doses (Stöhr, 2003). For the 2023-2024 season, vaccine manufacturers have supplied the United States with 156.2 to 170 million doses of influenza vaccines (CDC, 2023).

Severe acute respiratory syndrome coronavirus 2 (SARS-CoV-2) is also a virus of high importance, with significant cause of morbidity and mortality during the 2019 pandemic. The importance of the pandemic is apparent in the way it affected individuals, with its significant cause of morbidity and mortality (Sharma et al., 2020). In April 2022, almost 504 million coronavirus disease 2019 (COVID-19) cases were reported globally by the World Health Organisation (WHO). In addition, there were more than 6.2 million COVID-19-related deaths. The clinical severity of the disease can range from asymptomatic or mild disease of the upper airways to pneumonia and acute respiratory distress syndrome (ARDS). COVID-19 is a complex disease, affecting the respiratory and gastrointestinal tracts, as well as kidney function, resulting in immune system hyperstimulation. There are still no therapeutic approaches that are 100% effective for the prevention and treatment of the virus. From a global health perspective, there is a need for effective antiviral agents that can tackle a variety of viruses, due to the emergence of new viral diseases like COVID-19, as well as new viral strains.

1.2.4. Influenza virus and SARS-CoV2 clinical symptoms and diagnosis

Influenza A infection severity ranges from asymptomatic or mild symptoms of the upper airways to acute respiratory distress syndrome (ARDS) and pneumonia (Figure 1.1). Approximately 30-40% of hospitalised patients with confirmed influenza develop pneumonia, with a notable incidence of secondary bacterial infections (Kalil & Thomas, 2019; Daoud et al., 2019).

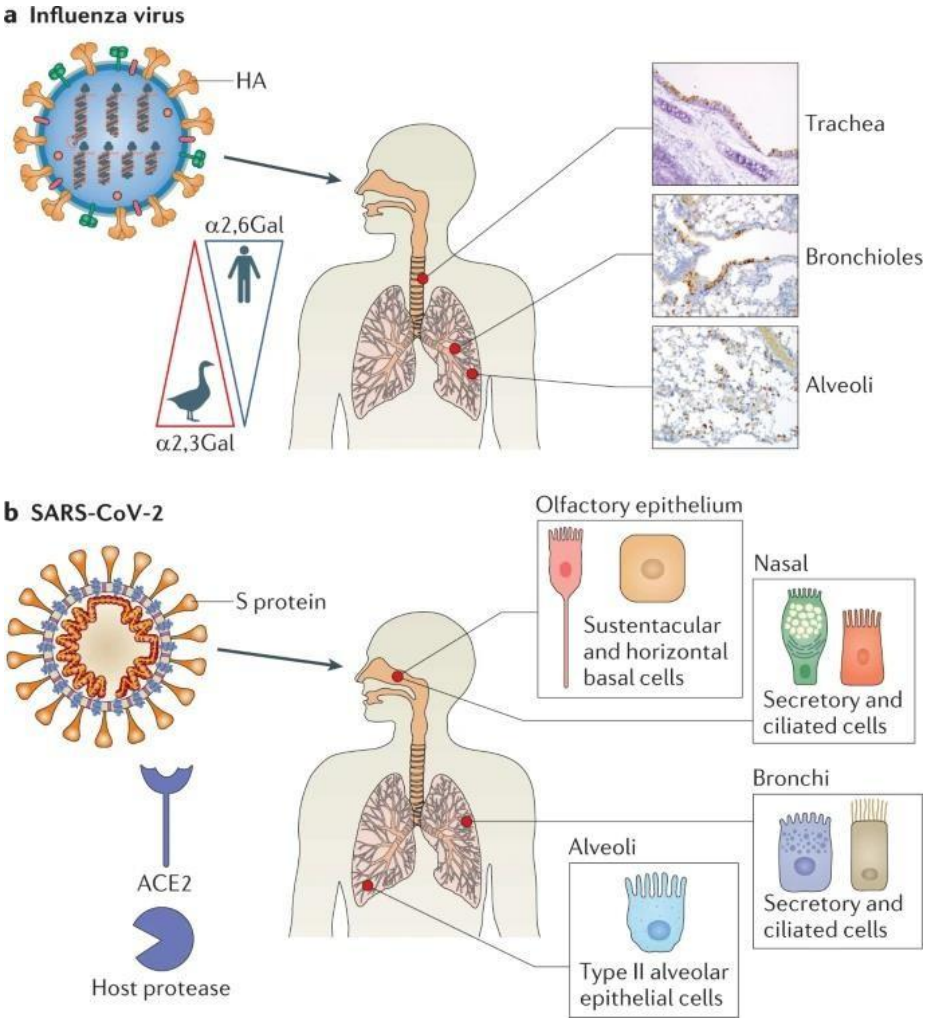

Figure 1.1 Binding mechanisms of influenza viruses and SARS-CoV-2 in respiratory epithelial cells.

a | The haemagglutinin (HA) protein of influenza viruses preferentially binds to the surface of pulmonary epithelial cells through binding sialosaccharides. Histopathological image courtesy of P. Vogel. **b |** severe acute respiratory syndrome coronavirus 2 (SARS-CoV-2) binds angiotensin-converting enzyme 2 (ACE2) via the spike (S) protein (Flerlage et al., 2021).

SARS-CoV-2 binds to ACE2, which is found on the surface of respiratory and olfactory epithelial

cells distributed along the human respiratory tract. The enzyme is activated by transmembrane serine protease 2 (TMPRSS2), as well as cathepsin L, neuropilin 1, and furin. (Flerlage et al., 2021). In comparison, influenza viruses bind to sialic acids linked to galactose. The difference between human and avian influenza viruses is that avian influenza viruses bind to SAα2,3Gal, whereas human IAV prefer sialic acids (SAs) linked to galactose by α (2,6) linkage (SAα2,6Gal). The distribution of these substances changes gradually across different parts of the human respiratory tract. The intracellular localisation of influenza viruses in epithelial cells from three different sites is depicted in Figure 1.1a, with immunohistochemistry staining, with samples from infected patients with influenza A virus. Due to this receptor distribution, human influenza viruses such as influenza A (H1N1) tend to infect the upper respiratory tract, leading to typical flu symptoms. On the other hand, avian influenza viruses, for example influenza A (H5N1), are more likely to infect deeper regions of the lungs where such receptors are more abundant.

1.2.5. Influenza virus and SARS-CoV2 treatment

COVID-19 and the Influenza virus have overlapping symptoms and signs. The only way to distinguish between the two is through testing. It is possible that coinfection between SARS-CoV-2 and influenza A and B can occur and should be considered, especially in hospitalised individuals with severe respiratory disease. Viral pneumonia can result in contagious acute respiratory infectious disease. This was the case in December 2019 in Wuhan, Hubei Province, China, due to the SARS-CoV-2 epidemic (Huang *et al.*, 2020). Mortality is higher in patients with ARDS, and according to a study, the overall hospital mortality rate for patients with ARDS in 2019 was 17.6%, with Influenza A/H1N1 patients having approximately three times the probability of death compared to others (Lobo et al., 2019). In addition, these patients develop co-infections and longer symptom durations, which led to the death of 38% of patients with ARDS developed from Influenza A, as reported in a cohort by Sun et al.

There are currently six antiviral drugs targeting the influenza virus that are approved in the USA. Four of them are approved by the U.S. Food and Drug Administration (FDA), and the rest are chemically based antiviral medications, known as neuraminidase inhibitors, that can block

the viral neuraminidase enzymes against influenza A and B (CDC, 2023). Current medications used for patients with influenza virus infection include inhaled zanamivir, oral oseltamivir, oral baloxavir, or intravenous peramivir (Gao et al., 2024). Zanamivir, oseltamivir, and peramivir are neuraminidase inhibitors, which block the viral neuraminidase enzyme, preventing the release of new virions from infected cells (Moscona, 2005). In contrast, baloxavir marboxil is a cap-dependent endonuclease inhibitor, targeting the PA subunit of the viral RNA polymerase complex, thus inhibiting viral mRNA transcription (Noshi et al., 2018).

Immediate antiviral treatment is recommended for any patients with suspected or confirmed influenza who are hospitalised, have severe complications, and are at a greater risk for influenza complications. These are considered priority groups for antiviral treatment of influenza. For non-higher-risk outpatients, clinicians can consider early antiviral treatment, which can be initiated upon 48 hours of illness, upon judgment (CDC, 2023b). Oseltamivir is recommended for hospitalised patients with confirmed or suspected influenza and can be administered either orally or enterically (Ariano et al., 2010). Oral oseltamivir is also recommended for outpatients with progressive disease or complications such as underlying chronic medical conditions and pneumonia (Kaiser et al., 2003). Inhaled zanamivir, oral oseltamivir, oral baloxavir, or intravenous peramivir are used for outpatients with suspected or confirmed influenza, depending on their age. A randomised study by Ison et.al (2020) baloxavir was more efficient in adults with the Influenza B virus compared to oseltamivir.

Immunocompromised individuals often experience prolonged viral replication and shedding with SARS-CoV-2 infections. This persistent infection can lead to intra-host viral evolution, resulting in mutations within variants and may decrease sensitivity to existing antivirals (Nooruzzaman et al., 2024). Treatments like nirmatrelvir-ritonavir (Paxlovid™), remdesivir (Veklury™), and molnupiravir (Lagevrio™) are effective in reducing viral loads and preventing severe disease in high-risk populations but are not as efficient in immunocompromised patients (Martinez et al., 2023). Prolonged treatment courses in these individuals can result in additional challenges for transmission control, since they may contribute to the emergence of resistant variants.

1.3. Natural products as antiviral treatments

Research into natural components as antivirals has gained momentum, particularly over the last two decades (Zhang *et al.*, 2021). Significant advancements were noted since 2010, with research of the antiviral properties of natural components focusing against Zika viruses and herpes simplex (Fong & Chu, 2022; Sun et al., 2021).

Phytochemicals play an essential role in complementary therapies, as 130 compounds have antiviral potential, and 94 metabolites have demonstrated bioactivity against coronaviruses (Naithani *et al.*, 2008). These compounds can be classified into different natural product groups, including terpenes, flavonoids, and alkaloids. An inhibitory activity against SARS-CoV-2 was shown by canthogelol E, isolated from Angelica keiskei, establishing the most ideal IC_{50} value of 1.2 μM, compared to other phytochemicals, against SARS-CoV papain-like protease PLpro. Other compounds with antiviral potential include hispidulin, glycyrrhizin, saikosaponin D, rutin, quercetin, and hesperetin, with quercetin also displaying activities against influenza A, COVID-19, and SARS-CoV (Chen *et al.*, 2023) (Solnier and Fladerer, 2020).

Certain plant species, such as Origanum, Thymus, and Cannabis, can limit SARS-CoV-2 infectivity by providing biobased formulations. Terpenes, obtained from essential oils produced by medicinal plants, exhibit anti-inflammatory and immunomodulatory properties and are effective against influenza and herpes simplex virus 1 and 2. These properties are observed in Artemisia glabella, Origanum acutidens, Melaleuca ericifolia, Thymus vulgaris, M. armillaris, and M. leucadendron. Molecular modelling studies have shown that several terpenoids are potent inhibitors of SARS-CoV-2 replication. Origanum vulgare and Thymus vulgaris EOs (essential oils) have been recognised for their therapeutic roles, mainly due to their flavonoids and terpenes, and have been shown to be effective against a variety of RNA viruses, including coronaviruses (Tomko et al., 2020).

Some natural products can also prevent and treat influenza due to their diverse chemical

structures and mechanisms of action. Flavonoids and terpenoids have shown strong antiviral activity, with the ability to modulate immune responses and inhibit viral replication. For instance, extracts from Isatis indigotica used in traditional Chinese medicine demonstrate dual antiviral and immunomodulatory effects, by inhibiting viral enzymes and modulating the cytokine storm (Zhang et al., 2020). Specifically, compounds such as indirubin, indigo, isatin, and isovitexin reduce the levels of pro-inflammatory cytokines and chemokines, including CCL5 (RANTES) and IFN-β. IFN-β production is inhibited through the RIG-I signaling pathway, mitigating extreme immune responses that are characteristic of the cytokine storm (Zhang et al., 2020). In addition, the ethanol extract of Caesalpinia decapetala reduced viral load and improved survival in mice that were infected with the following lethal strains of influenza A virus: H1N1, H3N2, H7N8, and the influenza B virus (Zhang et al., 2020), while a sesquiterpenoid from Phellinus ignarius has demonstrated strong inhibition to H5N1 in vitro, at low concentrations (Airong et al., 2014). Many of these compounds act by inhibiting neuraminidase which is an essential enzyme for Influenza replication (Sun & Huang, 2014), or by enhancing host immune responses with antiviral cytokine stimulation, activating immune cells like macrophages and natural killer cells, and regulating signaling pathways that improve the body's ability to recognise and clear the virus (Li et al.,2024).

1.4. Cannabinoids and their antiviral properties

A variety of cannabis-derived compounds have been evaluated for their potential against influenza and other viral infections. Previous research explored their mechanisms, gathering essential information for the knowledge and development of targeted therapies based on these compounds. Table 1.1 provides a detailed overview of several promising compounds, with a summary of each compound's antiviral activity, with the cytotoxic concentration reported on A549 human lung carcinoma cells, its effectiveness against specific viruses, and key references supporting its antiviral properties.

Cannabis constitutes a single diverse species called C. sativa L, with C. ruderalis, C. indica, and C. sativa being considered as varieties (Lowe *et al.*, 2021). The species can be found in different habitats and altitudes, from sea level to the Himalayan foothills (Paw *et al.*, 2020).

There are more than 100 cannabinoids with potential pharmacological properties. The cultivation of Cannabis sativa L. can be dated back to at least 12,000 years, suggesting that it is one of humanity's oldest cultivated crops (Preteroti et al., 2023).

Hemp consists of an understudied source of pharmacologically active compounds, and research on hemp has recently demonstrated antiviral activities, after years of legal restriction. The most common compounds studied in vitro, in silico, and in vivo are cannabidiol (CBD), cannabidiolic acid (CBDA), cannabigerolic acid (CBGA), and Δ9-tetrahydrocannabinol (Δ9-THC), which was first isolated in 1964 by Mechoulam and Gaoni. These compounds have been studied against SARS-CoV-2, γ-herpes viruses, and human immunodeficiency virus (HIV) (Nguyen et al., 2022; Polat et al., 2024; Medveczky et al., 2004; Tomer et al., 2022). The mechanisms of action of these compounds include inhibition of viral proteases, viral cell entry, and stimulation of cellular immune responses. Cannabinoids also possess anti-inflammatory properties, which can mitigate the cytokine storm of SARS-CoV-2 and control the inflammation in people living with HIV (Nguyen et al., 2022; Vallée, 2022; Langat, Chakrawarti and Klatt, 2025; Manuzak et al., 2018). There is a need for appropriately designed clinical trials for the review of the safety and efficacy of CBD, Δ9-THC, and cannabinoid mixtures, as well as to support their antiviral activities (van Breemen and Simchuk, 2023).

Table 1.1 Antiviral activity and cytotoxicity of cannabinoids that act against influenza and other viruses.

The table summarises the mechanism of action of the most effective compounds that act against influenza and other viruses, with their cytotoxicity on A549 cells.

Compound	Antiviral Properties	Cytotoxicity on A549 (μM)	Viruses Tested On	Primary Research References
THC	Dual action against viral proteases and ACE2. Efficacy against various DNA and RNA viruses (Sea et al., 2022).	27.2	SARS-CoV-2, Adenovirus, Influenza, RSV, Herpes Simplex Virus	van Breemen and Simchuk, 2023

CBD	Preliminary research suggests inhibition of SARS-CoV-2. Modulates immune response through CB1 and CB2 receptors (Nguyen et al., 2021).	20	Hepatitis B, Coronaviruses, Influenza A, ZIKV, HCV, ARDS, RSV, Nipah Virus, Rubella, Monkeypox, KSHV, Herpes SARS-CoV-2, Adenovirus, Influenza, RSV, Herpes	Nguyen et al., 2021
CBD-acid (CBDA)	Antiviral activity against SARS-CoV- 2 and HIV. Inhibits viral cell entry, proteases, stimulates immune responses (van Breemen et al., 2022).	37.1	SARS-CoV-2, Influenza, HIV, RSV, ARDS, Rubella, Hepatitis C, Kaposi's Sarcoma, Herpes Simplex	van Breemen et al., 2022
Cannabichromevarin (CBCV)	No verified primary research on antiviral effects. Included here as a candidate for future investigation.	Unknown	Predicted activity: Alphaviruses, Bunyavirales, non-enveloped Echovirus, adenovirus, herpes simplex, Cantagalo virus, Influenza	No primary research available
β- Caryophyllene	Antiviral and immunomodulatory properties. Inhibits viral replication and entry (Hassanin *et al.*, 2020).	28.18	Avian Influenza-A Virus (H5N1), Influenza, SARS-CoV-2, Zika Virus, DENV-2, RSV, HSV, Colitis	Gertsch et al., 2008
Cannaflavin A	No verified primary research on antiviral effects. Included here as a candidate for future investigation.	Unknown	Predicted activity: Influenza A and B, Dengue Virus, Hepatitis Virus, Rabies, Adenovirus, SARS-CoV-2, HPV, Rhinovirus, Herpesvirus	No primary research available

In 2019, there was a notable increase in studies focusing on cannabinoids as antivirals, due to the COVID-19 pandemic. Current treatments for SARS-CoV-2 are limited due to the lack of effective target-based therapeutics. Previous in silico and in vitro experiments demonstrated the potential of treating viral infections of SARS-CoV-2 with cannabinoids (CBDs). Two cannabinoid compounds, Δ-tetrahydrocannabinol (IC50 = 10.25 μM) and cannabidiol (IC50 = 7.91 μM), were observed to have greater antiviral activity against SARS-CoV-2 compared to standard drugs like chloroquine, lopinavir, and remdesivir (IC50 ranges of 8.16–13.15 μM). These molecules exhibit stable conformations within the active binding pocket of the SARS-CoV-2 Mpro through molecular dynamic simulation and density functional theory. Previous research suggests that these compounds could potentially be effective drugs against human coronaviruses when used in combination with other drug molecules (Raj et al., 2021). Both alpha and beta variants of SARS-CoV-2 can be targeted by CBGA and CBDA, which display similar effects. CBD has also been shown to inhibit viral replication during infection, as proven by an in vitro study (Janecki et al., 2022).

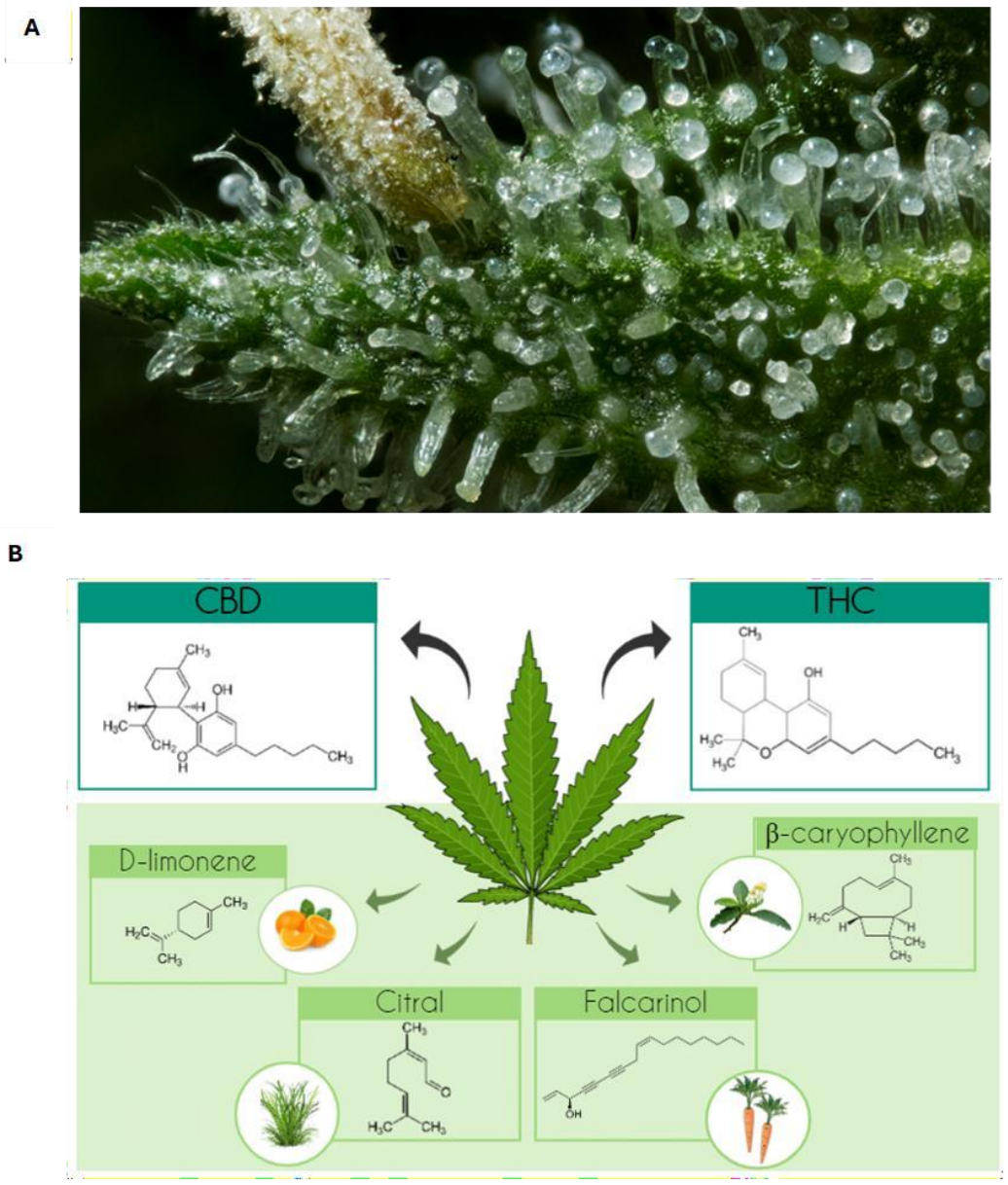

Figure 1.2 Morphological and molecular structures of Cannabis sativa and cannabis-derived compounds.

A) An individual Cannabis (*Cannabis sativa* L.) calyx epidermis covered in stalked glandular trichomes. The secretory disks line on the base of the trichome heads, where the biosynthesis of secondary metabolites takes place. Above the secretory disk cells, there is a clear subcuticular cavity for metabolite storage. The photograph was taken by Gina Coleman and sourced from Weedmaps. **B)** Molecular structures of some of the Cannabis sativa compounds (CBD, THC, D-limonene, β-caryophyllene, citral, and falcarinol). D-limonene, β-caryophyllene, citral, and falcarinol are also synthesised by other plants, such as Cordia verbenacea, lemon, Cymbopogon citratus, and carrot. This figure was adopted from the review by Gonçalves, E.C.D. et al. (2020)

1.4.1. Anti-Inflammatory properties of cannabinoids

The lungs act as the first line of defence against inhaled pathogens. The cells lining the airways constitute epithelial cells and alveolar macrophages. Cannabinoids may have numerous health benefits against pathogens that invade the lung epithelium and may help tame inflammation associated with chronic diseases. Cannabinoids can interact with the endocannabinoid system and can influence the immune response in the lungs; nevertheless, more research is needed to observe the beneficial responses, the health effects, and potential side effects, as these remain poorly understood.

Endocannabinoids can be metabolised into bioactive lipids that regulate inflammation through various mechanisms involving immune modulation, neurogenic inflammation control, and epigenetic alterations (Turcotte et al., 2015). 2-arachidonoyl glycerol (2-AG) and N-arachidonoyl ethanolamine (AEA), interact with cannabinoid receptors and other receptor families like transient receptor potential and peroxisome-proliferator-activation receptors to mediate anti-inflammatory effects in immune cells, such as macrophages, lymphocytes, and monocytes (Patel, Preedy and Martin, 2023). They alter gene expression related to inflammation by activating CB1 and CB2 receptors, leading to downstream signalling that suppresses pro-inflammatory cytokine production. In addition, they modulate transcription factors such as NF-κB, which results in decreased expression of inflammatory genes by promoting apoptosis and inducing T regulatory cells and myeloid-derived suppressor cells, which are immunosuppressive cells, while engaging epigenetic mechanisms that regulate the expression of cannabinoid receptors (Holloman et al., 2021). Macrophage polarisation is also influenced by these compounds, towards an anti-inflammatory phenotype (Creoli et al., 2025).

Exogenous cannabinoids can influence endocannabinoid metabolism and alter their availability and immunomodulatory impact. For instance, CBD is known to inhibit the enzyme fatty acid amide hydrolase (FAAH), which is responsible for anandamide (AEA) degradation. Through this inhibition, the breakdown of AEA levels becomes slower, prolonging the endocannabinoid's ability to activate cannabinoid receptors that are involved in reducing

inflammatory signalling (Janero, Vadivel and Makriyannis, 2009; Pertwee, 2005). Additionally, exogenous cannabinoids may interfere with the conversion of endocannabinoids by cyclooxygenase-2 (COX-2) into pro- or anti-inflammatory lipid derivatives such as prostamides and prostaglandin-glycerol esters. These interactions lead to the conclusion that cannabinoids not only exert direct anti-inflammatory effects but also modulate the metabolic pathways of endogenous signalling molecules that are associated with immune function.

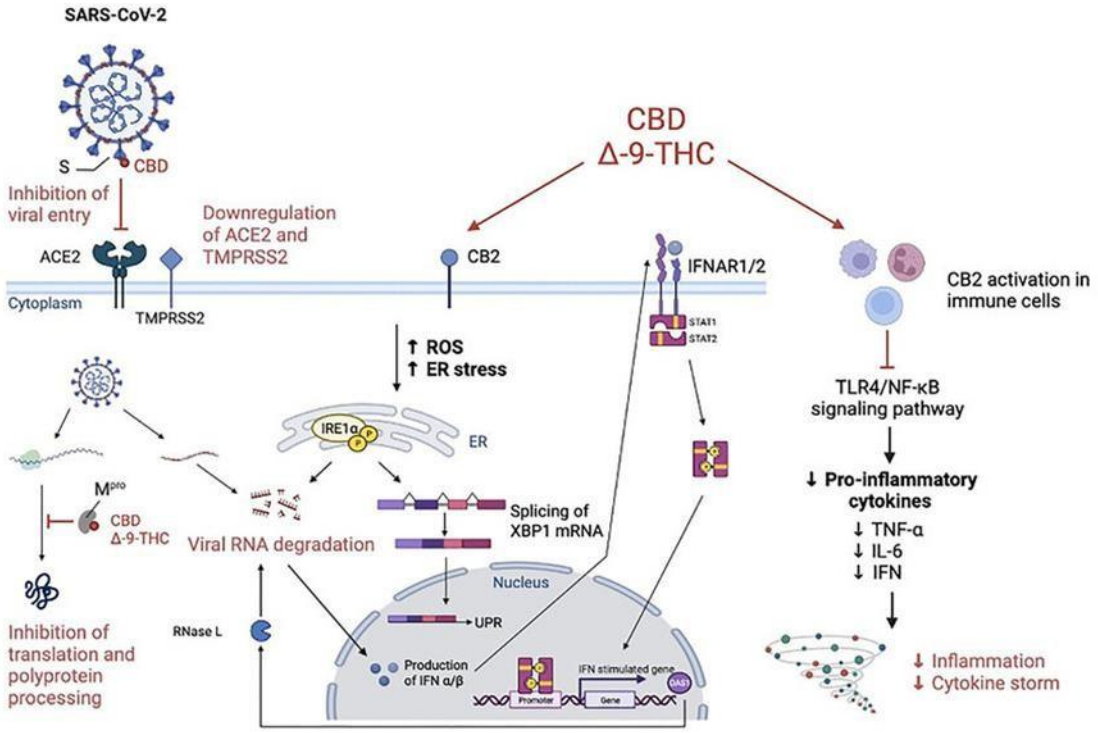

Figure 1.3 CBD and Δ-9-THC mechanism of action.

CBD is an allosteric antagonist of CB1andCB2 agonists. It inhibits viral cell entry, viral proteases, and stimulates innate immune responses against viruses like SARS-CoV-2, HIV, and γ-herpes viruses. In the case of SARS-CoV-2, CBD downregulates ACE2 and TMPRSS2 expression, necessary for viral entry into cells, via AKT pathway-mediated epigenetic control. THC mimics two endogenous cannabinoids that naturally occur in the body, anandamide (AEA) and 2-arachidonoylglycerol (2-AG), by acting as a partial agonist at CB1 and CB2. Image from Sea et al., 2022.

1.4.2. Interaction between cannabinoids and the endocannabinoid system

The endocannabinoid system (ECS) is a complex signalling system in humans and mammals

that regulates mood, memory, appetite, pain sensation, and immune response. It includes endocannabinoids, cannabinoid receptors (CB1 and CB2), and enzymes responsible for synthesizing and breaking down endocannabinoids.

Endogenous cannabinoids, such as anandamide (AEA) and 2-arachidonoylglycerol (2-AG), bind to the two key receptors of the ECS: cannabinoid type 1 (CB1) and cannabinoid type 2 (CB2), with enzymes like fatty acid amide hydrolase (FAAH) and monoacylglycerol lipase (MAGL) involved in their synthesis and degradation.

Phytocannabinoids can also bind to the ECS, by binding to these receptors. Through this binding, the phytocannabinoids interact with the ECS by mimicking the actions of endocannabinoids and are therefore able to regulate neurotransmitter release inflammation and immune responses (Pertwee, 2008). The most abundant psychoactive phytocannabinoid found in Cannabis is thought to be Δ9-tetrahydrocannabinol (Δ9-THC), and CBD is the most abundant non-psychoactive compound (Mechoulam et al., 2007). CBD is known to increase anandamide levels and acts on additional receptors, broadening the ECS's therapeutic potential (Leweke et al., 2012).

The CB1 receptor can be found in peripheral organs like muscles, the liver, pancreas, and adipose tissue, where it regulates food intake and energy expenditure. CB2 receptors, on the other hand, are expressed in immune cells such as lymphocytes, natural killer (NK) cells, CD8, monocytes, and neutrophils. These receptors present anti-inflammatory effects by reducing proinflammatory cytokine release, increasing anti-inflammatory cytokine production, regulating lymphocyte T activation, and inhibiting macrophage migration. Furthermore, cannabinoids also affect numerous other receptors, including G protein-coupled receptor 55 (GRP55), peroxisome proliferator-activated receptors (PPARs), and transient receptor potential vanilloid channels (TRPV) (Janecki et al., 2022).

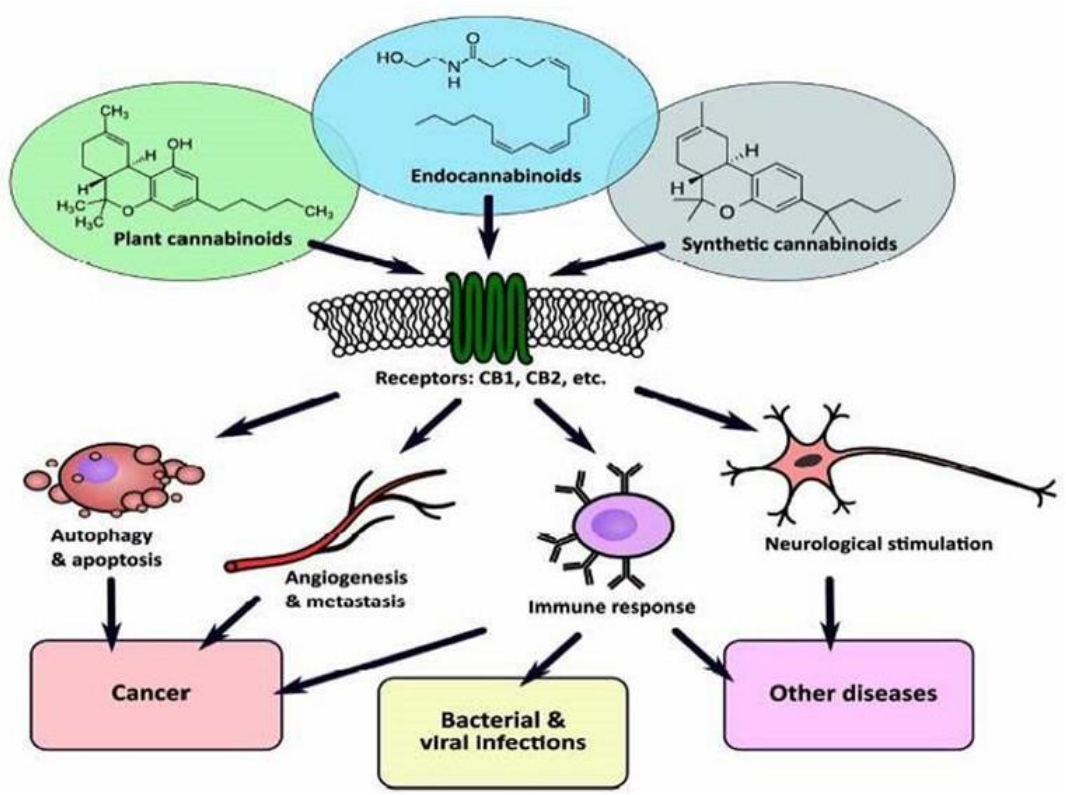

Figure 1.4 The regulatory role of the endocannabinoid system in immune modulation and disease management.

The endocannabinoid system (ECS) has a role in regulating internal processes and immune components such as antibodies, white blood cells, and the lymphatic system. This can result in benefits such as the control of viral infections, neurological disorders, cancer, and mood-related issues. Endocannabinoids, phytocannabinoids, and synthetic cannabinoids interact with the receptors CB1 and CB2 to mediate various physiological effects (Sledzinski et al., 2021).

1.4.3. Terpenoids and phenolic compounds

Terpenoids and phenolics are secondary organic compounds. Plants produce a great variety of primary compounds, including carbohydrates, lipids, nucleotides, and peptides, as part of their daily components and metabolites. Secondary compounds, which include terpenoids, are derived from primary components but are not central to metabolism. They can help protect against diseases and environmental stress, or be considered metabolic byproducts. Terpenoids are secondary metabolites consisting of five-carbon isoprene units and are found in many spices and fragrances (Padalia *et al.*, 2013).

In a study by Diniz et al. (2021), formulations were created (F1TC and F2TC) with different combinations of a variety of terpenes and CBD and demonstrated virucide effectiveness by reducing the infectivity of SARS-CoV-2. Specifically, the formulations reduced the infectivity of SARS-CoV-2 by 17% for CaCo-2 cells (Diniz *et al.*, 2021). In addition, the F2TC formulation also reduced infectivity by 24% for HaCat and 99% for A549 cells, while the F1TC formulation reduced infectivity by 43% for Hek293T, 37% for HaCaT, and 99% for Caco-2 cells. This approach of combining CBD with specific terpene groups against the virus in various cell lines could lead to new therapeutic strategies in the future.

CBD and terpenes are already used in both Western and folk medicine as treatments for autoimmune (Konstantin Kotschenreuther et al., 2020) and psychiatric disorders and cancer (Lior Chatow et al., 2024). Terpenes are known to modulate pro-inflammatory cytokines, a property that can alleviate symptoms of inflammatory diseases (Del Prado-Audelo et al., 2021). Monoterpenes specifically have a potential in respiratory therapies and can enhance the efficacy of treatments when used in combination, while reducing the side effects induced by those agents (Justia Patents, 2018; Wiktoria Potocka et al., 2023). Cannaflavin A, on the other hand, which is a flavonoid, may inhibit viral replication by interacting with key viral proteins, such as the papain-like protease (PLpro) of SARS-CoV-2 (Holmes et al., 2024).

1.5. Current cannabinoid regulatory products and research gaps

1.5.1. Current regulatory products of cannabis and cannabinoids

There are barriers when studying Cannabis and cannabinoids, surrounding cannabis production, use, and legalisation. Over the last couple of decades in America, 35 states and the District of Columbia have legalised cannabis for medical use (National Institute on Drug Abuse (NIDA), 2021). This complex legal landscape affects research and the application of cannabinoids.

A purified form of hemp-derived Cannabidiol (Epidiolex) has been approved by the Food and Drug Administration (FDA). Epidiolex is used as treatment for patients as young as one year of age, with Dravet or Lennox-Gastaut syndromes and more specifically for seizures (Nagarkatti et al., 2020).

1.5.2. Cannabis-based medication research gaps

Previous studies have investigated therapies to treat ARDS and the cytokine storm; however, their application can be clinically challenging. There are a few methods to treat the hyperimmune state caused by COVID. These include steroids, intravenous immunoglobulin, selective cytokine blockade, and JAK inhibition. However, none of these options are highly effective due to the involvement of inflammatory cytokines in the cytokine storm. There is also a risk of increasing the primary and secondary infections in the patients as they cannot overtly suppress the immune response. The researchers in the field of medical cannabis therapeutics have utilised methods including different routes of therapeutic administration, for instance oral oils, solutions, and capsules, such as Dronabinol and Nabilone. Furthermore, there are also oromucosal sprays such as Nabiximols and Sativex. It is known that the effects of medical cannabis differ by route of administration in terms of desired benefits, side effects, or onset actions, and there is a research gap in comparing the medicinal benefits across administration routes. To date, there is a broad range of cannabis-based products available around the world with a prescription. However, there is a lack of knowledge concerning their side effects and their efficacy. These products usually contain a combination of cannabinoids and hundreds of other compounds with unknown side effects. Many studies have recently investigated cannabinoid-based drugs as promising in preventing viral infections, as well as improving many SARS-CoV-2 infections. However, there are limitations in these results, as there are limited studies that have been conducted in assessing these therapies in young adults (Nagarkatti et al., 2020; Scott et al., 2023).

1.6. Aims

There are over 400 secondary metabolites found in the Cannabis plant, with 120 of these being cannabinoids. While the plant is used for both medical and recreational purposes, there are significant gaps in understanding the bioactivity and medical functions of these compounds. Previous research has explored the plant's antimicrobial, anticancer, and antioxidant properties. Additionally, as previously mentioned, there is evidence of its antiviral effects, such as blocking viral entry and replication for specific viruses. Some cannabinoids also exhibit anti-inflammatory properties, which could be beneficial for managing cytokine storms, but may also adversely affect the immune response.

The purpose of this project is to shortlist two cannabinoid compounds for antiviral drug development targeting influenza A virus (H1N1) strain A/PR/8/34 with the potential to act against a broader spectrum of various viruses. Cannabinoids like cannabidiolic acid (CBDA) and its derivative, CBDA methyl ester, have shown remarkable antiviral activity against different SARS-CoV-2 variants (Tamburello et al., 2023). Additionally, cannabinoids exhibit stable conformations that interact with key viral enzymes, inhibiting viral replication and entry (Mahmud et al., 2021). Furthermore, cannabinoids such as cannabidiol (CBD) and Δ9-THC downregulate ACE2 receptors, reducing viral infection, and act as protease inhibitors, blocking viral replication (Sea et al., 2022).

This investigation focused on the effects of cannabinoids on influenza A virus (H1N1) strain A/PR/8/34. The motivation of this project is based on the fact that while there is a growing body of evidence regarding the antiviral properties of cannabinoids against various viruses, including HIV, SARS-CoV-2, and HCV, studies addressing their efficacy against influenza A H1N1 are scarce. Given the historical impact of H1N1 outbreaks and the ongoing medical relevance of influenza viruses in public health, novel broad-spectrum antivirals are in need and of high priority. By concentrating on influenza A H1N1 PR8, this study aims to fill an important gap in the existing literature and contribute to the development of alternative antiviral strategies, and to provide exploitable information that could facilitate future clinical trials.

Specific Aims:

• To evaluate the cytotoxicity of 11 cannabis-derived compounds selected from an initial pool of over 400 secondary metabolites based on availability, safety, and reported antiviral potential.

• To test the antiviral activity of these 11 compounds against the influenza A (H1N1) virus in vitro.

• To shortlist two compounds with the strongest antiviral effects with potential for further testing against additional respiratory viruses and for future molecular investigation of further mechanisms.

Chapter 2 Materials and Methods

2.1. Materials and reagents

MDCK cells, A549 cells strain hACE2 TMPRSS2 were purchased from American Type Culture Collection (ATCC, Manassas, VA, USA), and influenza A virus (H1N1) strain A/PR/8/34 was kindly provided by Prof Munir Iqbal, The Pirbright Institute, UK. All media ingredients and the PrestoBlue™ cell viability kit were purchased from Thermo Fisher Scientific. The CytoTox-Glo™ cell viability assay kit was purchased from Promega Corporation. Cannabidiolol (CBD,15 mg/mL in ethanol, ≥95.0% purity, CAS # 13956-29-1), cannabigerol (CBG,1 mg/mL in methanol, ≥98% purity, CAS #25654-31-3), cannabichromene (CBC,1 mg/mL in methanol, ≥98% purity, CAS #20675-51-8), cannabivarin (CBV, 1 mg/mL in methanol, ≥98% purity, CAS #33745-21-0), β-caryophyllene (2000 µg/mL in methanol, ≥98% purity, CAS #87-44-5), cannabichromevarin (CBCV, 1 mg/mL in methanol, ≥90% purity, CAS #41408-19-9), cannabinol (CBN, 1 mg/mL in methanol, ≥98% purity, CAS #521-35-7), cannaflavin A (1 mg/mL in ethanol, ≥90% purity, CAS #76735-57-4) and Cannabidiolic acid (CBDA, 100mg/mL in ethanol, ≥95% purity, CAS #1244-58-2)were purchased from Sigma – Aldrich Company Ltd (Dorset, United Kingdom). Monoterpene and Sesquiterpene blends were prepared by Eybna Technologies (Pure™ line). These are food-grade compounds produced under ISO 9001, GMP, and kosher standards.

The monoterpene blend consisted of α-terpineol (1.0), α-pinene (0.66), β-pinene (0.33), and linalool (0.25). The sesquiterpene blend consisted of β-caryophyllene (1.0), caryophyllene oxide (0.33), α-humulene (0.33), and α-bisabolol (0.25). In both formulations, the values in parentheses represent the relative proportions of each compound, in relation to the quantity of the lead terpene set as the reference value of 1.0, and all compounds were combined accordingly to maintain these ratios during preparation. For the experiments, all stock compound aliquots were thawed and diluted directly into serum-free cell culture medium to achieve the desired working concentrations. Trypsin (10X), Versene, and Fetal Bovine Serum (FBS) were purchased from Thermo Fisher Scientific. The SPF chicken embryonated eggs for the inoculation of influenza A were purchased from Henry Stewart & Co Ltd., Fakenham, UK. The viral plaque assay overlay medium (2X) materials, including Minimum Essential Medium (10X), Gentamicin, Glutamax, HEPES, and Bovine Serum Albumin (BSA), were also provided by

Thermo Fisher Scientific. The low EEO Agarose powder used for plaque assay gel fixation was purchased from NBS Biologicals (Cambridge, UK). Corning™ 96-Well Clear Bottom White Polystyrene Microplates and Corning® 96 Well Clear Polystyrene Microplates were used for the cytotoxicity and cell viability assays, sourced from Thermo Fisher Scientific.

2.2. Cell culture

All media were supplemented with penicillin-streptomycin, glutamine (100X) (GIBCO), and 5% (v/v) fetal bovine serum (FBS) (Thermo Fisher). Both cell lines were seeded in T75 filter-top cell culture flasks with 10 mL of media. Cells were incubated at 37°C, 5% CO2, and passaged or subcultured routinely to maintain a confluency of 70–90%. Once confluent, both cell lines were passaged in a T75 flask twice per week by splitting them at a ratio of 1:2 for A549 cells and 1:15–1:20 for MDCK cells.

To detach cells from the T75 flasks, the culture medium was removed, and the cell monolayer was washed with PBS. For A549 cells, 5 mL of 0.25% trypsin was added for approximately 3 minutes. For MDCK cells, 10 mL of 1X trypsin-EDTA was added and incubated at 37°C for approximately 40 minutes. Once cells had detached, 10 mL of culture medium was added. The cells were carefully resuspended by pipetting up and down to create a single-cell suspension.

For subculture, 3 mL (for MDCK) and 5 mL (for A549) of this suspension were transferred into new T75 flasks containing 12 mL of fresh culture medium. This 1:4 and 1:2 dilution resulted in an 80–90% confluent flask the following day. For cell viability assays, a confluent T75 flask of A549 cells was split into a 96-well plate. For plaque assays, a confluent T75 flask of MDCK cells was split into four 6-well plates the day before to ensure cell confluency for infection.

The 1X Trypsin-EDTA solution was prepared with 220 mL of PBS, 5 mL of 10X Trypsin-EDTA with a concentration of 0.025%, and 25 mL of Versene. The final volume of the solution was 250 mL. The 10X Trypsin-EDTA stock used in this preparation has a concentration of 0.25% Trypsin, resulting in a final concentration of 0.025% Trypsin in the prepared solution.

2.3. Cell viability assessment following cannabinoid compound pre-treatment

A549 cells were plated in 96-well transparent and white microplates, in Dulbecco's Modified Eagle Medium (DMEM) supplemented with 5 % fetal bovine serum, with 1×10^4 cells/well. The plates were then incubated at 37 °C in 5 % CO2. After 24 h, once the cells reached 80% confluency, the medium was discarded, and 0.1mL of DMEM without fetal bovine serum was added to the cells, supplemented with the treatments of four compounds per plate in duplicates (cannabinoids, terpenes, or flavonoid). The compounds were diluted in a 1:10 ratio in culture medium with 0% FBS and were used to treat the cells at 11 different concentrations, with the aim of at least 45 µM as a maximum administered concentration. The cells were incubated for 24 h at 37 °C in 5 % CO2. As a negative control, 0.1mL of DMEM without fetal bovine serum was used. After 24 h of compound pre-treatment, 10 µL of PrestoBlue™ was added to the transparent microplates and 50 µL of AAF-Glo™ substrate from the CytoTox-Glo™ kit was added to the white plates. The cells were incubated for 10 minutes at 37 °C in 5% CO2. Both the cell viability and cell death were recorded with Tecan Infinite M200 plate reader model (Tecan Group Ltd., Männedorf, Switzerland), and the results were plotted and represented by a concentration-response, sigmoid curve, and the half maximal inhibitory concentration (IC_{50}) of cytotoxic compounds was determined.

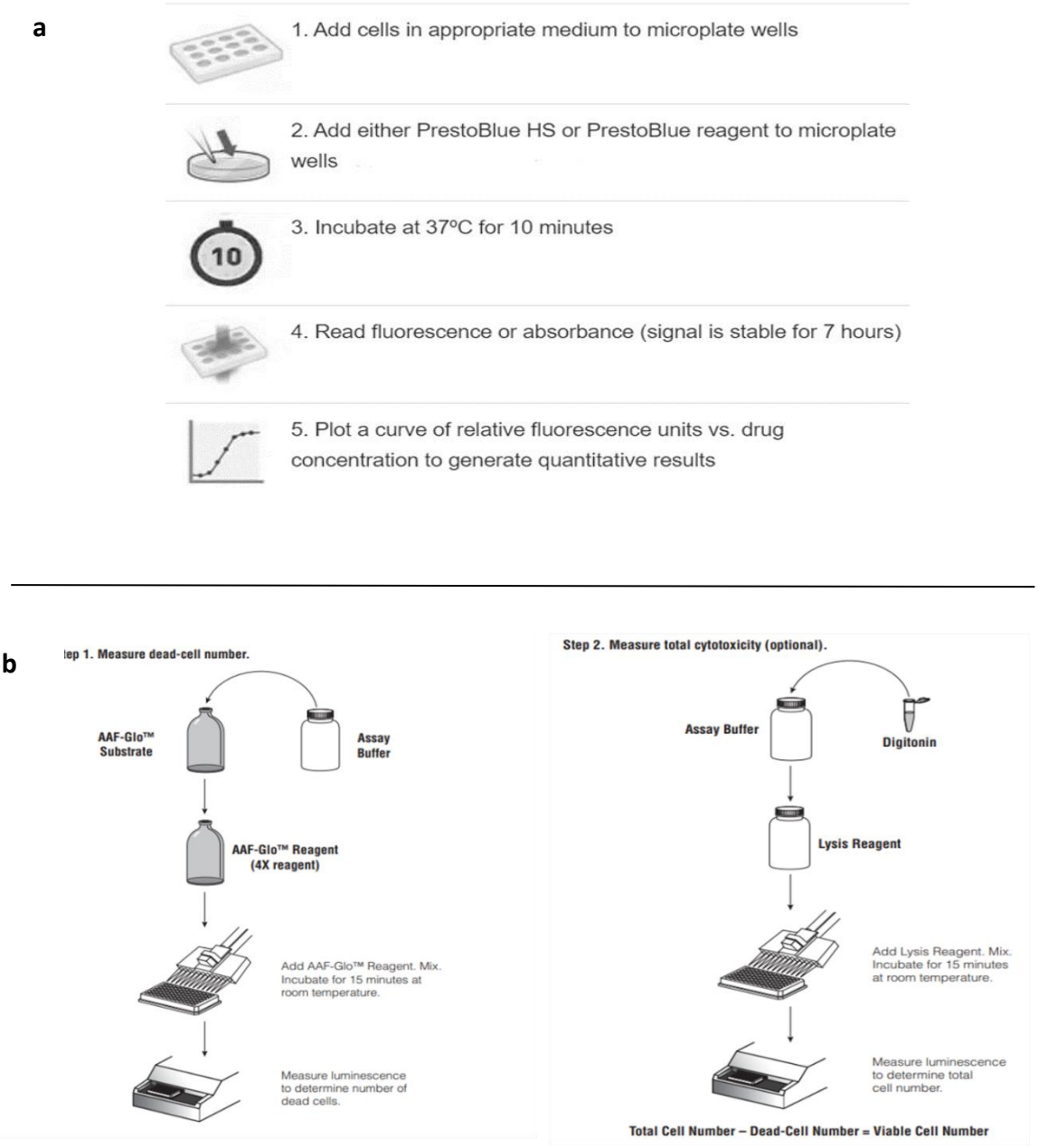

Figure 2.1 Cell viability and cytotoxicity assays with PrestoBlue™ and CytoTox-Glo™ methods

a) PrestoBlue™ Assay Protocol. Cells were seeded into a 96-well microplate and treated with 10 µL PrestoBlue™ reagent. The fluorescence represented the cell metabolic activity as an indicator of cell viability and was measured after a 10-minute incubation at 37°C, fluorescence was measured. Workflow adapted from the PrestoBlue™ assay protocol (Thermo Fisher Scientific). **b) Schematic diagram of the CytoTox-Glo™ Cytotoxic Assay.** The number of dead-cells was measured with luminescence in Step 1, with the addition of 50 µL AAF-Glo™ reagent. In Step 2, the total cell number was measured after adding 50µL lysis reagent. Both reagents required an incubation time of 15 minutes. The viable cell count was calculated by subtracting the dead-cell number from the total cell number. Schematic diagram adapted from the CytoTox-Glo™ Cytotoxicity Assay protocol (Promega).

PrestoBlue™ assay results represented the cell viability per compound concentration, and the level of cell death for the CytoTox-Glo™ assay results indicated both the cell viability compared to the cytotoxicity per concentration of each treatment at 24 h post-infection. The compounds were first titrated through serial dilutions to create a range of 11 different concentrations for the assessment of concentration-dependent effects on cell viability and cytotoxicity. Additionally, the cytotoxicity of ethanol and methanol was also evaluated, as these solvents were used as vehicles for dissolving compound stocks. This was done by diluting 100% ethanol and 100% methanol, using the same serial titration method, with concentration ranges matching those of the cannabinoid compound treatments.

2.3.1. PrestoBlue™ cell viability assay

PrestoBlue™ is a resazurin reduction to resorufin-based viability assay, as well as both a colorimetric and a fluorometric assay for the nonradioactive quantification of the metabolic activity of the cells, which is an indirect measure of cell viability and proliferation. The assay was performed as previously described [2.3]. At the end of each incubation period, when the seeded cells reached 80% confluency, the media were discarded from all wells, and 100 µL of fresh culture medium was added to the cells together with 100 µL of each compound dilution. The control wells included DMEM only as a non-toxic solution. The metabolic activity was measured at a wavelength of 590 nm (after the excitation of fluorophores at 560 nm).

2.3.2. CytoTox-Glo™ cytotoxicity assay

CytoTox-Glo™ cytotoxicity assay is an ATP detection-based cytotoxicity and cell death measurement assay. For the assay preparation, A549 cells were seeded in a 96-well round-bottom white plate, as previously described [2.3] in their culture medium, at 1×10^4 cells/well. The cells were allowed to attach for 24 h at 37 °C, in 5 % CO2. Then, the culture medium was discarded and 0.1 mL of assay media without FBS was added to the cells, supplemented with treatments (cannabinoids, flavonoids, or terpenes). The cells were incubated for 24 h at 37 °C, in 5 % CO2. The compounds were diluted sequentially 11 times using a 1:2 dilution factor and then added to the cells starting with the 10^{-1} dilution. The control wells included DMEM only as a non-toxic solution. The compounds were tested in duplicates, and the plates were incubated for 24 h. After 24 h, the medium was discarded, the

AAF-Glo™ and lysis substrate were thawed, and 50 µL of the AAF-Glo™ substrate was added to the plates first. The plates were incubated for 10 minutes at 37 °C in 5 % CO2 and were immediately taken to the plate reader for cell death reading. The cells were then lysed with 50 µL of the lysis reagent per well. Following an additional 10-minute incubation, the readings were performed again, this time capturing the total cell death. The cytotoxic concentration of each compound (µM) was calculated using a standard curve.

2.3.3. Half-maximal inhibitory concentration (IC_{50}) analysis

The IC_{50} is the concentration of the test compound that produces a response halfway between the 0% (no drug effect) and 100% (maximal response). This value is often determined by fitting the data to a sigmoidal dose-response curve, with a three- or four-parameter logistic. The curve's parameters include the lower and upper plateaus (min and max responses), the slope, and the concentration at which 50% of the maximal response occurs, which corresponds to the IC_{50} value (Sebaugh, 2011). The IC_{50} values were calculated using the AAT Bioquest IC_{50} calculator (AAT Bioquest, 2025), which fits concentration-response data to a nonlinear regression model. Since cell viability dropped steeply and approached zero at higher compound concentrations with no clear lower plateau, the three-parameter model was selected for compounds that showed cytotoxic effects, and a near-zero minimum response was assumed.

$$Y = \frac{Max}{1 + \left(\frac{X}{IC_{50}}\right)^{\text{Hill coefficient}}}$$

Figure 2.2 IC50 calculation using a three-parameter logistic model.

Y represented the response, and *Max* corresponded to the maximum response value. The concentration at which the response was reduced by 50% compared to the maximum response was equivalent to IC_{50}.

2.4. Virus propagation in chicken embryonated eggs

Virus propagation into eggs comprised the preparation of 10-fold serial dilutions of Influenza A virus H1N1 strain PR8 and inoculation of the material in 5 eggs per dilution via the chorioallantoic sac (CAS) route. The process involved marking the eggs and serialising them with ethanol. The eggs were then carefully punched for inoculation. The eggs were then sealed, incubated for 4 days, and candled daily, and dead embryos were discarded. The allantoic fluid is then collected, and after virus purification and chilling, the allantoic fluid was harvested for haemagglutination testing.

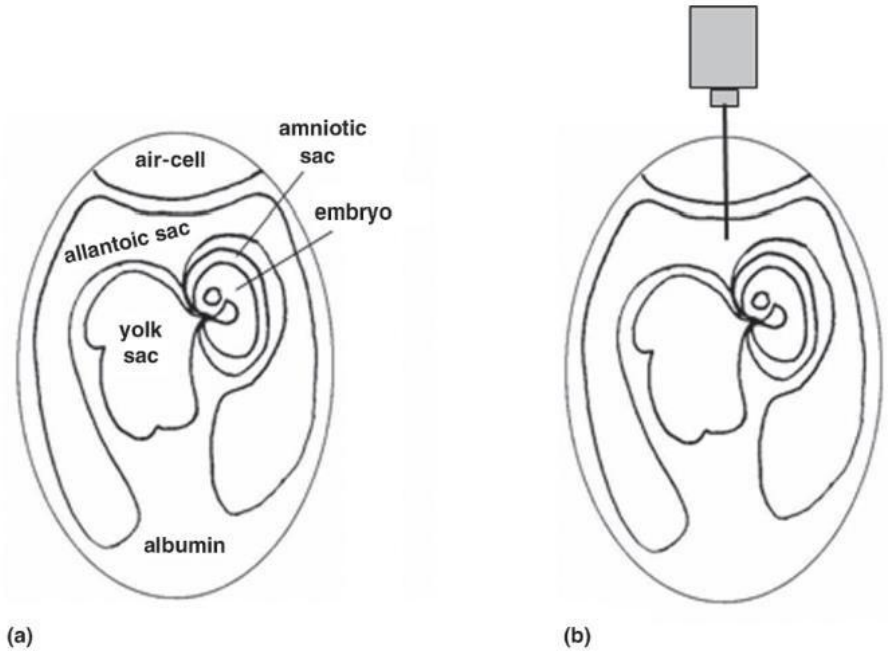

Figure 2.3 Inoculation sites in avian embryos.

Approximate structure of the avian embryo **(a)** relative to the inoculation sites for **(b)** the chorioallantoic sac (CAS), which is a membrane that contains fluid and surrounds the embryo. This route is commonly used for propagating influenza viruses due to the large surface area for virus replication and facilitated accessibility.

2.5. Virus titration and quantification

The isolation, propagation, purification, and titration of influenza viruses played an important role in the viral quantification experiments carried out, as well as the antiviral experiments. These steps were essential for the preparation of high-quality stocks, a critical component of the experiments. Successful isolation of viruses depended on the quality of the original

material and on the use of appropriate methods for the amplification of the primary isolates. The influenza virus H1N1 was propagated in chicken embryonated eggs, while following traditional propagation techniques specific to the virus.

Many methods can be used in assessing the antiviral properties of compounds by the quantification of infectious particles, such as tissue culture infectious dose 50 (TCID50), quantitative PCR (QPCR), haemagglutination assay, and plaque assays. However, the plaque assay was chosen in this case due to its sensitivity and accuracy. The results of this assay relied on the ability of influenza viruses to induce cytopathic effect (CPE) in certain cell types, which led to the formation of plaques in a cell monolayer overlaid with agar or suspensions of cellulose-derived polymers. These semisolid overlays allowed amplification of the virus to be restricted locally, resulting in well-defined holes in the cell monolayer. Each plaque represented an infection event initiated by a single virus particle, referred to as plaque forming unit (PFU).

The virus handling protocols were followed in compliance with biosafety containment guidelines suitable for CL3 facilities. Advanced precautions were taken for influenza A virus H1N1, which is classified as a BSL-2 pathogen. The manipulation of samples containing infectious influenza viruses was performed in a class II biosafety cabinet (BSC) in appropriate BSL-3 containment conditions. UV sterilisation took place between processing different samples for cross-contamination prevention. All experiments adhered to the appropriate governmental and institutional regulations.

2.6. Haemagglutination assay

The surface of influenza virus particles consists of the hemagglutinin protein particles that bind to the N-acetylneuraminic acid-containing proteins in mammalian and avian erythrocytes. When a high concentration of influenza virus is present, an agglutinin reaction takes place, and the erythrocytes form a diffuse lattice upon linkage. The amnioallantoic fluid (AAF) harvested from embryonating chicken eggs was screened via the haemagglutination assay to identify the presence of influenza virus following virus isolation passage. A single haemagglutinin unit (HAU) was equal to 5-6 logs of virus.

To perform the assay, a V-bottom microplate was tilted at 45 degrees and labelled for identification. 50µL of PBS was added to each well. 50 µL of antigen was added to the first well of each row, resulting in a 1:2 dilution. To dilute the antigen, the contents of the first row were mixed, then 50 µL from the first to the second well, repeating this two-fold dilution process across the wells. The positive control wells included 50µL of antigen and 50µL of PBS, while the negative control wells included 50 µL of negative allantoic fluid (without virus presence) and 50 µL of PBS. Then, 50 µL of 1% erythrocyte suspension was added to each well and, the plate was gently tapped to mix the contents. An adhesive plate sealer was applied, and the erythrocytes were allowed to settle for 30 minutes. The assay methodology was based on the protocol outlined by Spackman (2008).

2.7. Virus propagation in cell cultures

MDCK cells are optimal for the propagation of avian and mammalian influenza viruses, due to the presence of both α2,3- and α2,6-linked sialic acids on their cell surface proteins, as well as their lack of sensitivity towards trypsin-containing medium (Szretter *et al.*, 2006). Most vaccine candidates and isolates are efficiently amplified in cultures of Madin-Darby Canine Kidney (MDCK) epithelial cells (Hamamoto *et al.*, 2013). These cells were first described in 1966 and originally derived from the kidney of an adult female cocker spaniel (Gaush *et al.*, 1966). Replication of IAV and Influenza B virus strains is supported by MDCK cells; thus, a plaque assay system was adopted to quantify influenza virus with the support of these cells. Moreover, since the presence of trypsin in the culture medium enhances IAV and IBV growth on MDCK, a sensitive detection of influenza viruses from human specimens can be achieved. The way trypsin facilitates influenza infectiousness is by cleaving the viral surface glycoprotein precursor HA0 into the HA1 and HA2 subunits (Ueda *et al.*, 2008). Through this cleavage, the virus's genetic material is released into the infected cell (Matlin *et al.*, 1981).

2.8. Viral plaque assay

Confluent MDCK cells were seeded in a 6-well tissue culture plate (one plate per virus preparation to titrate). Influenza A virus (H1N1) strain A/PR/8/34 virus stock was diluted via a

10-fold dilution, and 500 µL of the virus was added to each well, for each dilution. Post the 2-hour infection of MDCK cells during the plaque assay process, the plates were washed with PBS and ana aliquots of 50 mL agar overlay medium (3 mL per well) was prepared, containing 25 mL of 2X minimum essential medium (MEM), 25 mL of 1.6% (w/v) low EEO agarose solution and 10 µL of L-1-Tosylamide-2-phenylethyl chloromethyl ketone (TPCK)-treated trypsin from bovine pancreas. The agarose solution was boiled in the microwave and kept at room temperature before the aliquot preparation.

For the preparation of 500mL of 2X MEM, 100 mL of 10X MEM was diluted with 10 mL Pen-Strep, 10 mL of 200 mM L-glutamine, 20mL of 7.5% sodium bicarbonate, 10 mL of 1M HEPES, and 6 mL of 35% endotoxin-free bovine serum albumin (BSA). Finally, 350 mL of ddH2O was added and the solution was filtered through a 0.2 µm membrane filter and stored at 4 °C.

After 4 days of incubation at 37°C, 5% CO_2, the cells were fixed with 3.7% formaldehyde solution in PBS (1 mL per well). The cells were then placed on a plate shaker to ensure uniform mixing. After 1 hour, the gels were carefully removed with a small spatula, followed by 0.5% crystal violet staining (2 mL per well) and stored at room temperature for 25 minutes. The stain was carefully removed by washing for plaque visualisation.

The clear zones represented the plaques that formed in a monolayer upon cell infection and lysis. Each plaque was equivalent to a localised area where a single virus particle initially infected a host cell, leading to subsequent cycles of infection and lysis. The plaques were counted to determine the viral titre of the sample in PFU/mL.

2.9. Antiviral assays

The main project objective was to assess the antiviral activity for each of the compounds with the production of viral stocks after pre-treatment exposure, with supernatants collected from infected biological samples (A549 cells) that were pretreated for 24 hours. The concentrations chosen per compound for the antiviral assay depended upon their safety and low cytotoxicity production, based on the results of cytotoxicity testing, aiming for at least 80% cell viability.

As performed in the previous protocol [2.8], the supernatant containing the virus was amplified in cultures of Madin-Darby Canine Kidney (MDCK) epithelial cells, in dilutions 10^{-1} to 10^{-6}. The supernatant stocks were stored in the -80°C freezer for later use in viral plaque assays.

Cell counting was performed during splitting of stock A549 cells. After trypsinisation, the cells were resuspended in 1 mL of media, from which 10 µL of the cell suspension was collected in an Eppendorf tube and counted with the use of the Neubauer improved haemocytometer. The cell counts were obtained by averaging measurements taken across four grids, each measuring 1 mm by 1 mm by 0.1 mm, with a volume of 0.1µL. The cells were seeded on 24-well plates, seeding 7.5×10^4 cells per well, and allowed to settle for a day.

The following day, the cells reached 90% confluency and were treated with the compounds. The plates were incubated at 35 °C, 5% CO2 for 24 hours. The cells were then washed with PBS and infected with 15 µL of the virus and 135 µL of DMEM without serum, aiming for an MOI of 1, for 2 hours. Then, the cells were washed again, and 500 µL for DMEM with 5% FBS was added to the wells. The supernatant was collected after 24 hours, and the antiviral activity of the compounds was assessed via a plaque assay. During the same day, 6-well plates of MDCK cells (3.0×10^5 cells per well) were prepared 48 hours before the titration, with each plate for a single replicate of a sample.

The plaque assay was then based on the influenza virus's ability to form well-defined plaques on agar overlaid cell monolayers after the pre-treatment. Each compound affected the CPE induced by the virus differently, leading to a different number of plaques, based on infected cell death. The addition of agar overlay restricted the infections to cells surrounding the original infected cells, forming subsequent plaques.

In order to reduce experimental bias during treatment preparation and viral burden quantification, a self-blinding procedure was implemented. Compound treatment and negative control samples were assigned to anonymised sample labels with random

alphanumeric codes, which were recorded in a separate notebook. All treatment samples were prepared in a separate room from where the plaque assays were conducted and then transferred into the containment area for the compound treatments and plaque assays, during which only the anonymised treatment labels were used.

Plaque counts and size measurements were performed using ImageJ software (Schneider, Rasband and Eliceiri, 2012), and the ViralPlaque macro (Cacciabue, Anabella Currá and Gismondi, 2019) in a blinded manner with image files being allocated separate alphanumeric codes, which were managed digitally with spreadsheet-based ID mapping. The average plaque size for each compound was calculated and compared to the averages of the positive control group. The codes were only accessed after the completion of all viral burden quantification.

Chapter 3 Compound cytotoxicity in A549 cells

3.1. Introduction

In order to evaluate the safety profile of selected cannabis-derived compounds in human lung epithelial cells, the following experiment investigated their cytotoxic and viability effects in vitro. A549 cells were treated with increasing concentrations of cannabinoids, flavonoids, terpenes, and vehicle solvents to assess potential toxicity on membrane integrity and metabolic activity. For this assessment, the PrestoBlue™ cell viability assay and the CytoTox-Glo™ assay were used.

The CytoTox-Glo™ cytotoxicity assay measures the activity of a specific dead-cell protease that is normally contained within viable cells but is released into the culture medium when the plasma membrane integrity is lost, indicating cell death. This protease activity cleaves a proprietary luminogenic peptide substrate linked to a luciferin derivative. Once the peptide substrate is cleaved by the dead cell protease, luciferin is released and converted to a luminescent signal by an included luciferase enzyme. This signal is directly proportional to the number of dead cells, allowing for an accurate and reproducible assessment of cell death (Promega, 2019).

Conversely, the PrestoBlue™ cell viability assay is based on the metabolic activity of viable cells. It uses a resazurin-based compound that is reduced to a highly fluorescent resorufin product by cellular enzymes in metabolically active cells. The fluorescence intensity correlates with the number of metabolically active cells. This correlation enables a sensitive and reproducible assessment of overall cell viability and proliferation (Thermo Fisher Scientific, 2024).

These assays complemented each other and provided a more comprehensive evaluation of both cell death through membrane integrity loss (CytoTox-Glo™) and cell metabolic function (PrestoBlue™).

The results of the cell viability assays are presented in Figures 31 – 3.7, with cell viability and cell death (%) plotted against the concentration in µM for the Cytotox-Glo assay. For the PrestoBlue assay, cell viability (%) was plotted against the concentration in µM. Eleven different concentrations were tested, as well as a negative control. The graphs were grouped based on cannabinoid structure similarities for cannabinoids (Figures 3.1 – 3.4), flavonoids and terpenes (Figures 3.5 – 3.6), and solvents (Figure 3.7).

3.2. Evaluation of cannabinoid cytotoxicity in A549 cells

In order to test whether cannabinoids affect the viability of A549 lung epithelial cells, a series of cytotoxicity assays was conducted. A549 cells were treated with 11 different increasing concentrations of selected cannabinoid compounds to determine their potential cytotoxic effects. Following treatment, cell viability and cytotoxicity were assessed using the PrestoBlue™ cell viability assay and the CytoTox-Glo™ cytotoxicity assay to quantify any reductions in viability correlated with increasing compound concentrations. This set of experiments aimed to evaluate the safety profile of the cannabinoids in a lung epithelial model, which is relevant for understanding and assessing the toxicity and therapeutic potential of compounds with possible respiratory exposure.

The data from the three groups of cannabinoid samples, except for β-caryophyllene, showed a significant concentration-dependent decrease in cell viability at a concentration of 50 µM

(Figure 3.1). For CBG, a 31.68 % decrease was observed for concentrations of 11.85 µM (Figure 3.1), for CBD a 89% decrease for 6.25 µM (Figure 3.2), for CBDA an 88% decrease for 697.25 µM (Figure 3.2), for CBN a 37% decrease for 11.63 µM (Figure 3.3), for CBC a 63% decrease for 23.55µM (Figure 3.3), for CBV a 48% decrease for 26.55 µM (Figure 3.4), and a 25% decrease for CBCV for 3.27µM (Figure 3.4). The PrestoBlue TM cell viability assay trends agreed with those of the CytoTox-Glo™ assay, and the concentrations that showed ≤ 20% decrease in cell viability were considered safe to use for the antiviral assays. The cytotoxicity values were inversely proportional to the % cell viability. CBD displayed the highest decrease in cell viability, at concentrations of ≥ 6.25 µM (Figure 3.2).

For all seven cannabinoid compounds that showed cytotoxicity, the decrease in cell viability was not directly correlated to the increase in concentration; rather, it showed a steep drop in viability at a given concentration, respective to each compound. This proposed the presence of threshold concentrations where the cannabinoids started to interact with cellular components or pathways, such as membrane integrity disruption or induction of mitochondrial dysfunction. Presumably, this led to decreased ATP production and increased reactive oxygen species (ROS), resulting in the activation of apoptotic pathways.

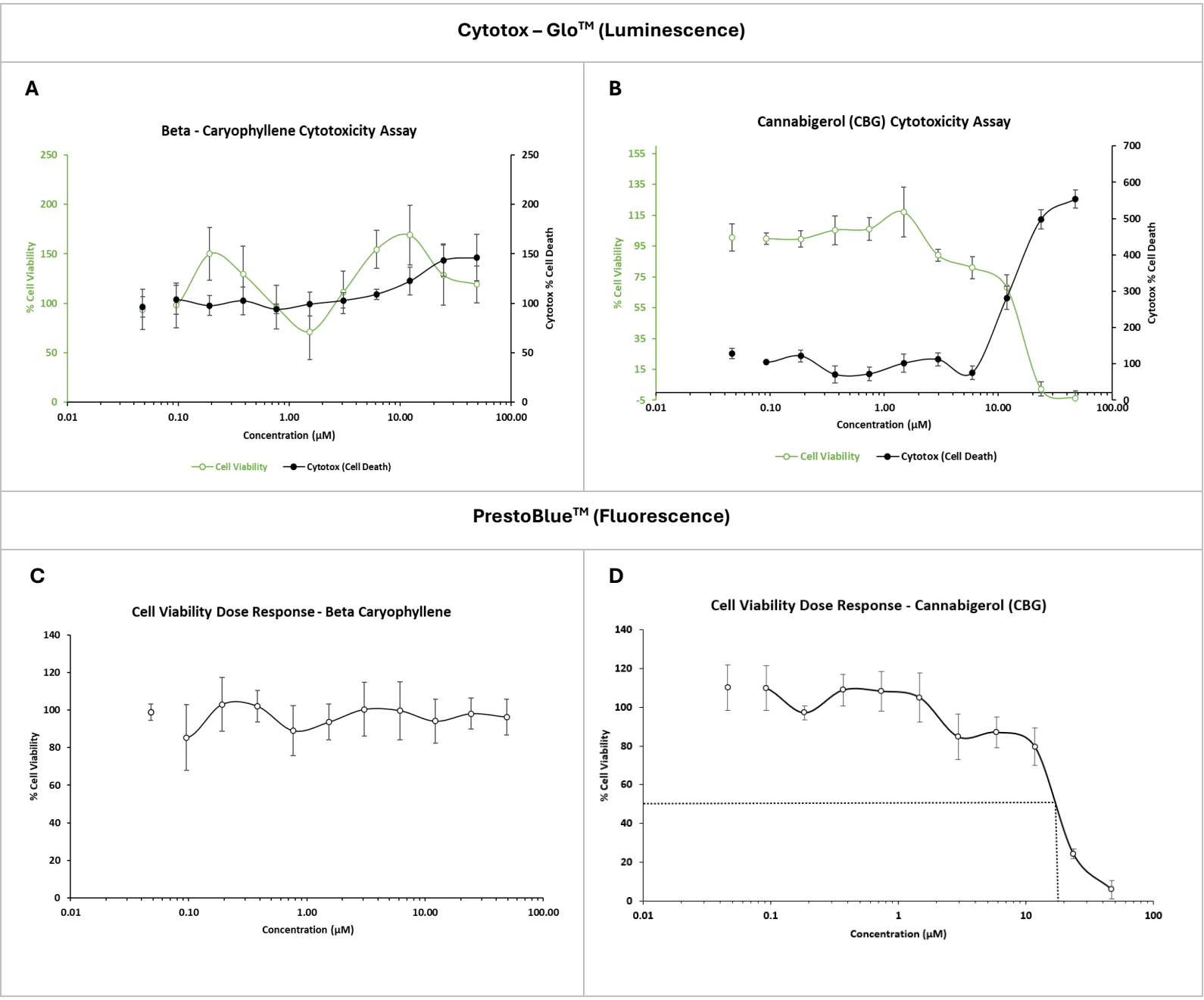

Figure 3.1 Cell viability and cytotoxicity of A549 cells treated with β-Caryophyllene or CBG.

Percentages of cell viability in A549 treated for 24 h with separate treatments of the cannabinoids β-caryophyllene and CBG, and negative controls. The Cytotox- Glo™ assay was used to evaluate cytotoxicity with the AAF-Glo™ substrate and cell viability with the PrestoBlue™ assay. The concentration is expressed in molarity and is dependent on the concentration of synthetic cannabinoid in the plant material, aiming for a maximum of ~50 µM. The graphs at the top represent the mean percentage cytotoxicity (cell death) ± standard error of the mean (SEM) and the percentage cell viability ± standard error of the mean (SEM) (n=6). The bottom graphs show the percentage cell viability ± standard error of the mean (SEM) of the same compound based on the PrestoBlue™ assay (n=6). A three-parameter logistic regression analysis was used to evaluate the IC_{50} value, which represented the concentration of the compound at which 50% of its maximal inhibitory effect was observed.

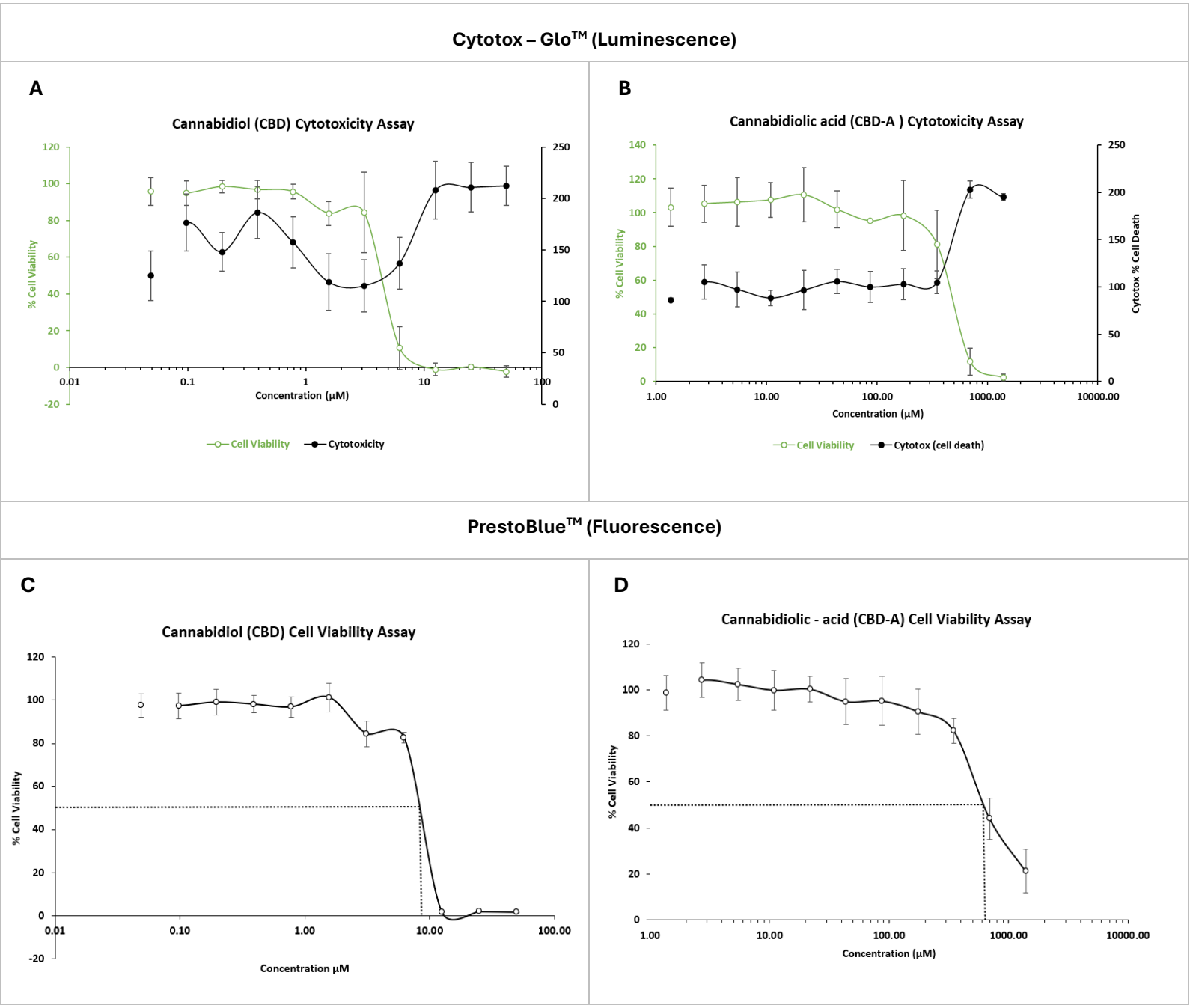

Figure 3.2 Cell viability and cytotoxicity of A549 cells treated with cannabidiol (CBD), or cannabidiolic – acid (CBDA)..

Percentages of cell viability in A549 treated for 24 h with separate treatments of the cannabinoids CBD and CBDA, and negative controls. The Cytotox- Glo™ assay was used to evaluate cytotoxicity with the AAF-Glo™ substrate and cell viability with the PrestoBlue™ assay. The concentration is expressed in molarity and is dependent on the concentration of synthetic cannabinoid in the plant material, aiming for a maximum of 50 µM for CBD and ~ 1300 Mm for CBDA. The graphs at the top represent the mean percentage cytotoxicity (cell death) ± standard error of the mean (SEM) and the percentage cell viability ± standard error of the mean (SEM) (n=6). The bottom graphs show the percentage cell viability ± standard error of the mean (SEM) of the same compound based on the PrestoBlue™ assay (n=6). A three-parameter logistic regression analysis was used to evaluate the IC_{50} value, which represented the concentration of the compound at which 50% of its maximal inhibitory effect was observed.

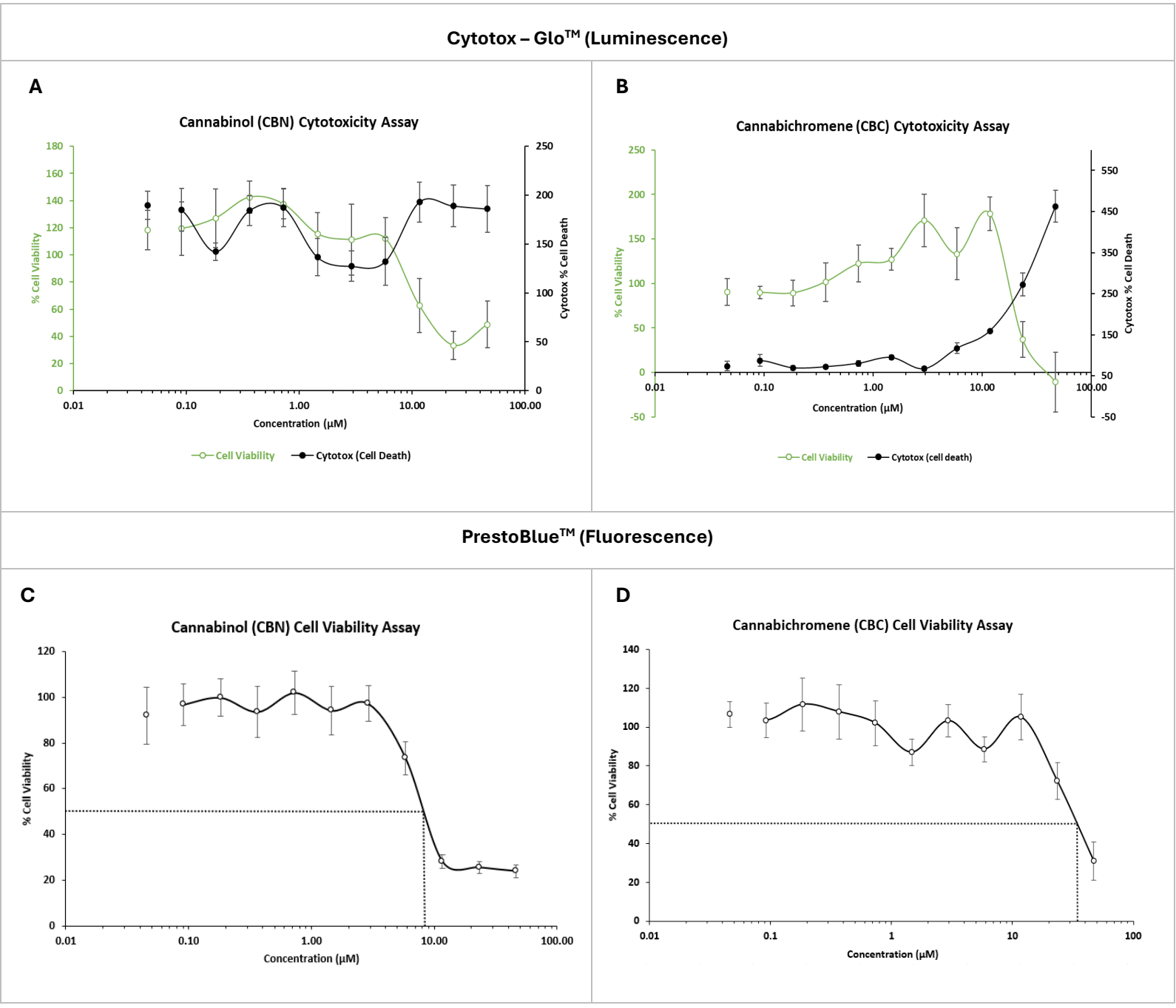

Figure 3.3 Cell viability and cytotoxicity of A549 cells treated with cannabinol (CBN) or cannabichromene (CBC).

Percentages of cell viability in A549 treated for 24 h with separate treatments of the cannabinoids CBN, CBC, and negative controls. The Cytotox- Glo™ assay was used to evaluate cytotoxicity with the AAF-Glo™ substrate and cell viability with the PrestoBlue™ assay. The concentration is expressed in molarity and is dependent on the concentration of synthetic cannabinoid in the plant material, aiming for a maximum of ~50 µM. The graphs at the top represent the mean percentage cytotoxicity (cell death) ± standard error of the mean (SEM) and the percentage cell viability ± standard error of the mean (SEM) (n=6). The bottom graphs show the percentage cell viability ± standard error of the mean (SEM) of the same compound based on the PrestoBlue™ assay (n=6). A three-parameter logistic regression analysis was used to evaluate the IC_{50} value, which represented the concentration of the compound at which 50% of its maximal inhibitory effect was observed.

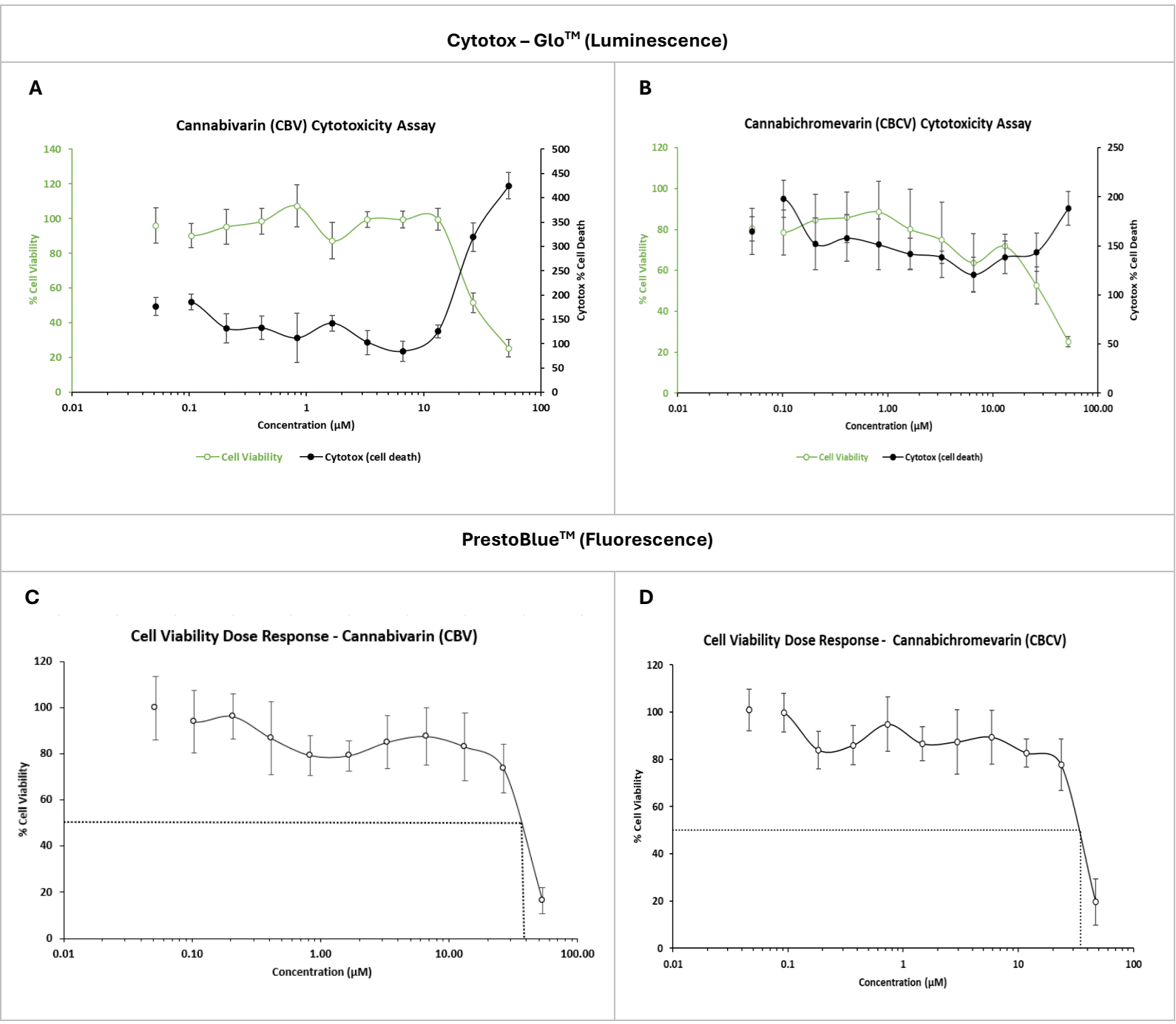

Figure 3.4 Cell viability and cytotoxicity of A549 cells treated with cannabivarin (CBV) or cannabichromevarin (CBCV).

Percentages of cell viability in A549 treated for 24 h with separate treatments of the cannabinoids CBN, CBC, and negative controls. The Cytotox- Glo™ assay was used to evaluate cytotoxicity with the AAF-Glo™ substrate and cell viability with the PrestoBlue™ assay. The concentration is expressed in molarity and is dependent on the concentration of synthetic cannabinoid in the plant material, aiming for a maximum of ~50 µM. The graphs at the top represent the mean percentage cytotoxicity (cell death) ± standard error of the mean (SEM) and the percentage cell viability ± standard error of the mean (SEM) (n=6). The bottom graphs show the percentage cell viability ± standard error of the mean (SEM) of the same compound based on the PrestoBlue™ assay (n=6). A three-parameter logistic regression analysis was used to evaluate the IC50 value, which represented the concentration of the compound at which 50% of its maximal inhibitory effect was observed.

3.3. Evaluation of flavonoid and terpene cytotoxicity in A549 cells

In order to test whether the flavonoid and terpenes affect the viability of A549 lung epithelial cells, a series of cytotoxicity assays was conducted. A549 cells were treated with 11 different increasing concentrations of selected flavonoid or terpene compounds to determine their potential cytotoxic effects. Following treatment, cell viability and cytotoxicity were assessed using the PrestoBlue™ cell viability assay and the CytoTox-Glo™ cytotoxicity assay to quantify any reductions in viability that were correlated with increasing compound concentrations. This experiment aimed to evaluate the safety profile of the cannabinoids in a lung epithelial model, which is relevant for understanding and assessing the toxicity and therapeutic potential of compounds with possible respiratory exposure.

When focusing on the flavonoid cannaflavin A, the cell viability decreased by 29% for a concentration of 46 µM (Figure 3.5). Monoterpenes and sesquiterpenes showed no cytotoxicity for the maximum concentration tested, which was 425 mg/mL for both (Figure 3.6). The PrestoBlue cell viability results were in similar ranges to the CytoTox-Glo™ results. The cytotoxicity results were inversely proportional to the cell viability results.

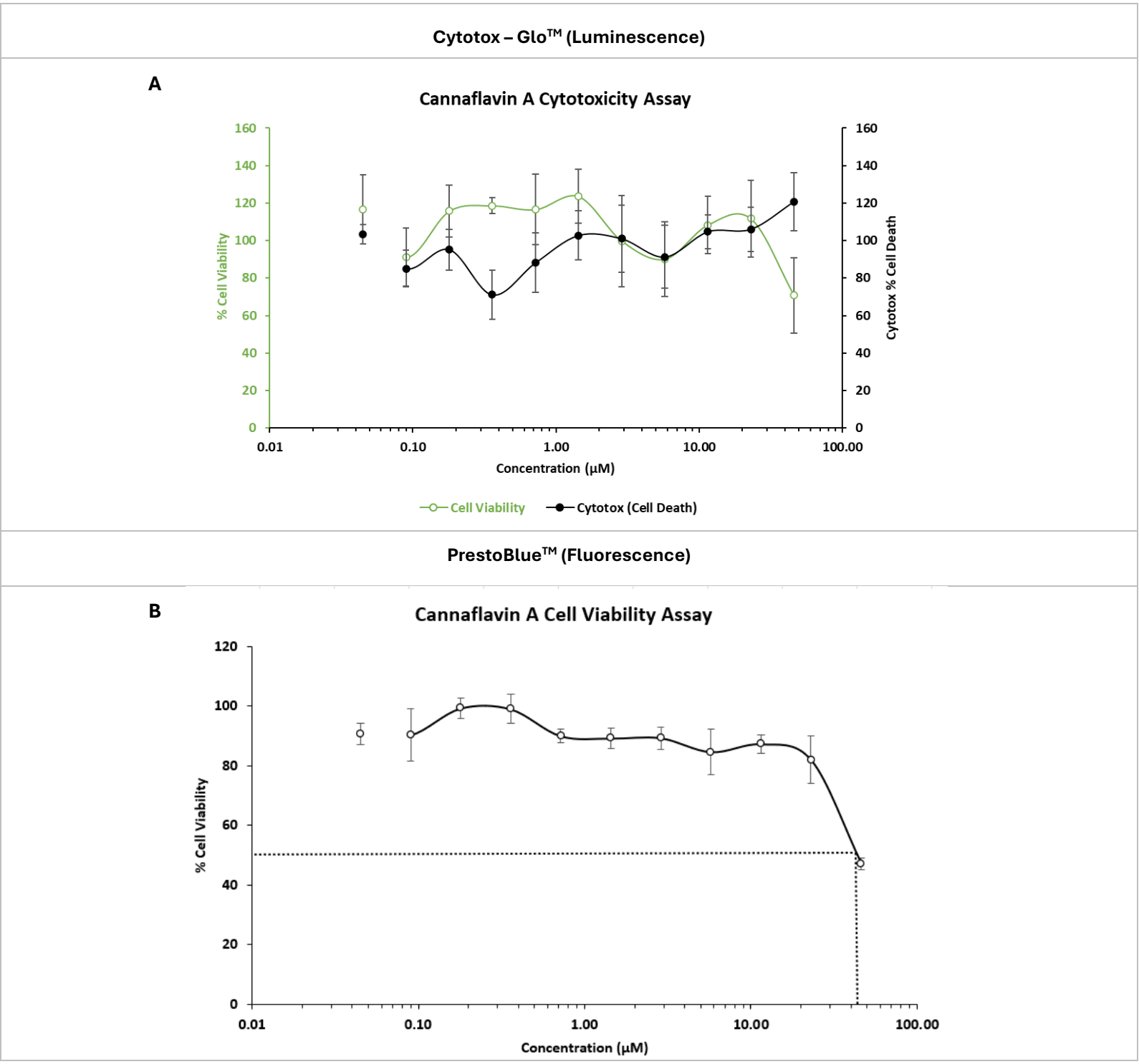

Figure 3.5 Cell viability and cytotoxicity of A549 cells treated with cannaflavin A.

Percentages of cell viability in A549 cells treated with cannaflavin A (flavonoid) with negative controls for 24 h. The concentration is expressed in molarity and is dependent on the concentration of synthetic cannabinoid in the plant material, aiming for a maximum of ~50 µM. The Cytotox-Glo™ assay was used to evaluate cytotoxicity with the AAF-Glo™ substrate and cell viability with the PrestoBlue™ assay. The graphs at the top represent the mean percentage cytotoxicity (cell death) ± standard error of the mean (SEM), as well as the percentage cell viability ± standard error of the mean (SEM) (n=6). The bottom graphs show the percentage cell viability ± standard error of the mean (SEM) of the same compound based on the PrestoBlue™ assay (n=6). A three-parameter logistic regression analysis was used to evaluate the IC_{50} value for cannaflavin A, which represented the concentration of the compound at which 50% of its maximal inhibitory effect was observed.

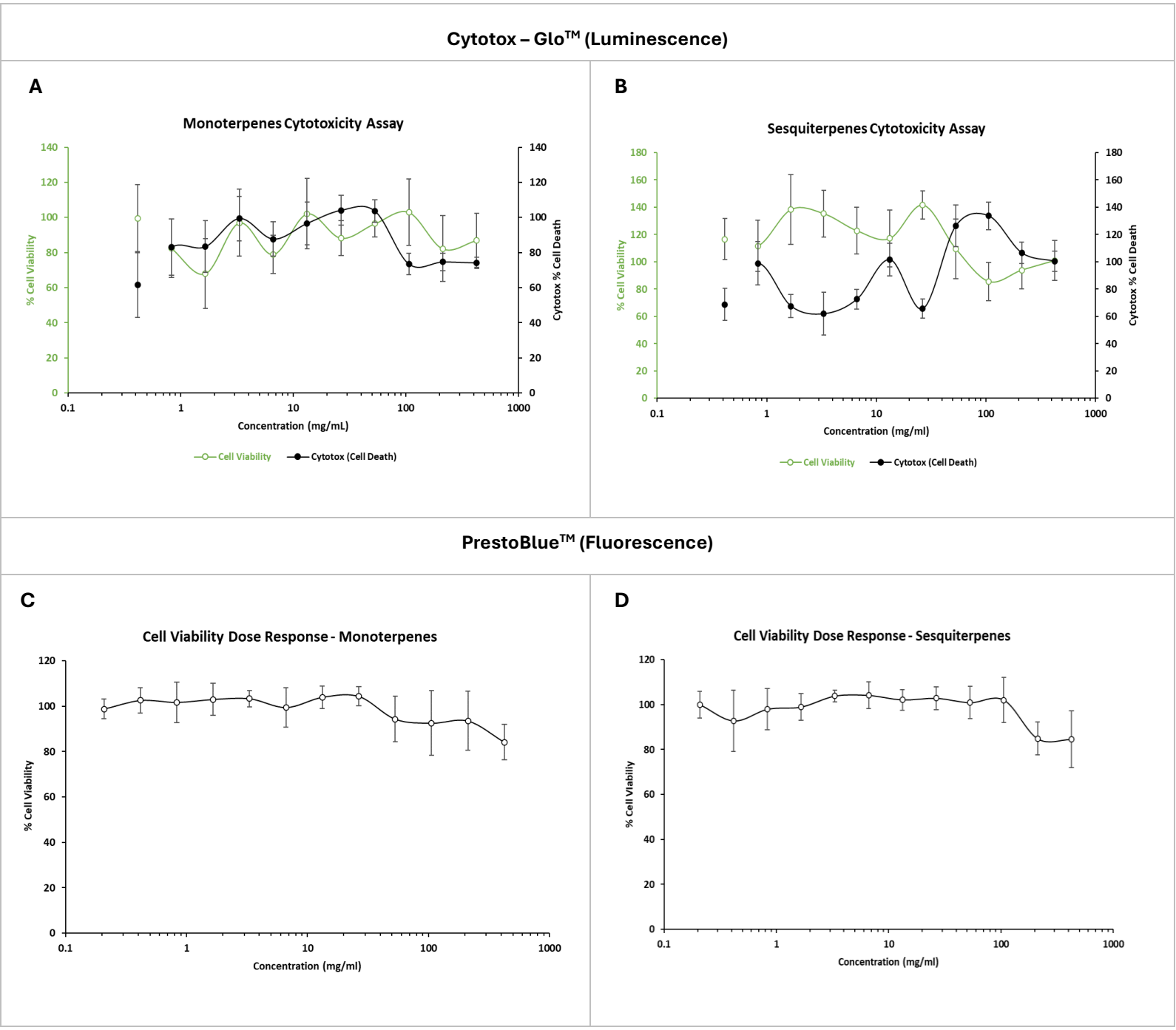

Figure 3.6 Cell viability and cytotoxicity of A549 cells treated with monoterpenes or sesquiterpenes.

Percentages of cell viability in A549 cells treated with either monoterpenes or sesquiterpenes, with negative controls for 24 h. The Cytotox-Glo™ assay was used to evaluate cytotoxicity with the AAF-Glo™ substrate and cell viability with the PrestoBlue™ assay. The concentration is expressed in mass concentration and is dependent on the concentration of synthetic terpenoids in the plant material, aiming for a maximum of 450 mg/mL. The graphs at the top represent the mean percentage cytotoxicity (cell death) ± standard error of the mean (SEM), as well as the percentage cell viability ± standard error of the mean (SEM) (n=6). The bottom graphs show the percentage cell viability ± standard error of the mean (SEM) of the same compound based on the PrestoBlue™ assay (n=6). A three-parameter logistic regression analysis was used to evaluate the IC50 value for cannaflavin A, which represented the concentration of the compound at which 50% of its maximal inhibitory effect was observed.

3.4. Evaluation of ethanol and methanol cytotoxicity in A549 cells

In order to test whether ethanol and methanol solvents affect the viability of A549 lung epithelial cells, a series of cytotoxicity assays was conducted. A549 cells were treated with 11 different increasing concentrations of the solvents chosen to match the main compound assays to determine their potential cytotoxic effects. Following treatment, cell viability and cytotoxicity were assessed using the PrestoBlue™ cell viability assay and the CytoTox-Glo™ cytotoxicity assay to quantify any reductions in viability correlated with increasing compound concentrations. This experiment aimed to evaluate the safety profile of the cannabinoids in a lung epithelial model, which is relevant for understanding and assessing the toxicity and therapeutic potential of compounds with possible respiratory exposure.

Cell proliferation occurred for all solvent concentrations (Figure 3.7). For ethanol, the most cytotoxic concentrations were 25 µM and 50 µM, with a 27% decrease in cell viability for 25 µM (Figure 3.7). Methanol showed no increased cytotoxicity for these concentrations (Figure 3.7).

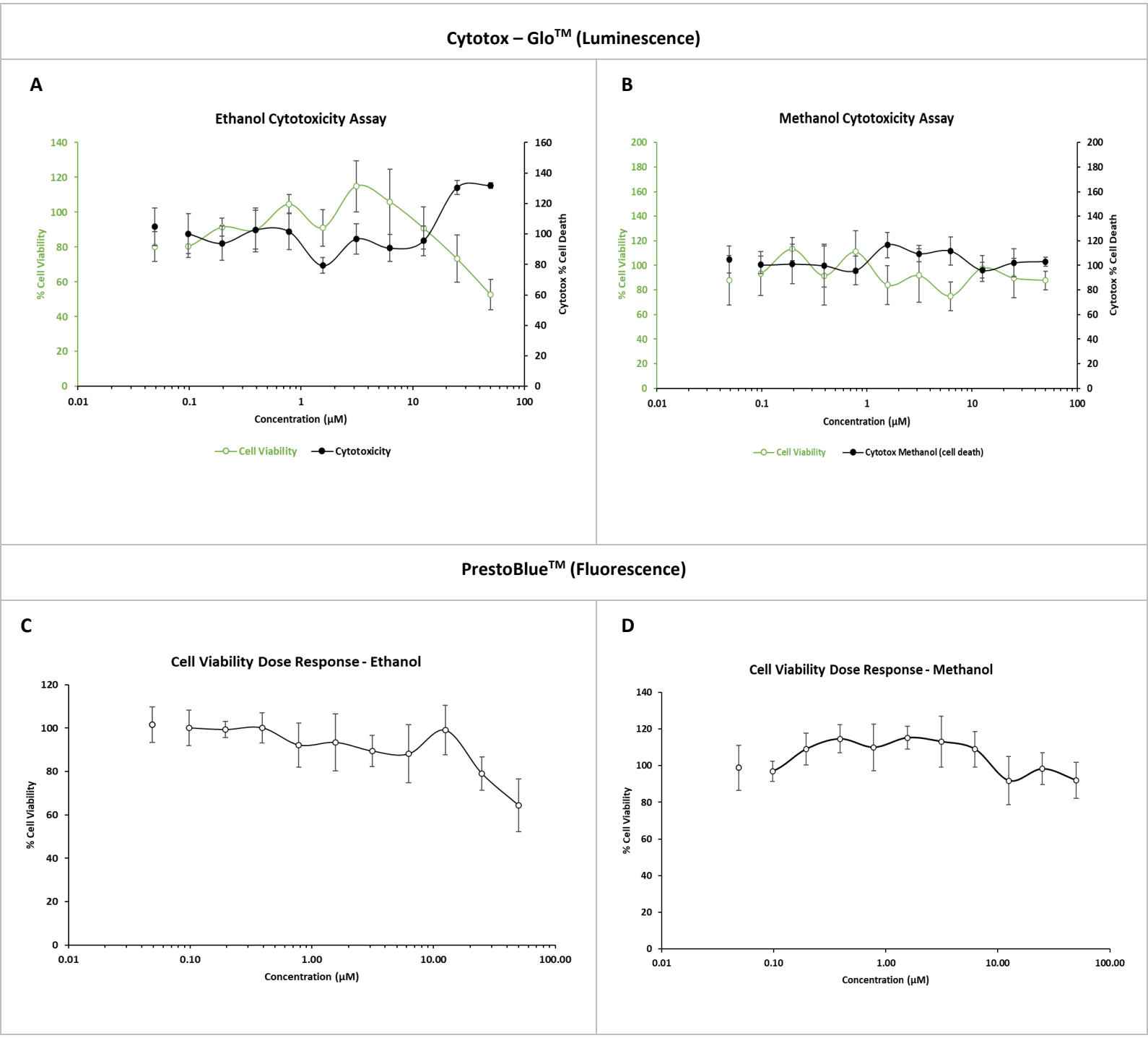

Figure 3.7 Cell viability and cytotoxicity of A549 cells treated with the vehicles: ethanol or methanol.

Concentration-effect curves for ethanol and methanol solvents after a 24 h treatment. The maximum concentration of the solvents tested was 50 µM. The Cytotox-Glo™ assay was used to evaluate cytotoxicity with the AAF-Glo™ substrate and cell viability with the PrestoBlue™ assay. The graphs at the top represent the mean percentage cytotoxicity (cell death) ± standard error of the mean (SEM), as well as the percentage cell viability ± standard error of the mean (SEM) (n=6). The bottom graphs show the percentage cell viability ± standard error of the mean (SEM) of the same compound based on the PrestoBlue™ assay (n=6).

3.5. IC_{50} values and 80% cell viability compound concentrations

Table 3.2 Assessment of IC50 concentrations in µM

The IC_{50}concentrations were determined using a sigmoidal (three-parameter) logistic model. The compound concentrations that corresponded to 80% cell viability were considered safe for subsequent antiviral assays.

Compound Name	**IC_{50} Concentration (µM or mg/mL)**	**Concentration for ≥ 80% Viability (µM or mg/mL)**
B-Caryophyllene	-	49.00 µM
CBG	16.38 µM	5.93 µM
CBD	7.79 µM	3.13 µM
CBDA	665.25 µM	348.63 µM
CBN	10.07 µM	5.83 µM
CBC	34.19 µM	11.78 µM
CBV	37.62 µM	13.27 µM
CBCV	34.83 µM	11.78 µM
Cannaflavin A	47.25 µM	23.00 µM
Monoterpenes	-	425 mg/mL
Sesquiterpenes	-	425 mg/mL

The viability of A549 cells exposed to approximately 0.05 to 50 µM, in 2-fold dilutions per cannabinoid for 24 h was assessed by Cytotox – Glo™ and PrestoBlue™ assays (Figures 3.1-3.5). The results indicated that cytotoxicity was increased with increased exposure concentration of cannabinoids. Exposure to CBN caused a pronounced effect on cell viability for the concentrations of ≥11,63, CBC and CBV at ≥23.55 µM, CBDA at 697.23 µM, CBCV at ≥3.27 µM, CBD at ≥6,25 µM and CBG at ≥11.85 µM. At the dosage of 50 µM of all

cannabinoids, A549 cells showed a 51.3% (CBN), 74.8% (CBCV and CBV), 97.7% (CBDA), and 100% (CBC, CBD, and CBG), cell viability loss at 24 h.

3.6. Chapter discussion

This study is the first to report the cytotoxicity of cannabinol (CBN), cannabichromevarin (CBCV), cannabivarin (CBV), and cannaflavin A on A549 cells. Previous studies have evaluated the cytotoxicity of the rest of the compounds. The IC_{50} values observed for the cannabinoids CBD (7.79 µM) and CBG (16.38 µM) are consistent with previously reported data on epithelial and cancer cell models. ChoiPark et al. (2008) investigated the effects of CBD on A549 lung cancer cells using an MTT assay and reported an IC_{50} of approximately 10 µM, confirming moderate cytotoxicity. The cytotoxic effect that CBD has on A549 cells is caused by the compound's ability to upregulate apoptosis-related proteins like p53, PARP, RIP1, and RIP3. It induces the formation of intracellular vesicles in A549 cells, most likely through PPARγ-dependent mechanisms (Park *et al.*, 2022). The CBD cytotoxicity results were also consistent with those achieved from a study of ChoiPark et al. (2008), pointing out that the cytotoxic effects at concentrations above 20 µM of this compound were induced in a concentration- and time-dependent manner. Likewise, Bęben et al. (2024) examined CBG in SW620 colon cancer cells and reported an IC_{50} of 24.1 µM, confirming the result that CBG demonstrates dose-dependent cytotoxicity in epithelial cells, although there might be some variability between different cell lines. Studies by Nguyen et al. (2021) and van Breemen and Simchuk (2023) showed that both CBG and CBD exhibit antiviral potential by downregulating ACE2 transcript levels and acting as a main protease inhibitor to block viral replication. In addition, these compounds inhibit viral cell entry, viral proteases, and stimulate innate immune responses against a variety of viruses, including respiratory viruses (Nguyen et al., 2021; van Breemen and Simchuk, 2023). Further studies by the same author demonstrated that CBD acts as an allosteric antagonist of CB1 and CB2 agonists (Nguyen et al., 2021; van Breemen and Simchuk, 2023).

In this study, CBC showed an IC_{50} of 34.19 µM, which is consistent with Anis et al. (2021), who observed an IC_{50} of approximately 40 µM for CBC in combination with THC in bladder cancer cell lines. Cannabinoids such as CBN, CBV, and CBCV indicated IC_{50} values ranging from 10–

38 µM, maintaining ≥80% viability at lower concentrations (~10 µM). However, due to the lack of existing data on the cytotoxicity of these compounds in lung epithelial cells, these findings offer a new contribution to the literature. Interestingly, CBDA showed a significantly lower cytotoxic profile, with an IC_{50} of 665.25 µM, which is substantially higher than all other cannabinoids tested. CBDA can target the cap-dependent endonuclease activity of the influenza virus transcriptase complex (Tomassini et al., 1994), while CBN was reported to interact with CB1 and CB2 (Karmaus et al., 2012). Chung et al. (2019) reported that β-caryophyllene caused no effects at concentrations up to 200 mM on the A549 cell line. The S-containing functional groups in caryophyllene oxide have been found to increase its antiviral properties (Gyrdymova et al., 2019). Cannaflavin A also demonstrated moderate cytotoxicity (IC_{50} = 47.25 µM); however, no directly comparable studies using A549 or similar respiratory models have been published to date. Cannaflavin A can inhibit viral ribonucleoprotein and neuraminidase activities, which are essential for influenza virus replication (Palese et al., 1974).

3.6.1. Known cannabinoid complications in humans

Several symptoms and side effects in humans induced by CBD have been reported by Taylor et al., including diarrhea, nausea, headache, and somnolence. The side effects were observed in phase I, randomised trial, administering a single dose of 1500, 3000, 4500, 6000 mg and placebo CBD, twice daily for six days. The time taken to reach maximum plasma concentration (Tmaxc) was 4-5 hours. CBD reached steady state after approximately 2 days, with moderate accumulation (1.8- to 2.6-fold) and the half-life estimates ranged from 10 to 17h. There was no consistent effect of CBD on sleep or sleepiness, and no clear evidence of any drug withdrawal syndrome during the trial. Furthermore, cannabinoids were found to be present in the breast milk of recent users (Taylor et al., 2018). Safety profiles and complications induced by the rest of the compounds need to be researched further.

Chapter 4 Antiviral potential evaluation of cannabis - derived compounds

4.1. Influenza A H1N1 virus propagation in chicken embryonated eggs

Embryonated eggs are a reliable source for influenza virus amplification (Szretter *et al.*, 2006). The avian influenza viruses preferentially replicate in the allantoic cavity by binding to α2,3-linked sialic acid, which is predominantly expressed in the allantoic membrane lined by the epithelial cells.

A

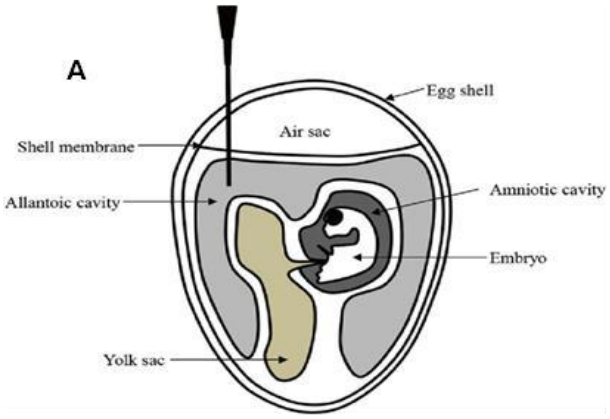

B

C

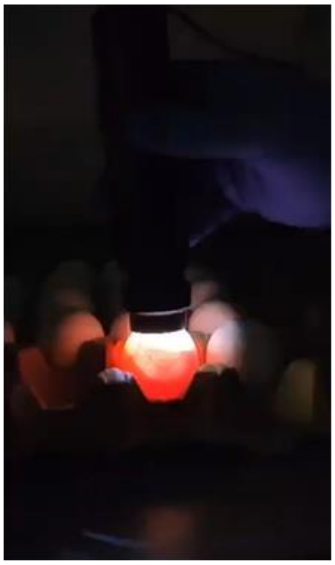

D

E

F

Figure 4.1 Embryonated egg inoculation and allantoic fluid collection.

(A) A graphical longitudinal section of an embryonated egg's anatomy. The allantoic cavity is the inoculation site, which is pointed with the needle (Zhang and Gauger, 2014). **(B)** Standard setup used for chicken egg inoculation, showing the mark that was made along the line of the air sac and a small "X" that was drawn to indicate the site for injection. **(C)** The candling procedure involves using a candling lamp to visualise the embryo for the amnion injection. **(D)** The egg was carefully cracked with forceps; the cap was removed above the air sac, and the egg content was exposed. **(F)** Standard setup for the virus collection procedure, where the allantoic fluid (AAF) was removed with a pipette.

Before inoculation, the eggs were individually illuminated to ensure the viability of the embryo. Using a pencil, a mark was made along the line of the air sac, and a small "X" was drawn with a pencil to indicate the site for injection. The shell was pierced just above the air sac, avoiding the blood vessels (Fig. 4.1A). The eggs were sprayed with 70% ethanol, the shell was pierced at the marked site, and 0.1 mL of PBS containing antibiotic and 100 µL of sample was drawn up into a syringe for each egg that was injected.

For virus amplification, 1000 PFU/egg of the virus stock was used in PBS containing antibiotic. The embryo was visualised with a candling lamp for direct amnion injection of 100 µL of inoculum into the allantoic fluid, and the syringe was slightly withdrawn. The injection of 0.1 mL of inoculum was made into the allantoic fluid. After the initial candlelight inspection and inoculation site determination, the eggs were injected directly without additional illumination (Fig. 4.1C). The holes were sealed with standard adhesive tape, and the eggs were incubated at 35°C for 4 days. After incubation, the eggs were chilled at 4 °C for 24 h before virus harvesting.

During virus harvesting, the eggs were sprayed with 70% ethanol. Forceps were used to carefully crack the egg, removing the cap above the air sac and exposing the egg content (Fig. 4.1 D and 4.1 E). The membrane of the egg was held back using a spatula, and a pipette were used to remove the allantoic fluid (Fig. 4.1 F). The HA activity and the viral titre was determined using the haemagglutination assay and the viral plaque assay.

Influenza virus purification was performed with centrifugation. Cell culture virus harvest (CVH) was centrifuged at 3,000 × g for 15 min to remove cell debris. At each step, the supernatant was transferred into a new centrifuge tube, and the pellet was discarded.
The allantoic fluid was aliquoted in Eppendorf tubes and stored at −80°C to preserve the virus infectivity titre. Repeated freezing and thawing were avoided. Once thawed for the antiviral assays, the virus stocks were kept on ice or at 4°C and used immediately.

4.2. Virus quantification using haemagglutination (HA) assays

Virus quantification experiments were performed prior to the plaque assays by Madin–Darby canine kidney plaque assay and haemagglutination, where the virus was quantified after inoculation and propagation in chicken embryonated eggs. By quantifying the virus before the plaque assays, the exact viral titre was determined, which allowed for precise standardisation of the virus concentration used in the assays. The precise determination of the viral load was necessary for experimental condition optimisation and achieving countable plaque numbers. Additionally, the virus quantification served as a quality control measure, ensuring consistency. The haemagglutination assay was also based on accurate and reliable viral concentrations (Figure 4.2).

To examine the concentration of influenza A virus that agglutinates red blood cells (RBCs), the hemagglutination assay was used, which is a method to titrate influenza virus based on the ability of the virus to attach to the surface of red blood cells. The viral suspension agglutinated the red blood cells, preventing them from settling out of suspension. This resulted in a cloudy appearance in the solution instead of forming a clear pellet at the bottom (Fig 4.2). This viral titre determination technique was performed by serial dilutions of virus in a round-bottom 96 - well plate and the addition of a fixed amount of chicken red blood cells (1%).

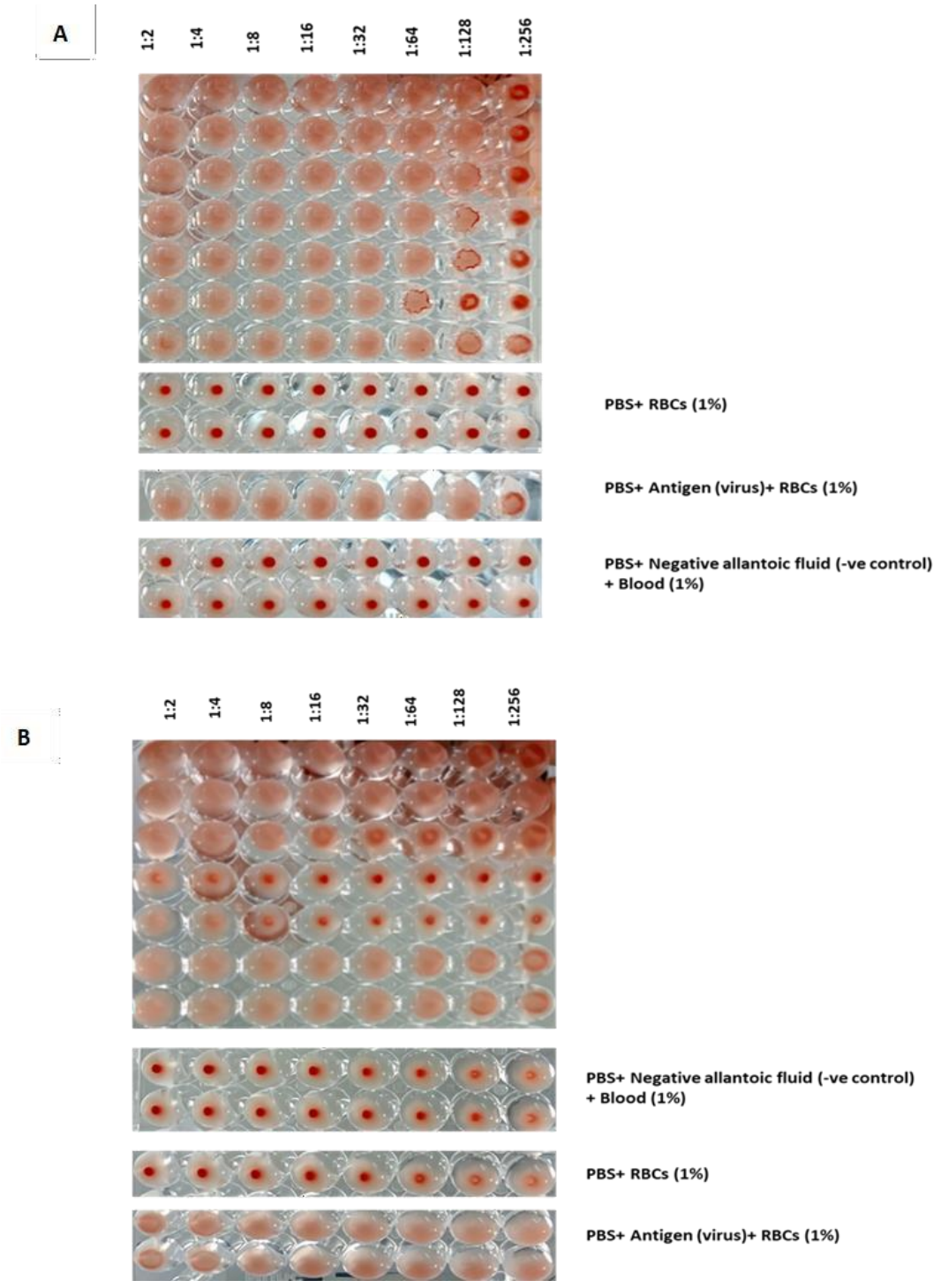

Figure 4.2 Hemagglutination (HA) assay to titre egg-derived PR8 influenza virus.

Wells containing negative allantoic fluid, without the presence of haemagglutinating agents, PBS, and 1% blood served as a negative control. 50 µL of AAF containing the virus was added to the first well of each column for columns 1-7. A 2-fold dilution was then performed in each row. The positive control consisted of PBS, 1% RBCs, and the virus. Chicken RBCs (0.5%, v/v) were added to each well. Panels A and B represent HI assay replicates used to determine the viral titre of Influenza A virus H1N1 by serial dilution. **(A)** The top seven rows contain the serial dilutions of the treatment compounds mixed with PBS and 1% RBCs; the next two rows include PBS with 1% RBCs (no virus);

followed by a row containing PBS, antigen (virus) and 1% RBCs; and the bottom two rows contain negative controls with PBS, negative allantoic fluid and 1% blood. **(B)** The top seven rows contain the serial dilutions; the following two rows contain PBS, negative allantoic fluid, and 1% blood; one row below includes PBS and 1% RBCs; and the bottom two rows contain PBS, antigen (virus), and 1% RBCs.

The virus was serially diluted 2-fold in PBS and mixed with 50 µL of 1% chicken RBCs. Pictures were taken after 30 minutes of incubation at RT, when the cell control wells had settled to form a solid button in the bottom of the well. Negative results appeared as dots in the centre of the wells, whereas positive results formed a uniform reddish colour across the well. A clearly negative result was observed in the fourth column, for dilutions 1:16 to 1:256, in columns 4 and 5, in Figure 4.2B. In Figure 4.2 A, hemagglutination is visible in the top left wells, where the positive results are indicated with a cloudy appearance. With further virus dilutions, the red dots started to form in the wells, signalling that there was an increased absence of hemagglutination, and therefore the negative results were indicated with a red dot formation, due to the sedimentation of RBCs at the bottom of the well. On average, the final titre was approximately 1:32, as hemagglutination consistently appeared in Figure 4.2 A) up to this dilution. Similarly, the second image follows a similar trend, with negative results appearing more consistently for dilutions 1:64 – 1:256. The endpoint of the virus titration is the highest dilution causing complete hemagglutination and is considered 1 hemagglutination unit (HAU), the number of HAUs/50 µL is the reciprocal of the highest dilution (Spackman, 2008). Therefore, the final titre was 640 HAU/mL.

4.3. Virus quantification using plaque assays

The plaque assay was based on the influenza virus's ability to form well-defined plaques on agar overlaid cell monolayers (Baer and Kehn-Hall, 2014). This event was caused by the CPE induced by the virus, which led to the death of infected cells. Because of the presence of an agar overlay, subsequent infections were restricted to cells surrounding the original infected cells. The circular zones of lysed cells appeared as clear plaques on the monolayer when stained with crystal violet. Plaque formation was exclusively caused by fully infectious viruses, which are referred to as plaque-forming units (PFUs). Therefore, the plaque assay was a quantitative measure of the number of infectious particles of the stock sample collected from the chicken embryonated egg inoculation. It was assumed that each plaque represents an

area initially infected by one single virus particle. The result of the titre of the virus sample was calculated in PFU per millilitre (PFU/mL). The plaque assay was carried out by preparing a tenfold dilution series of the stock virus to infect cell monolayers.

The control assay showed no virus activity and consequently no plaques appeared (Figure 4.3). The assay was initiated with the dilution of 10^{-4} to 10^{-9}. The plaques were observed in dilutions 10^{-4} to 10^{-6}. Among these dilutions, the plaques were measured in the 10^{-6} dilution since they were easily distinguished, and 30 plaques were counted in the well with the 10^{-6} dilution of virus. Because 0.5 mL of diluted viral stock was placed on the cells, the final titre is 6×10^{7} PFU/mL.

Since the titre of the virus was determined before exploring the antiviral potential of the cannabis derived compounds, this information was used for consistent virus quantity in the consequent antiviral experiments, and the multiplicity of infection (MOI) was calculated (MOI=1). This was the ratio of the infectious virus particles that targeted the cells. This was useful in understanding the dynamics of virus-cell interactions depending on the activity of cannabinoids. A known virus titre was also necessary in avoiding virus-induced cytopathic effects that could interfere with the antiviral effects of the compounds.

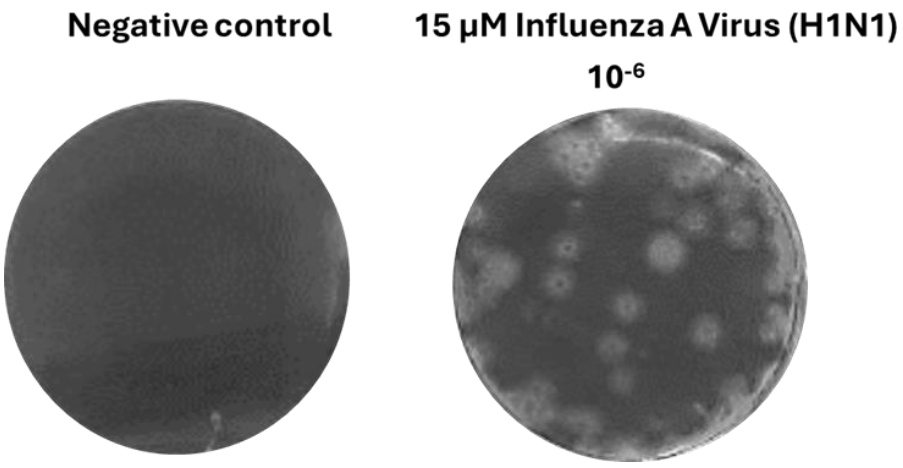

Figure 4.3 Quantification of influenza A H1N1/PR8 virus titre by plaque assay.

A monolayer of MDCK cells was infected with 10-fold serial dilutions of PR8 (10^{-4} – 10^{-9}) for 2 hr, washed, and then overlaid with a 0.8% agarose solution. After incubation at 37 °C for 72 hr, agar was carefully removed, and cells were fixed and stained with 0.25% crystal violet. Plaque formation was compared to that of an uninfected control.

4.4. Antiviral potential of selected cannabis-derived compounds (H1N1) strain A/PR/8/34

As outlined in chapter 2, section 2.9, A549 cells were pretreated for 24 hours with cannabis derived compounds and infected with chicken embryonated egg-derived influenza A virus over a 24h period. The concentrations chosen for the compounds were based on safety, i.e., the maximum concentration that displayed 80% cell viability on A549 cells and therefore no cytotoxicity was induced by the compounds. In A549 cells, the severity of the cytopathic effect (CPE) observed after the viral infection differed with each compound treatment. The cytopathic effects observed were cell shrinkage upon 6 hours of infection and detachment and fusion upon a 24-hour infection. For the plaque assays, when compared to the positive control of 15 µL of the virus, there was a trend towards significant antiviral potential over the post-infection period based on the biosynthesis pathway of the cannabinoid compounds that act as precursors of other cannabinoid compounds in the pathway, including CBG, and CBD . Similarly, all the compounds assessed *via* antiviral plaque assay showed some level of antiviral activity compared to controls (Figure 4.4), suggesting viral clearance was impaired by exposure to the compounds.

A

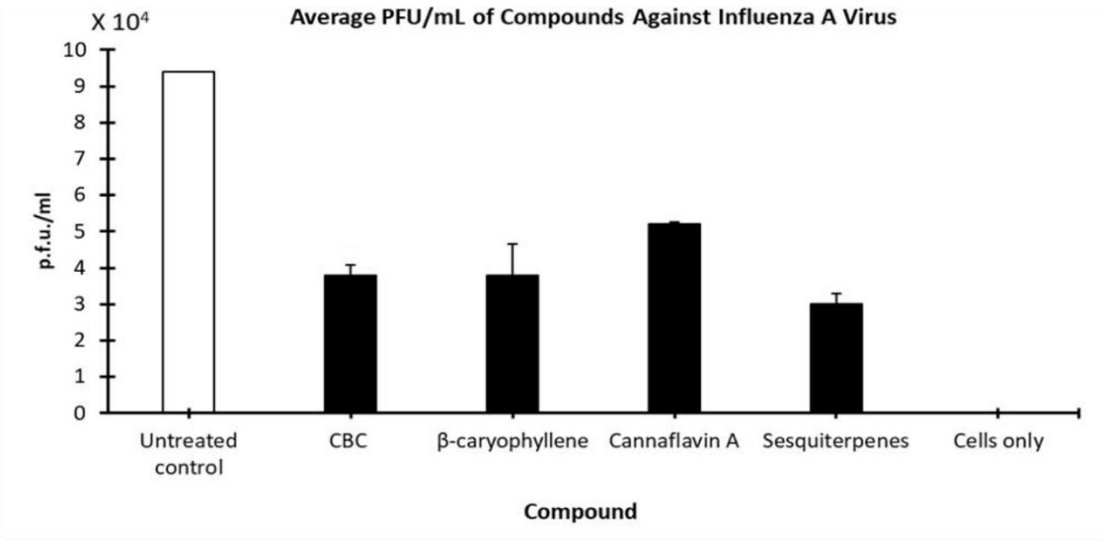

B

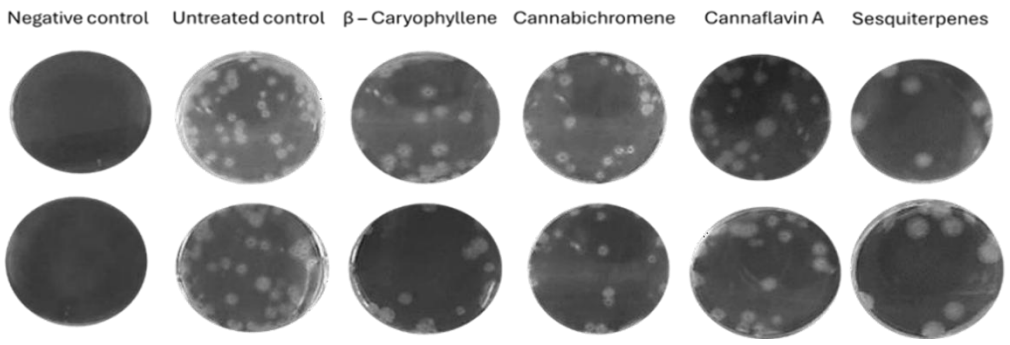

Figure 4.4 Cannabinoid pretreatment exposure showed antiviral activity following influenza A infection.

Viral burden was quantified by Madin–Darby canine kidney plaque assay and the results were assessed 24 h post infection. The plaque assays took place after the supernatant collection from pre-treated and infected A549 cells. The observed viral burden reductions of the effective cannabis-derived compounds were compared to the positive virus control (15 µL)-influenza A virus (IAV). Antiviral activity was quantified in MDCK cell culture *via* plaque assays for the compounds CBC, β–caryophyllene, cannaflavin A, and sesquiterpenes. Positive control included 15 µL of the virus, and negative control included DMEM without serum, where no plaques were observed. The viral infection was carried out with supernatant collected after 24 h cannabinoid pretreatment and 24 h virus infection. **A)** Bar graphs represent mean ± range; n=2 per compound. Viral burden reduction differences are descriptive only, and no statistical analysis was performed due to limited sample size. **B)** Plaque formation number and size correspond to the extent of viral replication under each compound treatment replicate.

CBC and β-caryophyllene treatments reduced the viral activity by approximately 60%, compared to the virus-only control (15 µL virus only) (Figure 4.4 A). Out of the set of compounds displayed in Figure 4.4, cannaflavin A reduced the viral burden the least (~50%), and sesquiterpenes achieved the highest antiviral activity (~70%). Overall, all compounds

shown in Figure 4.4 demonstrated reduced viral titres successfully compared to the virus-only control. While no statistical tests were applied due to low sample size, visual inspection of the data suggests potential antiviral trends that may become more evident with increased experimental replication.

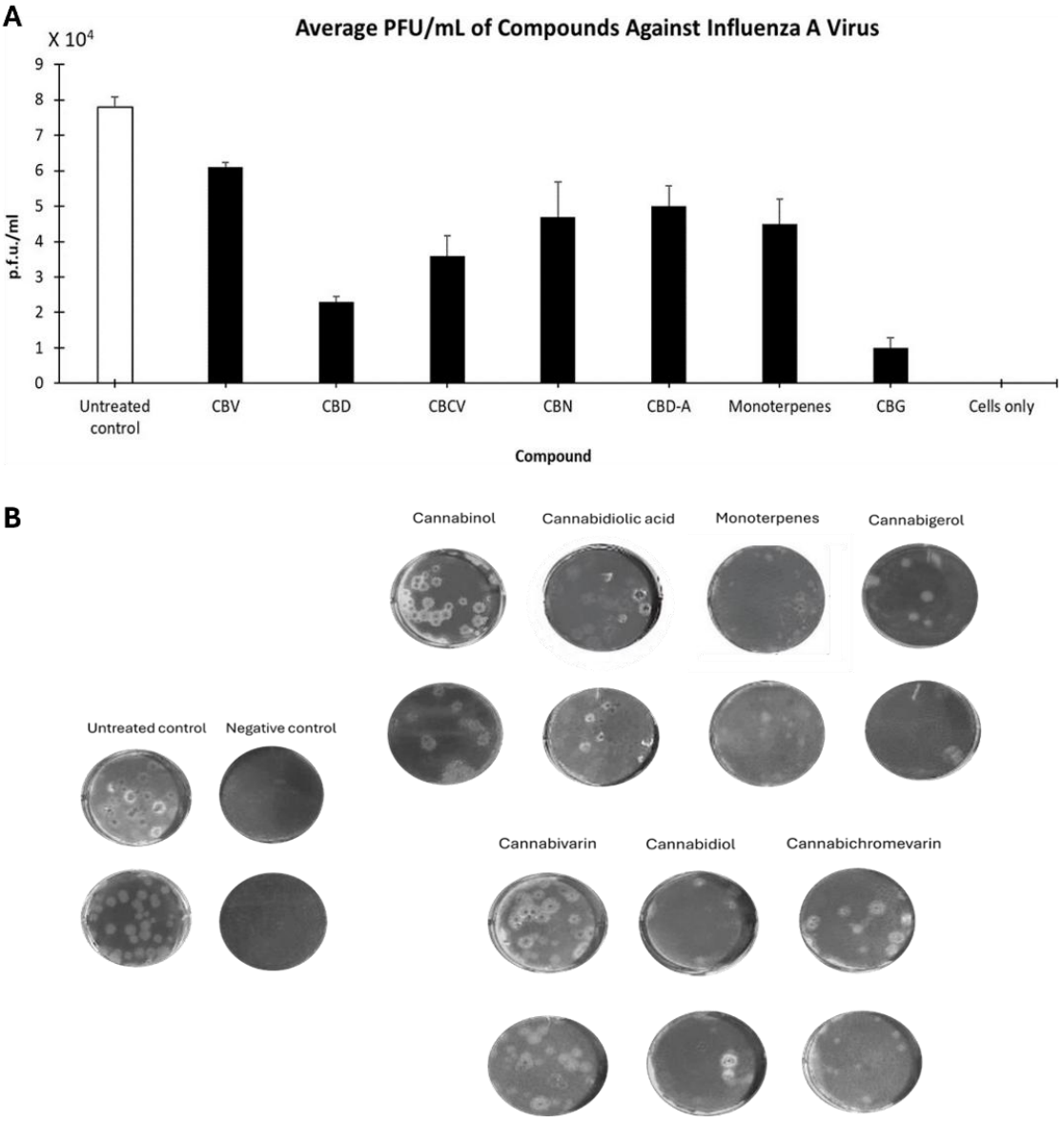

Figure 4.5 Cannabinoid pretreatment exposure showed antiviral activity following influenza A infection.

Viral burden was quantified by Madin–Darby canine kidney plaque assay, and the results were assessed 24 h post-infection. The plaque assays took place after the supernatant collection from pre-treated and infected A549 cells. The observed viral burden reductions of the effective cannabis-derived compounds were compared to the positive virus control (15 µl)-influenza A virus (IAV) and the antiviral activity of cannabis derived compounds. Results from antiviral assessment of cannabivarin (CBV), cannabidiol (CBD), cannabichromevarin (CBCV), cannabinol (CBN), monoterpenes, and cannabigerol (CBG). Positive control included 15 µl of the virus, and negative

control included DMEM without serum, where no plaques were observed. The viral infection was carried out with supernatant collected after 24 h cannabinoid pretreatment and 24 h virus infection. **A)** Bar graphs represent mean ± range; n=2 per compound. Viral burden reduction differences are descriptive only, and no statistical analysis was performed due to limited sample size. **B)** Plaque formation number and size correspond to the extent of viral replication under each compound treatment replicate.

In Figure 4.5, the viral activity was successfully decreased by all the treatments compared to the virus-only control. CBV showed the least antiviral activity (~20%) compared to all the compound treatments tested (Figures 4.4 and 4.5). CBN, CBDA, and monoterpenes were twice as effective as CBV and reduced the viral burden by ~40%. CBCV was slightly more effective, achieving ~55% reduction. However, the most effective compounds across all the assays (Figures 4.4 and 4.5) were CBD (~75% reduction) and CBG (~85% reduction).

The phytocannabinoids generally showed more consistent antiviral activity compared to the terpenes, although sesquiterpenes demonstrated a relatively strong reduction of ~70%. While statistical analysis was not feasible due to the limited sample size, the reductions observed were consistent across the antiviral compound treatment replicates; therefore, the results were reproducible under consistent assay conditions (Figures 4.4 B and 4.5 B). These preliminary results show a trend toward meaningful antiviral activity, particularly among CBG and CBD.

4.5. Chapter discussion

4.5.1. The cannabinoid compounds that reduced Influenza A H1N1 proliferation *in vitro*

As a result of the plaque assays, the cannabis compounds reduced IAV CPE induced in the cells. Firstly, some changes were observed for the pretreatment of CBC, β-Carophyllene, Cannaflavin A, and sesquiterpenes, but were not significant (Figure 4.4a). Their effects could target the virus cytokine levels, the viral surface protein hemagglutinin (HA) that binds to sialic acid receptors on the host cell. Previous research indicated that these compounds could modulate the immune response. For instance, β-caryophyllene has been shown to activate cannabinoid receptors, which may lead to anti-inflammatory effects and improved immune

function (Zaremba et al., 2024). Additionally, cannaflavin A has the potential to inhibit viral replication and reduce inflammation (Zaremba *et al.*, 2023). Sesquiterpenes, known for their diverse biological activities, may disrupt viral entry or replication processes (Romeo et al., 2024).

Cannabinol has only been previously investigated in the form of Δ9-tetrahydrocannabinol (Δ9-THC), which has shown effectiveness against influenza A (PR8). Karmaus *et al.* have suggested that Δ^9-THC potently suppressed myeloid cell immune function, in a manner involving CB_1 and/or CB_2, thereby impairing immune responses to influenza infection, and therefore, CBN could potentially behave similarly. Since CBN has not been addressed directly for its potential as an IAV treatment, this study is the first to investigate its potential effectiveness in targeting the virus.

Monoterpene derivatives, particularly those modified with sulphur-containing groups, demonstrate significant activity against the H1N1 strain of the influenza virus, while maintaining low cytotoxicity levels (Gyrdymova *et al.*, 2019). The derivatives of the specific monoterpene blend used (α-terpineol, α-pinene, β-pinene, and linalool) are hydrocarbon–based instead. Therefore, potential structural modifications in monoterpene blends could optimise their effectiveness against influenza A, making them promising candidates for further antiviral development.

CBG indicated the greatest antiviral potential as a pretreatment for the virus. This is a secondary cannabinoid and has been previously studied for its potential anti-inflammatory and antiviral properties, and although there is a lack of information on its potential in targeting IAV, it has been widely investigated for its effectiveness towards SARS-COV-2. According to Janecki *et al.*, CBG facilitated the inhibition of the cytokine storm associated with severe COVID-19 cases, reducing inflammation. In vitro studies by the same author suggested that phytocannabinoids, including CBG, can interact with SARS-CoV-2's main protease (Mpro), potentially blocking virus replication.

4.5.2. Indirect effectiveness of the cannabinoids on virus binding, entry and proliferation in immortalised A549 cells

In addition to the number of plaques, plaque morphology and dimensions can provide insights regarding the virulence and replication kinetics of the virus. The morphology of plaques has led to the distinguishment of viral isolates in previous studies and is also used as an indicator of virus attenuation (Moser *et al.*, 2018 & Mandary *et al.*, 2020). The area of the plaques was measured via ImageJ, an open-source image processing software, and ViralPlaque, which is an ImageJ macro. The area of individual plaques was measured with the LowRes method in single well mode and was determined in pixels squared (px^2).

Sesquiterpenes demonstrated a dual effect on the virus, with both less and larger plaques, compared to the positive control, which seems paradoxical. Possible explanations include local environment alteration or changes in the host cell response after the treatment. The specific blend of sesquiterpenes may have created conditions that altered viral entry, leading to fewer plaques, but the plaques that did form may have been more pronounced due to changes in host cell responses or enhanced local viral replication, proposing a potential synergistic effect of the different compounds used in the blend.

Chapter 5 General discussion

Each year, there are as many as 1 billion seasonal influenza infections around the world, and most cases occur during the winter season. 3–5 million of those cases are severe and can lead to 290,000–650,000 respiratory deaths annually (World Health Organization, 2023).

The first specific drug for the treatment of hospitalised COVID-19 patients was remdesivir. This involved drug repurposing, as it was originally used as an RNA polymerase inhibitor with broad antiviral activity against RNA viruses. Following this example, cannabis derived compounds could similarly be explored for broad-spectrum antiviral applications as well as reducing inflammation and modulating immune responses, for which they are traditionally known.

This investigation reported the antiviral potential of 11 compounds as pretreatments against the Influenza A virus (H1N1) strain A/PR/8/34, therefore investigating their indirect effects. Future investigations could involve exploring the different types of cannabinoid treatment formulations, i.e. oil, decoction or nasal spray and their effectiveness against a variety of viruses. Future studies may further explore the molecular functions of these compounds, such as their impact on inflammatory cytokines.

The effective in vitro concentrations for CBD (3.23 µM) and CBG (5.93 µM) against Influenza A H1N1 in this study suggest promising antiviral potential; however, whether such concentration levels are achievable in vivo remains uncertain. In mice, intraperitoneal administration of CBD at 120 mg/kg yields plasma concentrations that exceed 5 µM, which supports the feasibility of replicating the in vitro concentration in animal models (Deiana et al., 2011). In contrast, typical oral doses in humans (5–20 mg/kg) produce plasma levels of 0.03–1 µM, which is below the antiviral threshold (Millar et al., 2018; Perucca & Bialer, 2020). For CBG, high-dose administration in mice (120 mg/kg) results in detectable levels; however, there are no reports of plasma concentrations and antiviral efficacy (Deiana et al., 2011). The compounds CBC (11.78 µM), CBV (13.27 µM), CBCV (11.78 µM), CBN (5.83 µM), CBDA

(348.63 µM), and terpene mixtures (425 mg/mL) also showed in vitro activity, but evidence from in vivo pharmacokinetics remains scarce. Minor cannabinoids such as CBC and CBN have been detected in the brain and plasma after oral dosing in rats (3.2–100 mg/kg) (Moore et al., 2023). In addition, circulating concentrations of CBC, CBN, CBDV, and CBG have been confirmed in rodents (Deiana et al., 2011), but without antiviral evaluation.

The levels of cannabinoid compounds needed to inhibit the virus in vitro are higher than what can typically be achieved in the blood with standard doses for animals and humans; therefore, the optimisation of both dosing and delivery methods would likely be necessary. Despite the limitations related to pharmacokinetics and achievable plasma concentrations, this study's findings serve as a foundation in identifying compounds with promising antiviral properties and offer insights for future in vivo research and formulation development. As an example, targeted approaches such as inhalation aerosols or lipid nanoparticle formulations may help in the enhancement of tissue-specific bioavailability. (Millar et al., 2018; Child and Tallon, 2022).

In this study, the in vitro efficacy of the cannabinoid compounds was demonstrated, without any combinations, against the influenza A (H1N1) virus. Many of the cannabinoid compounds have been researched in previous studies on their potential against SARS-CoV-2. Influenza A and SARS-CoV-2 infections are caused by viruses that induce common symptoms such as fever, cough, and respiratory issues, but the symptoms of SARS-CoV-2 infections tend to last longer (CDC, 2020). When focusing on the differences of these two viruses, their genomes differ in polarity and segmentation, with the influenza virus having 8 negative-sense, single-stranded segments (Blut, 2009).

5.1. Limitations

Conducting viral plaque assays with cannabis-derived compounds, MDCK cells, and influenza H1N1 posed several methodological challenges that could affect the reliability and reproducibility of the results. The cannabis compounds may be cytotoxic at concentrations needed for antiviral activity. Due to this event, preliminary screening was carried out to identify

the optimised concentration necessary to maintain a balance, where the compounds are non-toxic yet effective.

Many cannabis compounds are hydrophobic, leading to solubility issues in the overlay medium used in plaque assays. Poor solubility can result in inconsistent delivery of the compounds to the cells. However, pre-treating the cells 24 hours before infection interfered with this issue, as the compounds had already diffused through the cell membrane due to their lipophilic nature. With pre-treatment, the results indicated the indirect effects of the compounds against the virus.

The sensitivity of the viral assay itself poses another set of challenges. Plaque size and clarity, essential for accurate quantification, can be affected by the presence of the compounds and cell confluency. Achieving consistent viral titres is critical for reproducibility, as variability in viral stocks can lead to inconsistent plaque numbers, thereby affecting the reliability of the assay outcomes. Experimental condition optimisation is important for the assay's success, including fine-tuning parameters such as incubation time and specific time points to suit both MDCK cells and the H1N1 virus. Any deviations can impact viral replication and cell viability significantly, due to the virus's sensitivity.

5.2. Maintaining consistency in viral plaque assays

Consistency is imperative for successful viral plaque assays, and precise planning was required throughout all experimental stages. This included the timing of key steps, such as viral infection, compound treatment, and plaque staining and visualization. Consistency of the concentration of trypsin (TPCK), which acted as a critical reagent, was also important. Similarly, uniform seeding density of MDCK cells across all assay plates was essential to prevent inconsistent data. Moreover, careful calculation and accurate dilution of the cannabis-derived compound concentrations were attained to establish both antiviral effectiveness and the maintenance of approximately 80% cell viability, as determined through preliminary cytotoxicity assays using A549 cells.

5.3. Indirect and direct antiviral properties of cannabinoids

This investigation focused solely on the indirect antiviral effectiveness of cannabinoids since the cells were pretreated. This allowed for the assessment of their potential to inhibit viral entry into the host cells or to enhance the cells' antiviral defences before exposure to the virus, observing the possibility of prophylactic effects and prevention of viral infection.

Another option would have been to observe their direct antiviral effectiveness via co-treatment (during viral infection) and post-treatment (after viral infection) methods. The co-treatment would involve administering the compounds simultaneously with viral infections, for evaluation of direct interference with viral replication and modulation of host cell responses during the early stages of infection, therefore observing the compounds' immediate antiviral activity. Post-treatment with the compounds was less commonly used in previous research, but can be used to investigate the potential of inhibition in viral spread or viral effect mitigation after the infection. This approach can provide perspective into the compounds' ability to target later stages of the viral life cycle or to contribute towards host immune responses for viral replication control.

The 24-hour pretreatment led to an extensive interaction between the cannabinoids and the cellular environment, for stronger effects on viral infection and replication. A longer pre-treatment period might have increased the risk of cellular adaptation and compound degradation. On the other hand, a 12-hour pretreatment would also be a suitable exposure timeframe for cellular pathway interaction. A 6-hour pretreatment would be an ideal timeframe for compounds with rapid effects.

The A549 cells used in the antiviral experiments expressed the angiotensin-converting enzyme 2 (ACE2) and transmembrane serine protease 2 (TMPRSS2). TMPRSS2 is responsible for viral protein entry into host cells for several viral infections, including influenza. Specifically, it cleaves viral proteins, such as haemagglutinin (HA) in influenza viruses and the spike (S) protein in coronaviruses, facilitating virus fusion with the host cell membranes. TMPRSS2 is mainly expressed in the respiratory and gastrointestinal tracts. A549 cells are also known to

produce cytokines and participate in immune responses, and therefore helped in evaluating cannabinoid pretreatment effects on the cellular inflammatory response to H1N1 infection.

5.4. Future perspectives

Since some of the assessed cannabinoid compounds have shown effectiveness in previous studies on their antiviral properties against SARS-CoV-2, they can therefore exhibit antiviral effects against other respiratory viruses, including influenza A H1N1, through the same or similar mechanisms of action. Cannabinoids interact with various biological pathways, including the modulation of the endocannabinoid system (ECS), cytokine storm reductions, and inhibition of viral entry, replication and assembly. Cannabinoids are also known for their anti-inflammatory effects, which lead to the reduction of disease severity. The reduction of the cytokine storms is an example of cannabinoid modulation of the host's immune response. Cannabinoids also have the ability to interact with ECS receptors (CB1 and CB2), impacting immune cell activity and reducing the viral load. The antiviral effects of these compounds can either be direct or indirect. Direct antiviral effects include viral entry inhibition and replication, preventing the virus's ability to bind to host cell receptors.

These effects were observed in previous studies investigating cannabinoid effectiveness against SARS-CoV-2, and these properties may also apply to influenza H1N1. This is due to the similarities in replication between these viruses. Although the entry receptors differ between the viruses, as Influenza A binds to sialic acid receptors and SARS-CoV-2 binds to ACE2 receptors, cannabinoids affect the receptor availability and cell membrane integrity and therefore disrupt the entry of both the viruses. There is less experimental evidence on the mechanistic effects of cannabinoids against influenza A H1N1, compared to the growing evidence supporting their effectiveness against SARS-CoV-2, and further research would be essential to conclude their molecular effects against influenza A.

This study however, investigated potential indirect effectiveness with a 24-hour pretreatment. The compounds were applied to A549 cells before influenza A H1N1 exposure. Since there was an observable decrease in plaque formation with certain treatments, this indicates signs

of immune modulation. These cannabinoids could therefore have the potential to increase the production of antiviral proteins, such as interferons, or reduce inflammation. Another possibility is that cannabinoids altered the cell surface receptor expressions or interfered with the signalling pathways of the virus. Changes in receptor availability and cell membrane composition may have created a ‘’protective barrier’’, preventing virus binding on the cells, which decreased the viral load and the plaque formation in the plaque assays. Direct testing of the compounds against the virus would also be beneficial in forming a complete picture of the antiviral potential and the specific effects of these compounds.

Although cannabivarin and cannabichromevarin have not been previously studied for their antiviral potential on IAV, CBD, which is a primary cannabinoid, is known to be effective as a pre-treatment targeting Influenza A virus (Lior Chatow et al., 2024). CBDA would be expected to have a similar effect, considering that it is a close structural derivative of CBD. Additional research with broader sampling is required to validate the observed trends and determine their statistical significance. Further mechanistic studies focusing on the modulation of ACE2 expression and viral entry inhibition, protease activity blockade, and enhancement of innate immune responses are needed to clarify the antiviral actions of these compounds and to therefore inform targeted therapeutic development (Nguyen et al., 2021; van Breemen and Simchuk, 2023).

In addition, the incorporation of repeated dosing of these compound treatments in vivo will provide insight into long-term effects, potential tolerance, sensitisation, and maintenance of antiviral efficacy, which cannot be fully assessed with single, short-term in vitro exposure (Cadoni et al., 2001; Thomas et al., 2018). Chronic administration of some of the cannabinoid compounds has been previously reported in preclinical models, providing an understanding of tolerance, receptor adaptation, and pharmacokinetics. For example, repeated dosing of THC in mice (10–60 mg/kg twice daily for 6.5 days) led to behavioural tolerance, with a 27-fold rightward shift in the ED_{50} for antinociceptive response, and CB1 receptor downregulation across brain regions such as the hippocampus and cerebellum (McKinney et al., 2007). Similarly, male rhesus monkeys receiving THC chronically (1 mg/kg every 12 h) displayed both tolerance and cross tolerance to other CB_1 agonists (McMahon, 2011). CBD showed a different profile. In mice, repeated CBD did not lead to tolerance of its

neuroprotective effects or CB_1 receptor desensitisation (Hayakawa et al., 2007), and co-administration with THC in rats resulted in altered THC metabolism and enhanced development of THC tolerance (Greene et al., 2018). These phenomena cannot be captured in single-exposure in vitro studies, and in vivo study results indicate that tolerance may change with different compound combinations.

5.5. Synergism and therapeutic combinations

Terpenes and flavonoids from cannabis plants may enhance the action of cannabinoids through synergism, potentially improving their efficacy in combating various human pathologies. Cannabidiol (CBD) Antagonises undesirable effects of THC such as intoxication, sedation and tachycardia. It enhances the analgesic, anti-emetic, and anti-carcinogenic properties of THC. THC and CBD demonstrated dual action against viral main proteases and human angiotensin-converting enzyme 2, with CBD being a potent viral main protease inhibitor (Toyang, Lowe and McLaughlin, 2017). Additionally, THC has been extensively researched for its efficacy against different DNA and RNA viruses (Pitakbut, Nguyen and Kayser, 2021).

This highlights an opportunity for further investigation into the synergistic effects of terpenes and flavonoids in conjunction with cannabinoids to produce enhanced antiviral therapies and broaden their range of applications. Additionally, investigating combinations of cannabinoids and terpenes with clinically approved antiviral agents (such as remdesivir or oseltamivir) could lead to formulations that present reduced toxicity profiles (Nguyen et al., 2021; van Breemen and Simchuk, 2023).

Chapter 6 References

AAT Bioquest (2025). IC50 Calculator | AAT Bioquest. Available at: https://www.aatbio.com/tools/ic50-calculator.

Agata Lewandowska & Graczyk, M. (2022) Anti-Inflammatory and Antiviral Effects of Cannabinoids. Agata Lewandowska. Available at: https://encyclopedia.pub/entry/22105.

Aizikovich, A. (2021) In vitro Activity of Novel Cannabinoids Derived from Tetrahydrocannabinolic Acid on Various Human Tumor Cell Lines. Journal of Oncology Research, 3(2).

Al-Naqeeb, A.A.A.G. & Raham, T.F. (2021) H1N1 and COVID-19: surprising mortality pattern correlation. International Journal Of Community Medicine And Public Health, 8(6), 2694.

Anderson, P.F., Jackson, D.M., Chesher, G.B. and R. Malor (1975) Tolerance to the effects of Δ 9-tetrahydrocannabinol in mice on intestinal motility, temperature and locomotor activity. Psychopharmacology, 43(1), pp.31–36. doi:https://doi.org/10.1007/bf00437611.

Anis, O., Vinayaka, A.C., Shalev, N., Namdar, D., Nadarajan, S., Anil, S.M., Cohen, O., Belausov, E., Ramon, J., Mayzlish Gati, E. and Koltai, H. (2021). Cannabis-Derived Compounds Cannabichromene and Δ9-Tetrahydrocannabinol Interact and Exhibit Cytotoxic Activity against Urothelial Cell Carcinoma Correlated with Inhibition of Cell Migration and Cytoskeleton Organization. Molecules, 26(2). doi:https://doi.org/10.3390/molecules26020465.

Ariano, R.E., Sitar, D.S., Zelenitsky, S.A., Zarychanski, R., Pisipati, A., Ahern, S., Kanji, S., Rello, J. and Kumar, A. (2010). Enteric absorption and pharmacokinetics of oseltamivir in critically ill patients with pandemic (H1N1) influenza. Canadian Medical Association Journal, 182(4), pp.357–363. doi:https://doi.org/10.1503/cmaj.092127.

Baek, S.H., Kim, S.H., Kim, M., Kim, S.H., and Lee, J. (2019). Clinical characteristics of influenza-associated acute respiratory distress syndrome in Korea.

Tuberculosis and Respiratory Diseases, 82(1), pp.9–14. doi: https://doi.org/10.4046/trd.2018.0067

Baer, A. & Kehn-Hall, K. (2014) Viral Concentration Determination Through Plaque Assays: Using Traditional and Novel Overlay Systems. Journal of Visualized Experiments, 93(93).

Bęben, D., Siwiela, O., Szyjka, A., Graczyk, M., Rzepka, D., Barg, E. and Moreira, H. (2024). Phytocannabinoids CBD, CBG, and their Derivatives CBD-HQ and CBG-A Induced In Vitro Cytotoxicity in 2D and 3D Colon Cancer Cell Models. Current Issues in Molecular Biology, 46(4), pp.3626–3639. doi:https://doi.org/10.3390/cimb46040227.

Blut, A. (2009) Influenza Virus. Transfusion Medicine and Hemotherapy, 36(1), 32–39.

Boncristiani, H.F., Criado, M.F. & Arruda, E. (2009). Respiratory viruses. In: *Encyclopedia of Microbiology*, 3rd edition, pp. 500–518. Academic Press.

Cacciabue, M., Anabella Currá and Gismondi, M.I. (2019). ViralPlaque: a Fiji macro for automated assessment of viral plaque statistics. PeerJ, 7(9), pp.e7729–e7729. doi:https://doi.org/10.7717/peerj.7729.

Cadoni, C., Pisanu, A., Solinas, M., Acquas, E. and Chiara, G. (2001). Behavioural sensitization after repeated exposure to Δ^9-tetrahydrocannabinol and cross-sensitization with morphine. Psychopharmacology, 158(3), pp.259–266. doi:https://doi.org/10.1007/s002130100875.

CDC (2020) Similarities and Differences between Flu and COVID-19. Available at: https://www.cdc.gov/flu/symptoms/flu-vs-covid19.htm

CDC (2022) Influenza Antiviral Medications: Clinician Summary. Available at: https://www.cdc.gov/flu/professionals/antivirals/summary-clinicians.htm#Table1

CDC (2023a) Frequently Asked Flu Questions: 2023–2024. Available at: https://www.cdc.gov/flu/season/faq-flu-season-2023-2024.htm

CDC (2023b) Influenza antiviral medications: Summary for clinicians. Available at:

https://www.cdc.gov/flu/professionals/antivirals/summary-clinicians.htm

Chen, J. et al. (2023) Natural Product-Based Screening for Lead Compounds Targeting SARS CoV-2 Mpro. Pharmaceuticals, 16(5), 767.

Chen, S. & Kim, J.-K. (2024) The Role of Cannabidiol in Liver Disease: A Systemic Review. International Journal of Molecular Sciences, 25(4), 2370–2370.

Child, R.B. and Tallon, M.J. (2022). Cannabidiol (CBD) Dosing: Plasma Pharmacokinetics and Effects on Accumulation in Skeletal Muscle, Liver and Adipose Tissue. Nutrients, 14(10), p.2101. doi:https://doi.org/10.3390/nu14102101.

ChoiPark, W.-H.-D., Baek, S.-H., Chu, J.-P., Kang, M.-H. and Mi, Y.-J. (2008). Cannabidiol Induces Cytotoxicity and Cell Death via Apoptotic Pathway in Cancer Cell Lines. Biomolecules & Therapeutics, 16(2), pp.87–94. doi:https://doi.org/10.4062/biomolther.2008.16.2.087.

Chung, K.-S. et al. (2019) β-Caryophyllene in the Essential Oil from Chrysanthemum Boreale Induces G1 Phase Cell Cycle Arrest in Human Lung Cancer Cells. Molecules, 24(20), 3754–3754.

Cilloniz, C. et al. (2022) Respiratory viruses: their importance and lessons learned from COVID-19. European Respiratory Review, 31(166), 220051.

Classen, N. et al. (2024) Cannabigerol and Cannabicyclol Block SARS-CoV-2 Cell Fusion. Planta Medica, 90(09).

Creative Bioarray (2024). CBD as a Drug: Pharmacokinetics and Current Formulations. Creative-bioarray.com. Available at: https://www.creative-bioarray.com/support/cbd-as-a-drug-pharmacokinetics-and-current-formulations.htm.

Creoli, M., Di Paola, A., Tarallo, A., Aziz, S., Miele, E., Martinelli, M., Casertano, M., Colucci, A., Cenni, S., Marrapodi, M.M., Staiano, A., Rossi, F. and Strisciuglio, C. (2025). Effects of CB2 Receptor Modulation on Macrophage Polarization in Pediatric Inflammatory Bowel Disease. International Journal of Molecular Sciences, 26(8), p.3720. doi:https://doi.org/10.3390/ijms26083720.

Daoud, A. et al. (2019) Pulmonary complications of influenza infection: a targeted narrative review. Postgraduate Medicine, 131(5), 299–308.

Deiana, S., Watanabe, A., Yamasaki, Y., Amada, N., Arthur, M., Fleming, S., Woodcock, H., Dorward, P., Pigliacampo, B., Close, S., Platt, B. and Riedel, G. (2011). Plasma and brain pharmacokinetic profile of cannabidiol (CBD), cannabidivarine (CBDV), Δ9-tetrahydrocannabivarin (THCV) and cannabigerol (CBG) in rats and mice following oral and intraperitoneal administration and CBD action on obsessive–compulsive behaviour. Psychopharmacology, 219(3), pp.859–873. doi:https://doi.org/10.1007/s00213-011-2415-0.

Del Prado-Audelo, M.L. et al. (2021) Therapeutic Applications of Terpenes on Inflammatory Diseases. Frontiers in Pharmacology, **12**, 704197 doi: 10.3389/fphar.2021.704197.

Devi, M. & Yadav, V. (2023) *Screening and Simulation Study of Efficacious Antiviral Cannabinoid Compounds as Potential Agents Against SARS-CoV-2.* ChemRxiv [preprint]. doi: 10.26434/chemrxiv-2023-nf6mq

Devinsky, O., Kraft, K., Rusch, L., Fein, M. and Leone-Bay, A. (2021). Improved Bioavailability with Dry Powder Cannabidiol Inhalation: A Phase 1 Clinical Study. Journal of Pharmaceutical Sciences, 110(12), pp.3946–3952. doi:https://doi.org/10.1016/j.xphs.2021.08.012.

Diniz, L.R.L. et al. (2021) Bioactive Terpenes and Their Derivatives as Potential SARS-CoV-2 Proteases Inhibitors from Molecular Modeling Studies. Biomolecules, 11(1), 74.

Fantegrossi, W.E., Franks, L.N., Vasiljevik, T. and Prather, P.L. (2013). Tolerance and cross-tolerance among high-efficacy synthetic cannabinoids JWH-018 and JWH-073 and low-efficacy phytocannabinoid Δ9-THC. The FASEB Journal, 27(S1). doi:https://doi.org/10.1096/fasebj.27.1_supplement.1097.1.

Flerlage, T. et al. (2021) Influenza virus and SARS-CoV-2: pathogenesis and host responses in the respiratory tract. Nature Reviews Microbiology, 19(7), pp.1–17.

Forbes, R.L. et al. (2012) Pregnant Women Have Attenuated Innate Interferon Responses to 2009 Pandemic Influenza A Virus Subtype H1N1. The Journal of Infectious Diseases, 206(5), pp.646–653.

Gao, Y., Guyatt, G., Uyeki, T.M., Liu, M., Chen, Y., Zhao, Y., Shen, Y., Xu, J., Zheng, Q., Li, Z., Zhao, W., Luo, S., Chen, X., Tian, J. and Hao, Q. (2024). Antivirals for treatment of severe influenza: a systematic review and network meta-analysis of randomised controlled trials. The Lancet, 404(10454), pp.753–763. doi:https://doi.org/10.1016/s0140-6736(24)01307-2.

Gaoni, Y. & Mechoulam, R. (1964) Isolation, Structure, and Partial Synthesis of an Active Constituent of Hashish. Journal of the American Chemical Society, 86(8), 1646–1647.

. Gaush, C.R., Hard, W.L., & Smith, T.F. (1966). Characterization of an Established Line of Canine Kidney Cells (MDCK). *Proceedings of the Society for Experimental Biology and Medicine*, **122**(3), 931–935.

Gertsch, J., Leonti, M., Raduner, S., Racz, I., Chen, J.-Z., Xie, X.-Q., Altmann, K.-H., Karsak, M. and Zimmer, A. (2008). Beta-caryophyllene is a dietary cannabinoid. Proceedings of the National Academy of Sciences of the United States of America, 105(26), pp.9099–9104. doi:https://doi.org/10.1073/pnas.0803601105.

Gomez, D.M., Everett, T.J., Hamilton, L.R., Ranganath, A., Cheer, J.F. and Oleson, E.B. (2021). Chronic cannabinoid exposure produces tolerance to the dopamine releasing effects of WIN 55,212-2 and heroin in adult male rats. Neuropharmacology, 182, p.108374. doi:https://doi.org/10.1016/j.neuropharm.2020.108374.

Gonçalves, E.C.D. et al. (2020) Terpenoids, Cannabimimetic Ligands, beyond the Cannabis Plant. Molecules. Available at: https://www.mdpi.com/1420-3049/25/7/1567

Greene, N.Z., Wiley, J.L., Yu, Z., Clowers, B.H. and Craft, R.M. (2018). Cannabidiol modulation of antinociceptive tolerance to Δ9-tetrahydrocannabinol. Psychopharmacology, 235(11), pp.3289–3302.

doi:https://doi.org/10.1007/s00213-018-5036-z.

Grotenhermen, F. (2003) Pharmacokinetics and Pharmacodynamics of Cannabinoids. Clinical Pharmacokinetics, 42(4), 327–360.

Gyrdymova, Y.V. et al. (2019) Anti-Influenza Activity of Several Caryophyllane Hiosesquiterpenoids. Chemistry of Natural Compounds, 55(6), 1179–1181.

Hamamoto, I. et al. (2013). High Yield Production of Influenza Virus in Madin Darby Canine Kidney (MDCK) Cells with Stable Knockdown of IRF7. PLoS ONE, 8(3), e59892.

Hassanin, O. et al. (2020). In vitro and in vivo experimental trials to assess the modulatory influence of β-caryophyllene on NDV replication and immunopathogenesis. Comparative Immunology, Microbiology and Infectious Diseases, 73, 101547.

Hayakawa, K., Mishima, K., Nozako, M., Ogata, A., Hazekawa, M., Liu, A.-X., Fujioka, M., Abe, K., Hasebe, N., Egashira, N., Iwasaki, K. and Fujiwara, M. (2007). Repeated treatment with cannabidiol but not Δ9-tetrahydrocannabinol has a neuroprotective effect without the development of tolerance. Neuropharmacology, 52(4), pp.1079–1087. doi:https://doi.org/10.1016/j.neuropharm.2006.11.005.

Hayden, F.G., Sugaya, N., Hirotsu, N., Lee, N., de Jong, M.D., Hurt, A.C., Ishida, T., Sekino, H., Yamada, K., Portsmouth, S., Kawaguchi, K., Shishido, T., Arai, M., Tsuchiya, K., Uehara, T. and Watanabe, A. (2018). Baloxavir Marboxil for Uncomplicated Influenza in Adults and Adolescents. New England Journal of Medicine, 379(10), pp.913–923. doi:https://doi.org/10.1056/nejmoa1716197.

Holloman, B.L., Nagarkatti, M. and Nagarkatti, P. (2021). Epigenetic Regulation of Cannabinoid-Mediated Attenuation of Inflammation and Its Impact on the Use of Cannabinoids to Treat Autoimmune Diseases. International Journal of Molecular Sciences, 22(14), p.7302. doi:https://doi.org/10.3390/ijms22147302.

Holmes, J. et al. (2024). Exploring Cannabinoids as Potential Inhibitors of SARS-

CoV-2 Papain-like Protease: Insights from Computational Analysis and Molecular Dynamics Simulations. Viruses, 16(6), 878–878..

Hu, B., Guo, H., Zhou, P. and Shi, Z.-L. (2020). Characteristics of SARS-CoV-2 and COVID-19. Nature Reviews Microbiology, 19(19), pp.1–14. Available at: https://www.nature.com/articles/s41579-020-00459-7

Huang, Y. et al. (2020). Structural and functional properties of SARS-CoV-2 spike protein: potential antivirus drug development for COVID-19. Acta Pharmacologica Sinica, 41(9), 1141–1149.

Ison, M.G. et al. (2020). Early treatment with baloxavir marboxil in high-risk adolescent and adult outpatients with uncomplicated influenza (CAPSTONE-2): a randomised, placebo-controlled, phase 3 trial. The Lancet Infectious Diseases, 20(10), pp.1204–1214.

Iván Martínez-Baz, Fernández-Huerta, M., Navascués, A., Pozo, F., Camino Trobajo-Sanmartín, Casado, I., Echeverria, A., Ezpeleta, C. and Castilla, J. (2023). Influenza Vaccine Effectiveness in Preventing Laboratory-Confirmed Influenza Cases and Hospitalizations in Navarre, Spain, 2022–2023. Vaccines, 11(9), pp.1478–1478. doi:https://doi.org/10.3390/vaccines11091478.

Jackson, C.B., Farzan, M., Chen, B. and Choe, H. (2021). Mechanisms of SARS-CoV-2 Entry into Cells. Nature Reviews Molecular Cell Biology, 23(1), pp.1–18. doi: https://doi.org/10.1038/s41580-021-00418-x.

Janecki, M. et al. (2022a). Anti-Inflammatory and Antiviral Effects of Cannabinoids in Inhibiting and Preventing SARS-CoV-2 Infection. International Journal of Molecular Sciences, 23(8), 4170.

Janecki, M. et al. (2022b). Anti-Inflammatory and Antiviral Effects of Cannabinoids in Inhibiting and Preventing SARS-CoV-2 Infection. International Journal of Molecular Sciences, 23(8), 4170.

Janero, D.R., Vadivel, S.K. and Makriyannis, A. (2009). Pharmacotherapeutic modulation of the endocannabinoid signalling system in psychiatric disorders: Drug-discovery strategies. International Review of Psychiatry,

21(2), pp.122–133. doi: https://doi.org/10.1080/09540260902782778.

Jin, K.-S., Bak, M.-J., Jun, M., Lim, H.-J., Jo, W.-K. and Jeong, W.-S. (2010). α-pinene triggers oxidative stress and related signaling pathways in A549 and HepG2 cells. Food Science and Biotechnology, 19(5), pp.1325–1332. doi: https://doi.org/10.1007/s10068-010-0189-5.

Job, E.R. et al. (2010). Pandemic H1N1 Influenza A Viruses Are Resistant to the Antiviral Activities of Innate Immune Proteins of the Collectin and Pentraxin Superfamilies. The Journal of Immunology, 185(7), pp.4284–4291.

Justia Patents (2018) *US Patent for Monoterpenes for treating respiratory diseases, in particular bronchopulmonary diseases Patent (Patent # 11,135,194 issued October 5, 2021) - Justia Patents Search*. Available at: https://patents.justia.com/patent/11135194.

Kaiser, L., Wat, C., Mills, T., Mahoney, P., Ward, P. and Hayden, F. (2003). Impact of Oseltamivir Treatment on Influenza-Related Lower Respiratory Tract Complications and Hospitalizations. Archives of Internal Medicine, 163(14), p.1667. doi: https://doi.org/10.1001/archinte.163.14.1667.

Kalil, A.C. & Thomas, P.G. (2019). Influenza virus-related critical illness: pathophysiology and epidemiology. Critical Care, 23(1)..

Karmaus, P.W.F. et al. (2012). Δ9-Tetrahydrocannabinol Impairs the Inflammatory Response to Influenza Infection: Role of Antigen-Presenting Cells and the Cannabinoid Receptors 1 and 2. Toxicological Sciences, 131(2), pp.419–433.

Konstantin Kotschenreuther et al. (2020). Cannabinoids drive Th17 cell differentiation in patients with rheumatic autoimmune diseases. Cellular and Molecular Immunology, 18(3), pp.764–766. Springer Nature.

Kuramoto, K., Wang, N., Fan, Y., Zhang, W., Schoenen, F.J., Frankowski, K.J., Marugan, J., Zhou, Y., Huang, S. and He, C. (2016). Autophagy activation by novel inducers prevents BECN2-mediated drug tolerance to cannabinoids. Autophagy, 12(9), pp.1460–1471. doi: https://doi.org/10.1080/15548627.2016.1187367.

Lamtha, T. et al. (2022). Structural analysis of cannabinoids against EGFR-TK leads a novel target against EGFR-driven cell lines. Current Research in Pharmacology and Drug Discovery, 3, 100132.

Leweke, F.M., Piomelli, D., Pahlisch, F., Muhl, D., Gerth, C.W., Hoyer, C., Klosterkötter, J., Hellmich, M. and Koethe, D. (2012). Cannabidiol enhances anandamide signaling and alleviates psychotic symptoms of schizophrenia. Translational Psychiatry, 2(3), pp.e94–e94. doi: https://doi.org/10.1038/tp.2012.15.

.

Lior Chatow et al. (2024). Terpenes and Cannabidiol against Human Corona and Influenza Viruses - Anti-Inflammatory and Antiviral in Vitro Evaluation. Biotechnology Reports, 47, e00829. doi: https://doi.org/10.1016/j.btre.2024.e00829

Li, R., Han, Q., Li, X., Liu, X. and Jiao, W. (2024). Natural Product-Derived Phytochemicals for Influenza A Virus (H1N1) Prevention and Treatment. Molecules, 29(10), pp.2371–2371. doi: https://doi.org/10.3390/molecules29102371.

Li, X. et al. (2019). Crystal Structure of the Human Cannabinoid Receptor CB2. Cell, 176(3), pp.459-467.e13.

Liu, C. et al. (2022). Identification of SARS-CoV-2 Main Protease Inhibitors from a Library of Minor Cannabinoids by Biochemical Inhibition Assay and Surface Plasmon Resonance Characterized Binding Affinity. Molecules, 27(18), p.6127. doi: https://doi.org/10.3390/molecules27186127.

Lowe, H. et al. (2021). Non-Cannabinoid Metabolites of Cannabis sativa L. with Therapeutic Potential. Plants, 10(2), p.400 Available at: https://pmc.ncbi.nlm.nih.gov/articles/PMC7923270/.

Lucas, S. (2010). Predictive clinicopathological features derived from systematic autopsy examination of patients who died with A/H1N1 influenza infection in the UK 2009–10 pandemic. Health Technology Assessment, 14(55).

Mahmud, M.S. et al. (2021). Antimicrobial and Antiviral (SARS-CoV-2) Potential of Cannabinoids and Cannabis sativa: A Comprehensive Review. Molecules, 26(23), 7216.

Mandary, M.B. et al. (2020). Characterization of Plaque Variants and the Involvement of Quasi-Species in a Population of EV-A71. Viruses, 12(6), 651.

Manuzak, J.A., Gott, T.M., Kirkwood, J.S., Coronado, E., Hensley-McBain, T., Miller, C., Cheu, R.K., Collier, A.C., Funderburg, N.T., Martin, J.N., Wu, M.C., Isoherranen, N., Hunt, P.W. and Klatt, N.R. (2018). Heavy Cannabis Use Associated With Reduction in Activated and Inflammatory Immune Cell Frequencies in Antiretroviral Therapy–Treated Human Immunodeficiency Virus–Infected Individuals. Clinical Infectious Diseases, 66(12), pp.1872–1882. doi: https://doi.org/10.1093/cid/cix1116.

Martinez, D.R., Moreira, F., Zweigart, M.R., Gully, K.L., De, G., Brown, A.J., Adams, L.E., Catanzaro, N., Yount, B., Baric, T.J., Mallory, M.L., Conrad, H., May, S.R., Dong, S., Scobey, T., Montgomery, S.A., Perry, J.K., Babusis, D., Barrett, K.T. and NguyễnA. (2023). Efficacy of the oral nucleoside prodrug GS-5245 (Obeldesivir) against SARS-CoV-2 and coronaviruses with pandemic potential. bioRxiv (Cold Spring Harbor Laboratory). doi: https://doi.org/10.1101/2023.06.27.546784.

Matlin, K.S. et al. (1981). Infectious entry pathway of influenza virus in a canine kidney cell line. Journal of Cell Biology, 91(3), 601–613.

McKinney, D.L., Cassidy, M.P., Collier, L.M., Martin, B.R., Wiley, J.L., Selley, D.E. and Sim-Selley, L.J. (2007). Dose-Related Differences in the Regional Pattern of Cannabinoid Receptor Adaptation and in Vivo Tolerance Development to Δ9-Tetrahydrocannabinol. Journal of Pharmacology and Experimental Therapeutics, 324(2), pp.664–673. doi: https://doi.org/10.1124/jpet.107.130328.

McMahon, L.R. (2011). Chronic Δ9-tetrahydrocannabinol treatment in rhesus monkeys: differential tolerance and cross-tolerance among cannabinoids. British Journal of Pharmacology, 162(5), pp.1060–1073. doi:

https://doi.org/10.1111/j.1476-5381.2010.01116.x.

Medveczky, M.M., Sherwood, T.A., Klein, T.W., Friedman, H. and Medveczky, P.G. (2004). Delta-9 tetrahydrocannabinol (THC) inhibits lytic replication of gamma oncogenic herpesviruses in vitro. BMC Medicine, 2, p.34. doi: https://doi.org/10.1186/1741-7015-2-34.

Mechoulam, R. et al. (2007). Cannabidiol – Recent Advances. Chemistry & Biodiversity, 4(8), 1678–1692. https://doi.org/10.1002/cbdv.200790147

Millar, S.A., Stone, N.L., Yates, A.S. and O'Sullivan, S.E. (2018). A Systematic Review on the Pharmacokinetics of Cannabidiol in Humans. Frontiers in Pharmacology, 9(1365). doi: https://doi.org/10.3389/fphar.2018.01365.

Moser, L.A. et al. (2018). Growth and adaptation of Zika virus in mammalian and mosquito cells. PLOS Neglected Tropical Diseases, 12(11), e0006880.

Moore, C.F., Weerts, E.M., Kulpa, J., Schwotzer, D., Dye, W., Jantzi, J., McDonald, J.D., Lefever, T.W. and Bonn-Miller, M.O. (2023). Pharmacokinetics of Oral Minor Cannabinoids in Blood and Brain. Cannabis and Cannabinoid Research, 8(S1), pp.S51–S61. doi: https://doi.org/10.1089/can.2023.0066.

Moscona, A. (2005). Neuraminidase Inhibitors for Influenza. New England Journal of Medicine, 353(13), pp.1363–1373. doi: https://doi.org/10.1056/nejmra050740.

Nagarkatti, P. et al. (2020). Use of Cannabinoids to Treat Acute Respiratory Distress Syndrome and Cytokine Storm Associated with Coronavirus Disease-2019. Frontiers in Pharmacology, 11.

Naithani, R. et al. (2008). Antiviral activity of phytochemicals: a comprehensive review. Mini Reviews in Medicinal Chemistry, 8(11), 1106–1133.

National Institute on Drug Abuse (NIDA) (2021) *NIDA Drug Supply Program*. Available at: https://nida.nih.gov/research/research-data-measures-resources/nida-drug-supply-program

Nguyen, L.C., Yang, D., Nicolaescu, V., Best, T.J., Gula, H., Saxena, D., Gabbard, J.D., Chen, S.-N., Ohtsuki, T., Friesen, J.B., Drayman, N., Mohamed, A., Dann, C.,

Silva, D., Robinson-Mailman, L., Valdespino, A., Stock, L., Suárez, E., Jones, K.A. and Azizi, S.-A. (2022). Cannabidiol inhibits SARS-CoV-2 replication through induction of the host ER stress and innate immune responses. Science Advances, 8(8). doi: https://doi.org/10.1126/sciadv.abi6110.

Nguyen, L.C., Yang, D., Nicolaescu, V., Best, T.J., Ohtsuki, T., Chen, S.-N., Friesen, J.B., Drayman, N., Mohamed, A., Dann, C., Silva, D., Gula, H., Jones, K.A., Millis, J.M., Dickinson, B.C., Tay, S., Oakes, S.A., Pauli, G.F., Meltzer, D.O. and Randall, G. (2021). Cannabidiol Inhibits SARS-CoV-2 Replication and Promotes the Host Innate Immune Response. bioRxiv, 6(39), p.2021.03.10.432967. doi: https://doi.org/10.1101/2021.03.10.432967.

Noor, R., Indwiani Astuti and Mustofa (2014). Cytotoxicity of α-terpineol in HeLa cell line and its effects to apoptosis and cell cycle. Journal of the Medical Sciences (Berkala Ilmu Kedokteran), 46(01), pp.1–9. doi: https://doi.org/10.19106/jmedscie004601201401.

Nooruzzaman, M., Katherine, J., Rani, R., Finkelsztein, E.J., Caserta, L.C., Kodiyanplakkal, R.P., Wang, W., Hsu, J., Salpietro, M.T., Banakis, S., Albert, J., Westblade, Lars F, Zanettini, C., Marchionni, L., Soave, R., Ghedin, E., Diel, D.G. and Salvatore, M. (2024). Emergence of transmissible SARS-CoV-2 variants with decreased sensitivity to antivirals in immunocompromised patients with persistent infections. Nature Communications, 15(1), pp.1–16. doi: https://doi.org/10.1038/s41467-024-51924-3.

Noshi, T., Kitano, M., Taniguchi, K., Yamamoto, A., Omoto, S., Baba, K., Hashimoto, T., Ishida, K., Kushima, Y., Hattori, K., Kawai, M., Yoshida, R., Kobayashi, M., Yoshinaga, T., Sato, A., Okamatsu, M., Sakoda, Y., Kida, H., Shishido, T. and Naito, A. (2018). In vitro characterization of baloxavir acid, a first-in-class cap-dependent endonuclease inhibitor of the influenza virus polymerase PA subunit. Antiviral Research, 160, pp.109–117. doi: https://doi.org/10.1016/j.antiviral.2018.10.008.

Pacher, P. & Mechoulam, R. (2011). Is lipid signaling through cannabinoid 2 receptors part of a protective system? Progress in Lipid Research, 50(2),

193–211.

Padalia, R.C. et al. (2013). Volatile terpenoid compositions of leaf and rhizome of Curcuma amada Roxb. from Northern India. The Journal of Essential Oil Research, 25(1), 17–22.

Palese, P. et al. (1974). Inhibition of influenza and parainfluenza virus replication in tissue culture by 2-deoxy-2,3-dehydro-N-trifluoroacetylneuraminic acid (FANA). Virology, 59(2), 490–498.

Palese, P. (2004). Influenza: old and new threats. Nature Medicine, 10(S12), S82–S87. doi: https://doi.org/10.1038/nm1141.

Park, Y.-J. et al. (2022). Cannabidiol Regulates PPARγ-Dependent Vesicle Formation as well as Cell Death in A549 Human Lung Cancer Cells. Pharmaceuticals, 15(7), 836.

Patel, V.B., Preedy, V.R. and Martin, C.R. (2023). Neurobiology and Physiology of the Endocannabinoid System. Academic Press.

Paw, M. et al. (2020). Estimation of variability, genetic divergence, correlation studies of Curcuma caesia Roxb. Journal of Applied Research on Medicinal and Aromatic Plants, 17, 100251.

Pérez, R., Glaser, T., Villegas, C., Burgos, V., Ulrich, H. and Paz, C. (2022). Therapeutic Effects of Cannabinoids and Their Applications in COVID-19 Treatment. Life, 12(12), 2117. doi: https://doi.org/10.3390/life12122117.

Pertwee, R.G. (2005). The therapeutic potential of drugs that target cannabinoid receptors or modulate the tissue levels or actions of endocannabinoids. The AAPS Journal, 7(3), E625–E654. doi: https://doi.org/10.1208/aapsj070364.

Pertwee, R.G. (2008). The diverse CB1 and CB2 receptor pharmacology of three plant cannabinoids: Δ9-tetrahydrocannabinol, cannabidiol and Δ9-tetrahydrocannabivarin. British Journal of Pharmacology, 153(2), 199–215. doi: https://doi.org/10.1038/sj.bjp.0707442.

Petrova, V.N. and Russell, C.A. (2017). The evolution of seasonal influenza viruses. Nature Reviews Microbiology, 16(1), 47–60. doi:

https://doi.org/10.1038/nrmicro.2017.118.

Piscura, M.K., Henderson-Redmond, A.N., Barnes, R.C., Mitra, S., Guindon, J. and Morgan, D.J. (2023). Mechanisms of cannabinoid tolerance. Biochemical Pharmacology, 214, 115665. doi: https://doi.org/10.1016/j.bcp.2023.115665.

Pitakbut, T., Nguyen, G.-N. and Kayser, O. (2021). Activity of THC, CBD, and CBN on Human ACE2 and SARS-CoV1/2 Main Protease to Understand Antiviral Defense Mechanism. Planta Medica, 88(12), pp.1047–1059. doi: https://doi.org/10.1055/a-1581-3707.

Polat, H.U., Yalcin, H.A., Köm, D., Aksoy, Ö., Abaci, I., Ekiz, A.T., Serhatli, M. and Onarici, S. (2024). Antiviral effect of cannabidiol on K18-hACE2 transgenic mice infected with SARS-CoV-2. Journal of Cellular and Molecular Medicine, 28(17), e70030. doi: https://doi.org/10.1111/jcmm.70030.

Preteroti, M. et al. (2023). Modulation of pulmonary immune function by inhaled cannabis products and consequences for lung disease. Respiratory Research, 24(1).

Promega (2019). CytoTox-GloTM Cytotoxicity Assay. Available at: https://www.promega.co.uk/products/cell-health-assays/cell-viability-and-cytotoxicity-assays/cytotox_glo-cytotoxicity-assay/?catNum=G9290

Racaniello, V. (2009) Influenza hemagglutination inhibition assay | Virology Blog. *Virology Blog*, 27 May. Available at: https://virology.ws/2009/05/27/influenza-hemagglutination-inhibition-assay/

Raj, V. et al. (2021). Assessment of antiviral potencies of cannabinoids against SARS-CoV-2 using computational and in vitro approaches. International Journal of Biological Macromolecules, 168, 474–485.

Ramirez, J., Peyrani, P., Wiemken, T., Chaves, S.S. and Fry, A.M. (2018). A randomized study evaluating the effectiveness of oseltamivir initiated at the time of hospital admission in adults hospitalized with influenza-associated lower respiratory tract infections. Clinical Infectious Diseases,

67(5), 736–742. doi: https://doi.org/10.1093/cid/ciy163.

Romeo, R. et al. (2024). Antiviral compounds to address influenza pandemics: An update from 2016-2022. Current Medicinal Chemistry, 31(18), 2507–2549..

Russo, C. et al. (2021). Comparative assessment of antimicrobial, antiradical and cytotoxic activities of cannabidiol and its propyl analogue cannabidivarin. Scientific Reports, 11(1).

Saraswat, A., Vartak, R., Patki, M. and Patel, K. (2021). Cannabidiol inhibits in vitro human liver microsomal metabolism of remdesivir: A promising adjuvant for COVID-19 treatment. Cannabis and Cannabinoid Research, 12(12). doi: https://doi.org/10.1089/can.2021.0109.

Scott, C. et al. (2023). Cannabinoids and the endocannabinoid system in early SARS-CoV-2 infection and long COVID-19—a scoping review. Journal of Clinical Medicine, 13(1), 227.

Sea, Y.L. et al. (2022). Cannabis as antivirals. Journal of Applied Microbiology, 134(1).

Sebaugh, J.L. (2011). Guidelines for accurate EC50/IC50 estimation. Pharmaceutical Statistics, 10(2), 128–134.

Shabana, S.M., Gad, N.S., Othman, A.I., Mohamed, A.F. and El-Missiry, M.A. (2023a). Antioxidant promotion and oxidative stress downregulation by β-caryophyllene oxide attenuate lung cancer A549 cell proliferation. Asian Journal of Cell Biology, 40(7). doi: https://doi.org/10.21203/rs.3.rs-2489411/v1.

Shabana, S.M., Gad, N.S., Othman, A.I., Mohamed, A.F. and El-Missiry, M.A. (2023b). β-caryophyllene oxide induces apoptosis and inhibits proliferation of A549 lung cancer cells. Medical Oncology, 40(7). doi: https://doi.org/10.1007/s12032-023-02022-9.

Sharma, A. et al. (2020). Severe acute respiratory syndrome coronavirus-2 (SARS-CoV-2): A global pandemic and treatment strategies. International Journal of Antimicrobial Agents, 56(2), 106054.

Shi, T. et al. (2019). Global disease burden estimates of respiratory syncytial virus–associated acute respiratory infection in older adults in 2015: A systematic review and meta-analysis. The Journal of Infectious Diseases, 222(Supplement_7), S577–S583.

Śledziński, P. et al. (2020). Cannabinoids in medicine: Cancer, immunity, and microbial diseases. International Journal of Molecular Sciences, 22(1), 263.

Slivicki, R.A., Yi, J., Brings, V.E., Huynh, P.N. and Gereau, R.W.I. (2022). The cannabinoid agonist CB-13 produces peripherally mediated analgesia in mice but elicits tolerance and signs of central nervous system activity with repeated dosing. PAIN, 163(8), 1603–1621. doi: https://doi.org/10.1097/j.pain.0000000000002550.

Solnier, J. & Fladerer, J.-P. (2020). Flavonoids: A complementary approach to conventional therapy of COVID-19? Phytochemistry Reviews, 13.

Song, A.-R., Sun, X.-L., Kong, C., Zhao, C., Qin, D., Huang, F. and Yang, S. (2013). Discovery of a new sesquiterpenoid from Phellinus ignarius with antiviral activity against influenza virus. Archives of Virology, 159(4), 753–760. doi: https://doi.org/10.1007/s00705-013-1857-6.

Spackman, E. (2008). Avian influenza virus. Totowa, NJ:.

Stöhr, K. (2003). The WHO global influenza program and its animal influenza network. Avian Diseases, 47(s3), 934–938.

Szulc, M., Kujawski, R., Pacholak, A., Poprawska, M., Czora-Poczwardowska, K., Geppert, B. and Mikołajczak, P.Ł. (2023). Cannabidiol as a modulator of the development of alcohol tolerance in rats. Nutrients, 15(7), 1702. doi: https://doi.org/10.3390/nu15071702.

Sun, F. and Huang, R. (2014). The medicinal potential of natural products for the development of anti-influenza agents. Current Drug Targets, 15(2), 175–183. doi: https://doi.org/10.2174/13894501113146660203.

Sun, Z.-G. et al. (2021). Recent advances in natural products with antiviral activities. Mini-Reviews in Medicinal Chemistry, 21(14), 1888–1908..

Suryavanshi, S.V., Zaiachuk, M., Pryimak, N., Kovalchuk, I. and Kovalchuk, O. (2022). Cannabinoids alleviate the LPS-induced cytokine storm via attenuating NLRP3 inflammasome signaling and TYK2-mediated STAT3 signaling pathways in vitro. Cells, 11(9), 1391. doi: https://doi.org/10.3390/cells11091391.

Szretter, K.J. et al. (2006). Influenza: Propagation, quantification, and storage. Current Protocols in Microbiology, 3(1), 15G.1.1–15G.1.22.

Schneider, C.A., Rasband, W.S. and Eliceiri, K.W. (2012). NIH Image to ImageJ: 25 years of image analysis. Nature Methods, 9(7), 671–675. doi: https://doi.org/10.1038/nmeth.2089.

Tamburello, M. et al. (2023). Antiviral activity of cannabidiolic acid and its methyl ester against SARS-CoV-2. Journal of Natural Products, 86(7), 1698–1707..

Taylor, L. et al. (2018). A phase I, randomized, double-blind, placebo-controlled, single ascending dose, multiple dose, and food effect trial of the safety, tolerability and pharmacokinetics of highly purified cannabidiol in healthy subjects. CNS Drugs, 32(11), 1053–1067.

Thermo Fisher Scientific (2024) *PrestoBlue Cell Viability Reagent for Microplates Protocol | Thermo Fisher Scientific - UK*. Available at: https://www.thermofisher.com/cy/en/home/references/protocols/cell-and-tissue-analysis/protocols/prestoblue-cell-viability-reagent-for-microplates-protocol.html.

Tomassini, J. et al. (1994). Inhibition of cap (m7GpppXm)-dependent endonuclease of influenza virus by 4-substituted 2,4-dioxobutanoic acid compounds. Antimicrobial Agents and Chemotherapy, 38(12), 2827–2837.

Tomko, A.M. et al. (2020). Anti-cancer potential of cannabinoids, terpenes, and flavonoids present in cannabis. Cancers, 12(7), 1985.

Tomer, S., Mu, W., Suryawanshi, G., Ng, H., Wang, L., Wennerberg, W., Rezek, V., Martin, H., Chen, I., Kitchen, S. and Zhen, A. (2022). Cannabidiol modulates expression of type I IFN response genes and HIV infection in macrophages. Frontiers in Immunology, 13. doi:

https://doi.org/10.3389/fimmu.2022.926696.

Troeger, C.E. et al. (2019). Mortality, morbidity, and hospitalisations due to influenza lower respiratory tract infections, 2017: an analysis for the Global Burden of Disease Study 2017. The Lancet Respiratory Medicine, 7(1), 69–89.

Turcotte, C., Chouinard, F., Lefebvre, J.S. and Flamand, N. (2015). Regulation of inflammation by cannabinoids, the endocannabinoids 2-arachidonoyl-glycerol and arachidonoyl-ethanolamide, and their metabolites. Journal of Leukocyte Biology, 97(6), 1049–1070. doi: https://doi.org/10.1189/jlb.3ru0115-021r.

Ueda, M. et al. (2008) Maturation efficiency of viral glycoproteins in the ER impacts the production of influenza A virus. Virus Research, 136(1-2), 91–97.

UK (2024) Surveillance of influenza and other seasonal respiratory viruses in the UK, winter 2023 to 2024. GOV.UK. Available at: https://www.gov.uk/government/statistics/surveillance-of-influenza-and-other-seasonal-respiratory-viruses-in-the-uk-winter-2023-to-2024/surveillance-of-influenza-and-other-seasonal-respiratory-viruses-in-the-uk-winter-2023-to-2024#:~:text=Influenza%20hospital%20admissions%20peaked%20in

van Breemen, R.B., Muchiri, R.N., Bates, T.A., Weinstein, J.B., Leier, H.C., Farley, S., & Tafesse, F.G. (2022). Cannabinoids block cellular entry of SARS-CoV-2 and the emerging variants. Journal of Natural Products, 85, 176-184 doi: https://doi.org/10.1021/acs.jnatprod.1c00946.

van Breemen, Richard B. & Simchuk, D. (2023). Antiviral activities of hemp cannabinoids. Clinical Science, 137(8), 633–643. doi: https://doi.org/10.1042/cs20220193.

Wang, Y., Song, T., Li, K., Jin, Y., Yue, J., Ren, H. and Liang, L. (2019). Different Subtypes of Influenza Viruses Target Different Human Proteins and Pathways Leading to Different Pathogenic Phenotypes. BioMed Research International, 2019, pp.1–7. doi: https://doi.org/10.1155/2019/4794910.

Wen, C.-C. et al. (2007). Specific Plant Terpenoids and Lignoids Possess Potent Antiviral Activities against Severe Acute Respiratory Syndrome Coronavirus. Journal of Medicinal Chemistry, 50(17), 4087–4095.

Wiktoria Potocka et al. (2023). Current and Potential Applications of Monoterpenes and Their Derivatives in Oral Health Care. Molecules, 28(20), 7178–7178..

World Health Organization (2023). Influenza (Seasonal). Available at: https://www.who.int/news-room/fact-sheets/detail/influenza-(seasonal)?gad_source=1&gclid=Cj0KCQjwt4a2BhD6ARIsALgH7DrXy5CNXt6Nvk15_n5asJHM2yJ9awokL484W4uS0dr4UkwbHDGc6kgaAj-yEALw_wcB.

World Health Organization (2024) *The burden of influenza*. Available at: https://www.who.int/news-room/feature-stories/detail/the-burden-of-influenza

Wu, S., Peng, L., Sang, H., Ping Li, Q. and Cheng, S. (2018). Anticancer effects of α-Bisabolol in human non-small cell lung carcinoma cells are mediated via apoptosis induction, cell cycle arrest, inhibition of cell migration and invasion and upregulation of P13K/AKT signalling pathway. Journal of B.U.ON. : official journal of the Balkan Union of Oncology, 23(5), pp.1407–1412. Available at: https://pubmed.ncbi.nlm.nih.gov/30570866/.

Xu, C., Chang, T., Du, Y., Yu, C., Tan, X. and Li, X. (2019). Pharmacokinetics of oral and intravenous cannabidiol and its antidepressant-like effects in chronic mild stress mouse model. Environmental Toxicology and Pharmacology, 70, p.103202. doi: https://doi.org/10.1016/j.etap.2019.103202.

Yuhui Deborah Fong & Jang, J. (2022). Natural products as Zika antivirals. Medicinal Research Reviews, 42(5), 1739–1780. .

Zaremba, P. et al. (2023). In vitro and in silico studies of the antiviral activity of polyhydrated fullerenes against influenza A (H1N1) virus. Scientific Reports, 13(1), 10879.

Zaremba, P.Yu. et al. (2024). Antiviral Activity of Low-Molecular-Weight Fluorinated Compounds Against Influenza A (H1N1) Virus.

Mikrobiolohichnyi Zhurnal, 86(2), 51–64..

Zhang, J. & Gauger, P.C. (2014). Isolation of Swine Influenza Virus in Cell Cultures and Embryonated Chicken Eggs. Methods in Molecular Biology, 1161, 265–276.

Zhang, L., Chen, J., Ke, C., Zhang, H., Zhang, S., Tang, W., Liu, C., Liu, G., Chen, S., Hu, A., Sun, W., Xiao, Y., Liu, M. and Chen, X. (2020). Ethanol Extract of Caesalpinia decapetala Inhibits Influenza Virus Infection In Vitro and In Vivo. Viruses, 12(5), p.557. doi: https://doi.org/10.3390/v12050557.

Zhang, M. et al. (2021). Development of Broad-Spectrum Antiviral Agents—Inspiration from Immunomodulatory Natural Products. Viruses, 13(7), 1257–1257.